# PSD-95: Genomic Characterisation, Generation of a Conditional Allele and Role in Anaesthesia in the mouse

**Matthew Bence**


**Doctor of Philosophy**
**The University of Edinburgh**
**2002**

## Declaration

I declare that the work presented in this thesis is my own, except where otherwise stated.

8/12/02

Matthew Bence

# Acknowledgements

Thanks to my supervisor, Seth Grant, for his advice and support throughout my PhD. Thanks also to everyone in the lab, the Centre for Genome Research and Department of Neuroscience who has helped with advice, reagents or allowing me to bend their ear. I would particularly like to thank Mags McClean and Noboru Komiyama for teaching me all things molecular, and Andrew Smith, Rick Lathe, Val Wilson and Richard Morris for the time and help they have given me. Thanks also to everyone involved in mouse matters, particularly Jane Robinson.

Finally, thanks to all my pals in Edinburgh and down South who have kept me entertained, especially Al (Begg), Al, (Easter), Al (Farley), Al (Plumbe), Julie, Lillian and Tony. Thanks also to Mum, for supporting me throughout. Big thanks to Clare, for always being there and getting me through the dark days. Cheers.

# Abbreviations

| | |
|---|---|
| AKAP | PKA anchoring protein |
| AMP | Adenosine monophosphate |
| AMPA | α-amino-3-hydroxy-5-methylisoxazole-4-propionic acid |
| arc | activity-regulated cytoskeleton-associated protein |
| arg3.1 | activity-regulated gene 3.1 |
| ATP | Adenosine triphosphate |
| BAI1 | Brain-specific angiogenesis inhibitor 1 |
| bp | Base pairs |
| CaMKII | Calcium/calmodulin dependent kinase II |
| CASK | Calcium/calmodulin-dependent serine protein kinase |
| cDNA | Complementary DNA |
| CNS | Central nervous system |
| Cre-Pr | Cre-progesterone binding domain fusion protein |
| CREB | cAMP response element binding protein |
| CRIPT | Cysteine-rich interactor of PDZ3 |
| DAP-1 | hDLG and PSD-95 associated protein-1 |
| DEPC | Diethylenepyrocarbonate |
| DIA | Differentiation inhibiting activity |
| dlg/DLG | Discs large |
| DNA | Deoxyribonucleic acid |
| DOB | Date of birth |
| DOC | Deoxycholate |
| E | Embryonic day |
| EGTA | Ethylene glycol-bis(2-aminoethylether)-N,N,N',N'-tetraacetic acid |
| EM | Electron microscopy |
| fEPSP | Field excitatory postsynaptic potential |
| mEPSP | Minature excitatory postsynaptic potential |
| ER | Endoplasmic reticulum |
| ERK | Extracellular signal-regulated kinase |
| ES cell | Embryonic stem cell |
| EST | Expressed sequence tag |
| gDNA | Genomic DNA |
| GFP | Green fluorescent protein |
| GK | Guanylate kinase |
| GKAP | Guanylate kinase-associated protein |
| GRIP | Glutamate receptor interacting protein |
| hDLG | Human Discs large (a.k.a. SAP97) |
| HEK | Hamster embryonic kidney cell line |
| HGMP | Human genome mapping project |
| INAD | Inactivation no after-potential D |
| kb | Kilobase pairs |

| | |
|---|---|
| IEG | Immediate early gene |
| IRES | Internal ribosome entry site |
| KDa | Kilo Daltons |
| LIF | Leukaemia inhibitory factor |
| LORR | Loss of righting reflex |
| LR-PCR | Long range PCR |
| LTD | Long term depression |
| LTP | Long term potentiation |
| MAGUK | Membrane-associated guanylate kinase |
| MAPK | Mitogen-activated protein kinase |
| MEK | MAPK/extracellular signal-regulated kinase kinase |
| neo | Neomycin phosphotransferase |
| NMDA | N-methyl-D-aspartate |
| NMJ | Neuromuscular junction |
| NR2AΔC | NR2A C-terminal deletion |
| NR2BΔC | NR2B C-terminal deletion |
| NRC | NMDA receptor-associated complex |
| PAC | P1 artificial chromosome |
| PAGE | Polyacrylamide gel electrophoresis |
| PBS | Phosphate buffered saline |
| PCR | Polymerase chain reaction |
| PDZ | PSD-95/DLG/ZO-1 |
| PGK | Phosphoglycerate kinase I |
| PI3K | Phosphoinositol 3-kinase |
| PKA | cAMP-dependent kinase |
| PKC | Protein kinase C |
| PMSF | Phenylmethylsulfonyl fluoride |
| PSD | Postsynaptic density |
| PSD-93 | Postsynaptic density protein 93 (a.k.a. chapsyn 110) |
| PSD-95 | Postsynaptic density protein 95 |
| RACE | Rapid amplification of cDNA ends |
| RSK | Ribosomal protein S6 kinase |
| RT | Room temperature |
| SAP90 | Synapse associated protein 90 (a.k.a. PSD-95) |
| SAP97 | Synapse associated protein 97 |
| SAP102 | Synapse associated protein 102 |
| SDS | Sodium dodecylsulphate |
| SH3 | Src homology 3 |
| SSR | Subsynaptic reticulum |
| Tet | Tetracycline |
| tetO | tetracycline resistance operon |
| tk | Thymidine kinase |
| tTA | Tetracycline-controlled transcriptional activator |

| | |
|---|---|
| uORF | Upstream open reading frame |
| UTR | Untranslated region |

Amino acid single letter code:

| | | | |
|---|---|---|---|
| A | Alanine | M | Methionine |
| C | Cysteine | N | Asparagine |
| D | Aspartate | P | Proline |
| E | Glutamate | Q | Glutamine |
| F | Phenylalanine | R | Arginine |
| G | Glycine | S | Serine |
| H | Histidine | T | Threonine |
| I | Isoleucine | V | Valine |
| K | Lysine | W | Tryptophan |
| L | Leucine | Y | Tyrosine |

# Abstract

PSD-95 is a synaptic adaptor molecule that binds a wide range of proteins, including transmembrane receptors and channels, signalling molecules and adhesion proteins to form a large multiprotein complex. PSD-95 has been implicated in a number of NMDA receptor dependent processes including excitotoxicity, spinal hyperalgesia and learning and memory, and our understanding of these processes has been advanced by the generation of a PSD-95 mutant mouse. However, this conventional knockout mutation did not allow spatial or temporal control over gene inactivation, properties that would enable better dissection of PSD-95's role in behavioural responses such as learning and anaesthesia. The aim of this thesis was therefore to characterise the *PSD-95* locus and generate a conditional allele of PSD-95 such that the gene could be deleted in specific brain regions, ideally with temporal control.

Murine *PSD-95* consists of 23 exons spanning 27kb of genomic sequence, with similar organisation and identical intron-exon boundaries to the human homologue, *DLG4*. Additionally, a novel mouse splice variant and an alternative transcriptional start site were identified, indicating a greater potential variety in PSD-95 protein structure. The generation of a conditional allele, using Cre-loxP technology is also described, including generation of the targeting construct and embryonic stem cell targeting.

The volatile anaesthetic halothane has been reported to bind PSD-95. To explore the role of PSD-95 in anaesthesia, the halothane sensitivity of PSD-95 mutant mice was tested using a behavioural test. Halothane dose response curves generated for PSD-95 mutants and wild type littermates demonstrated a reproducible increase in sensitivity to halothane in PSD-95 mutant mice, while association of PSD-95 with ion channels was unaffected.

# Table of Contents

# Chapter 1: INTRODUCTION

The functioning of the brain requires the electrical activity of neurons and the chemical transmission (called neurotransmission) of information between neurons. Neurons are bipolar in structure, forming dendritic and axonal processes that receive and transmit information respectively. The branched structure of dendrites and axons enables neurons to form numerous connections such that a single neuron can receive information from many thousands of others. Neurons are able to integrate and modulate this large input of information, and the connections between neurons may be important sites for such modulation.

The connections between neurons are called synapses and the structure of a synapse is shown in the electron micrograph and simple schematic in figure 1.1. Vesicles containing neurotransmitters are clustered at the presynaptic active site and electrical activity in the presynaptic neuron stimulates the release of neurotransmitter from these vesicles. In close apposition to the presynaptic active site is the postsynaptic membrane, where neurotransmitter receptors are clustered. Release of neurotransmitter into the synapse will activate the postsynaptic receptors, transmitting information to the postsynaptic cell. The short distance between neurons at synapses and the juxtaposition of release and receptive sites allows the very rapid transmission of information between neurons that is essential for brain function.

In addition to the clustering of neurotransmitter receptors at synapses, many cytoplasmic proteins are also enriched at these sites and some, such as postsynaptic density protein 95 (PSD-95), are directly associated with neurotransmitter receptors (Kornau *et al.* 1995). PSD-95 is important in modulating the strength of signal transmitted to the postsynaptic cell and in learning and memory (Migaud *et al.* 1998). This protein has therefore attracted considerable attention and is the focus of this thesis.

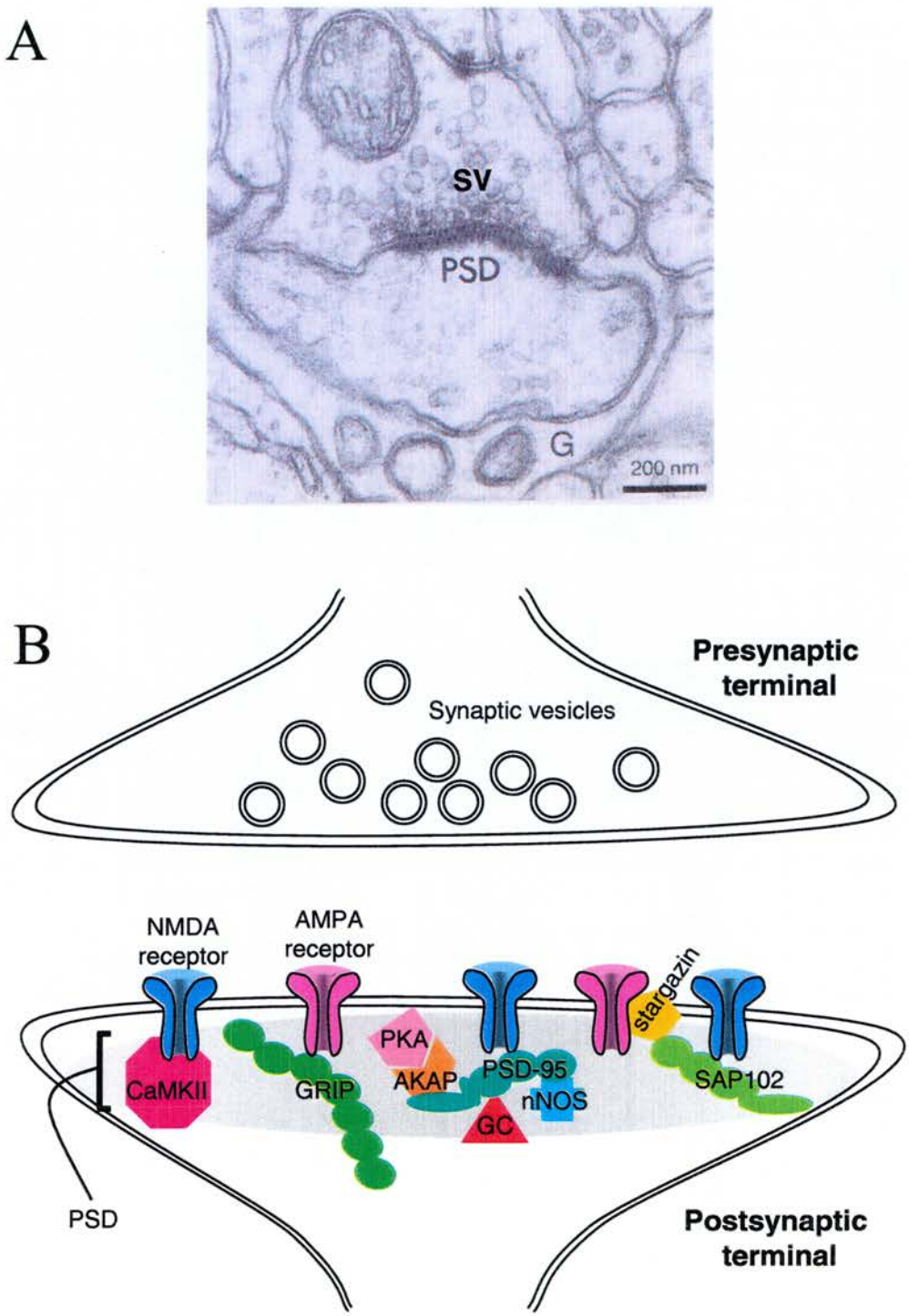


**Figure 1.1 Structure of excitatory synapses.** ***A.*** Electron micrograph of an excitatory synapse showing synaptic vesicles (SV) clustered at the presynaptic terminal and the postsynaptic density (PSD) just below the postsynaptic membrane. Picture adapted from Cowan *et al.,* 2001 ***B.*** Schematic representation of an excitatory synapse showing postsynaptic NMDA and AMPA receptors associated with some of their known binding partners: CaMKII, PSD-95 or SAP102 can bind NMDA receptors. GRIP and stargazin interact with AMPA receptors, stargazin also being capable of binding SAP102 or PSD-95. Adaptor proteins such as GRIP, SAP102 and PSD-95 are capable of multiple interactions, as shown by PSD-95 binding nNOS, guanylyl cyclase (GC) and AKAP. AKAP in turn can interact with PKA. It should be noted that this depiction of interactions is far from exhaustive.

While it is clear that neurotransmitters activate postsynaptic receptors, the complex molecular events triggered by receptor activation are less well understood. The cytoplasmic proteins associated with synapses are therefore of great interest. The synapse-associated cytoplasmic proteins form an organised network beneath the postsynaptic membrane, interacting with surface receptors, ion channels and adhesion molecules as well as cytoplasmic adaptor proteins, signalling molecules and cytoskeletal components (Kennedy 1997; Garner *et al.* 2000). The density of the clustered postsynaptic proteins is such that it appears as a dark strip along the postsynaptic membrane in the electron micrograph and is termed the postsynaptic density (PSD; Fig. 1.1). The PSD was first observed at excitatory synapses by Palay and Gray (Palay 1958; Gray 1959), however the constituents of the PSD were to remain a matter of conjecture until a method for its purification by subcellular fractionation was developed (Cotman *et al.* 1974; Cohen *et al.* 1977).

To better understand the molecular composition and function of the PSD, Cotman and colleagues identified a 95 KDa antigen in the PSD, termed PSD-95 (Nieto Sampedro *et al.* 1981). The PSD-95 antibodies also recognised a 95 KDa antigen in synaptic junction preparations from numerous other species from sharks to mammals (Nieto Sampedro *et al.* 1982), suggesting an important, conserved role for PSD-95 at the synapse. This was further supported by evidence that PSD-95, in addition to the PSD, was lost from deafferented synapses (Nieto Sampedro *et al.* 1982).

In 1992, rat cDNA encoding a protein with the same electrophoretic mobility as PSD-95 was independently cloned by two groups and referred to as PSD-95 and SAP90 respectively (Cho *et al.* 1992; Kistner *et al.* 1993). PSD-95/SAP90 was found to be homologous to the product of a *Drosophila* tumour suppressor gene, *dlg* (Woods and Bryant 1991), a protein present at epithelial septate junctions and neuromuscular synaptic junctions (NMJ) (Woods and Bryant 1991; Lahey *et al.* 1994). The conservation of this gene between fly and rat allowed some functions for PSD-95/SAP90 to be inferred from studies of the neuronal phenotype of *dlg* mutant flies.

## 1.1 Drosophila Discs large (DLG)

The *Drosophila dlg* locus was first identified in 1972 as *lethal(1)discs large-1*, a recessive oncogenic mutation (Stewart *et al.* 1972) and subsequently cloned in 1989 (Woods and Bryant 1989) . Mutation of *dlg* produced neoplastic growth of the imaginal discs and abnormal development of septate and synaptic junctions (Woods and Bryant 1991; Lahey *et al.* 1994; Budnik *et al.* 1996; Woods *et al.* 1996). Comparisons between *Drosophila* DLG (Woods and Bryant 1991) and the mammalian proteins PSD-95 and zona occludens-1 (ZO 1), associated with neuronal synaptic junctions and tight junctions respectively (Cho *et al.* 1992; Kistner *et al.* 1993; Willott *et al.* 1993), identified three repeated domains in their N-terminal sequence, termed PDZ (PSD-95, DLG, ZO-1) domains. DLG, ZO-1 and PSD-95 also all contained an SH3 domain and an enzymatically inactive guanylate kinase (GK) homology domain (Kistner *et al.* 1995; Kuhlendahl *et al.* 1998), and were categorised as a new protein family: the membrane associated guanylate kinases (MAGUKs).

Compared to other MAGUKs, DLG contains an extended linker sequence between the SH3 and GK domains, termed the HOOK domain. Expression of deletion constructs in *Drosophila* indicated that correct localisation of DLG requires the presence of the HOOK and GK domains in addition to either PDZ 1 or 2 (Hough *et al.* 1997; Thomas *et al.* 2000). However, DLG localisation only required the GK domain in the absence of endogenous DLG (Thomas *et al.* 2000), suggesting wild type DLG can traffic GK-deleted DLG to the NMJ through direct or indirect association. Due to the known role of calcium-calmodulin dependent kinase II (CaMKII) in the regulation of *Drosophila* synaptic development (Wang *et al.* 1994) and behavioural plasticity (Griffith *et al.* 1993), studies were performed to determine the effect of CaMKII on DLG localisation. Expression of a constitutively active CaMKII mutant (T287D) reduced DLG staining at NMJ synapses while expression of a CaMKII inhibitory peptide enhanced DLG localisation to synaptic boutons (Koh *et al.* 1999).

DLG is required for correct localisation of the Shaker potassium channel and the cell adhesion molecule FASII to the NMJ synapse (Thomas *et al.* 1997), both of which DLG

binds (Tejedor *et al.* 1997; Thomas *et al.* 1997; Zito *et al.* 1997). NMJ synaptic development is regulated by the amount of FASII at the synapse. In the $fas^{e86}$ and $fas^{e76}$ hypomorphs, synaptic FASII is respectively ~50% and ~10% that of wild type animals yet the number of synaptic boutons are increased and decreased respectively (Schuster *et al.* 1996). In CaMKII T287D mutant flies, the induced DLG relocation also results in dispersion of FASII from the synapse (Koh *et al.* 1999). Combined these data suggest that regulation of FASII levels at synaptic boutons via CaMKII mediated DLG dispersal may be one mechanism for the action of CaMKII in *Drosophila* synaptic plasticity.

## 1.2 Mammalian Neuronal MAGUKs

In mammals, gene duplication has distributed the roles of DLG across a large number of MAGUKs. Located at tight junctions, thought to be the mammalian equivalent of the *Drosophila* septate junction, are zona occludens-1, -2 and -3 (Stevenson *et al.* 1986; Jesaitis and Goodenough 1994; Haskins *et al.* 1998), while in the central nervous system (CNS) four related MAGUKs were identified: synapse associated protein 97 KDa (SAP97; Muller *et al.* 1995)/ human discs large (hDLG; Lue *et al.* 1994); synapse associated protein 102 KDa (SAP102; Muller *et al.* 1996)/neuronal and endocrine dlg (NE-dlg; Makino *et al.* 1997); channel-associated protein of synapses-110 KDa (chapsyn-110; Kim *et al.* 1996)/postsynaptic density protein 93 KDa (PSD-93; Brenman *et al.* 1996a) and postsynaptic density protein 95 KDa (PSD-95; Cho *et al.* 1992)/synapse associated protein 90KDa (SAP90; Kistner *et al.* 1993). For simplicity, these proteins will be referred to as SAP97, SAP102, chapsyn-110 and PSD-95 respectively.

The PSD-95, SAP102, chapsyn-110 and SAP97 have been shown to bind a wide range of important synaptic proteins including the NR2 subunits of the N-methyl-D-aspartate (NMDA) receptor (Kornau *et al.* 1995; Muller *et al.* 1996; Niethammer *et al.* 1996), neuronal nitric oxide synthase (nNOS; Brenman *et al.* 1996a; Brenman *et al.* 1996b) and cytoskeletal proteins such as protein 4.1 (Lue *et al.* 1994) and MAP1A (Brenman *et al.* 1998). They form multifunctional complexes that can influence processes as diverse as synaptic plasticity (Migaud *et al.* 1998) and cell cycle progression (Ishidate *et al.* 2000).

Analyses of the tissue distribution pattern of the CNS MAGUKs identified PSD-95 as nervous system specific in the adult (Cho *et al.* 1992; Kistner *et al.* 1993; Muller *et al.* 1996), while chapsyn-110 message was identified in the embryonic thymus and submandibular gland in addition to the nervous system (Brenman *et al.* 1996a). SAP102 message was observed in brain, spinal cord, pancreas, thyroid, trachea and prostate (Makino *et al.* 1997) while SAP97 message had the widest distribution, being found in adult brain, heart, spleen, lung, liver, muscle, kidney, placenta, pancreas and testes (Lue *et al.* 1994; Muller *et al.* 1995; McLaughlin *et al.* 2002). Western blotting confirmed the presence of SAP97 in brain, muscle, liver and heart (Muller *et al.* 1995), and SAP97 was shown to co-immunoprecipitate with the inward rectifier potassium channel Kir2.2 in the heart (Leonoudakis *et al.* 2001).

Further interest in SAP97 was generated when its interaction with the tumour suppressor adenomatosis polyposis coli (APC) protein was discovered (Matsumine *et al.* 1996). Overexpression of SAP97 or APC in NIH3T3 cells blocked cell cycle progression, while mutation of any one domain in SAP97 or deletion of the C-terminal PDZ binding motif of APC blocked their activity (Ishidate *et al.* 2000). SAP97 was further implicated in tumour suppression when two groups showed human adenovirus and human papillomavirus (HPV) oncoproteins to bind the PDZ domains of SAP97 (Kiyono *et al.* 1997; Lee *et al.* 1997), and that the C-terminal PDZ recognition motif of HPV 16E6 protein was required for morphological and tumourigenic transformation of transfected cell lines (Kiyono *et al.* 1997).

The mouse *SAP97* gene was mutated by the insertion of a gene trap vector (Caruana and Bernstein 2001). Gene trap vectors are promotorless, so selected clones result from the gene trap vector inserting into an endogenous gene that drives expression of the selection cassette. This event necessarily interrupts the endogenous gene, resulting in a truncation of the endogenous transcript. The *SAP97* gene trap mutant produces a fusion protein of SAP97 PDZ domain 1, 2 and 3 and β-geo, therefore lacking the SH3 and GK domains (Caruana and Bernstein 2001). Although truncation of the GK domain in

*Drosophila dlg* mutants results in neoplasia (Woods *et al.* 1996), *SAP97* gene trap mutants displayed a mildly retarded growth *in utero* instead of an overgrowth phenotype (Caruana and Bernstein 2001). The perinatal lethality of the *SAP97* gene trap mutant (Caruana and Bernstein 2001) precluded further analyses of the tumour suppressor activity of SAP97 in these animals, though it should be noted that SAP97 and SAP102 could rescue both the neoplasia and NMJ abnormalities in *dlg Drosophila* mutants when overexpressed at sufficiently high levels (Thomas *et al.* 1997).

These studies demonstrate some similarity in function between *Drosophila* and mammalian MAGUKs, however, MAGUKs also display specificity for certain ligands, for example, specific PDZ-mediated interactions have been observed between the AMPA GluR1 subunit and SAP97, but not SAP102 or PSD-95 (Leonard *et al.* 1998). Further specificity is likely achieved by differential distribution of the MAGUKs and functional variety engendered by splice variants.

### 1.2.1 Splice Variants

*PSD-95*, *SAP97*, *SAP102* and *chapsyn-110* all generate alternative isoforms, as indicated in figure 1.2. *SAP102* transcripts have been reported to include 2 insertions: I1, an 18aa insertion prior to PDZ1, and I2, a 14aa insertion between the SH3 and GK domains (Muller *et al.* 1996). Chapsyn-110 can contain three alternate splice insertions at 2 sites, a 52aa insertion between PDZ2 and 3 and a 34aa or 15aa insertion between the SH3 and GK domians. Additionally, four chapsyn-110 cDNA clones were identified with distinct 5' sequences leading to the utilisation of four different translation initiation methionines (Brenman *et al.* 1996a). Utilisation of alternative transcriptional start sites by *PSD-95* produces distinct N-termini (PSD-95α and PSD-95β) (Chetkovich *et al.* 2002). Finally, SAP97 can contain five different insertions at three sites: I1A (33aa) and/or I1B (18aa) insert before PDZ1; I2 (12aa) and/or I3 (34aa) insert at one site between the SH3 and GK domains, I5 (13aa) and I4 (13aa) insert between SH3 and GK domains at sites progressively more C-terminal from the I2/I3 site (Lue *et al.* 1994; Mori *et al.* 1998; McLaughlin *et al.* 2002).

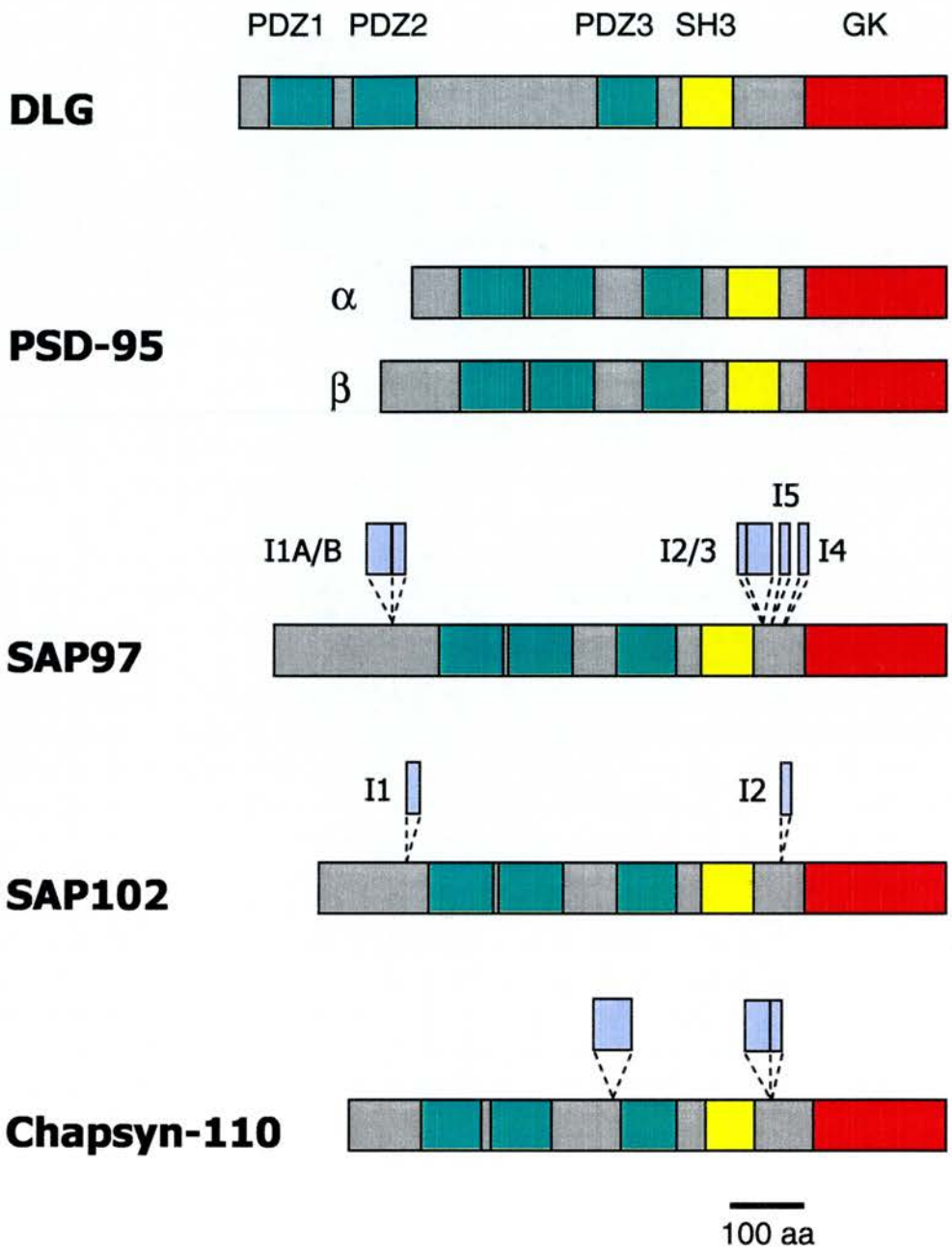


**Figure 1.2 Organisation of MAGUK domains and alternate variants.** Proteins are drawn to scale and show PDZ domains (green), SH3 domains (yellow), GK domains (red) and alternate splice insertions (blue). Also shown are PSD-95α and β variants resulting from alternate transcriptional start sites. Chapsyn-110 variants resulting from alternate transcriptional start sites are not shown.

In some instances these diverse splice isoforms have been show to engender functional differences. Inclusion of SAP97 I3 versus I2 results in differential cellular localisation. I3 promotes localisation to sites of cell-cell contact when expressed as an SH3-I3-GK fusion protein in epithelial cells or colon carcinoma CX-1 cells (Lue *et al.* 1996), while the I2 insertion showed no preferential localisation in these cells (Lue *et al.* 1996). However, immunostaining for I2 variants transfected into the human epithelial MCF10F cell line indicated an enrichment in the nucleus (McLaughlin *et al.* 2002). Another MAGUK, CASK, has been shown to bind the transcription factor Tbr-1 and activate transcription in neurons (Hsueh *et al.* 2000). Combined, these data suggest that a subclass of MAGUK proteins may be involved in transcriptional regulatory events, and that this specificity may be gained via regulated splicing.

Other variants produce differential binding activities. For example, the SAP97 I1A+B variant conferred SH3 binding activity through insertion of proline-rich sequences (McLaughlin *et al.* 2002) while the PSD-95β variant, which makes up ~10% of expressed PSD-95 protein, encodes a unique N-terminus containing an L27 motif that enables PSD-95β to bind CASK (Chetkovich *et al.* 2002).

## 1.2.2 MAGUK Localisation in the Brain

### *1.2.2.1 Developmental Distribution of MAGUK mRNAs*

*In situ* analysis of developing mouse brain showed overall similarities in the expression patterns of MAGUKs (Fukaya *et al.* 1999). PSD-95 and SAP102 were widely expressed at the earliest time point analysed, E13. Chapsyn-110 expression was weak at E15, stronger from E18 and highly restricted to the telecephalon. SAP102 expression remained relatively uniform through development, however, PSD-95 appeared more dynamic, with expression levels briefly dipping at P1/P7 followed by a large increase in expression at P14 (Fukaya *et al.* 1999). *In situ* analysis has not been performed for SAP97 transcripts, however postnatal Northern analysis of SAP97 showed a 4.9kb transcript present at P1 that reached peak levels at P15 and a 4.4kb transcript that appears abruptly at P15, then declined to P75 (Muller *et al.* 1995). Utilising the SAP97-βGeo fusion protein in SAP97 gene trap mice, a snapshot of embryonic development

was provided by lacZ staining that detected signal in hippocampus and cerebellum at E10.5 (Caruana and Bernstein 2001). During postnatal development, SAP102 protein levels decline while PSD-95 protein levels rise. These changes are associated with decreased SAP102 synaptic staining with increased PSD-95 staining (Sans *et al.* 2000).

#### *1.2.2.2 Regional distribution of MAGUK Proteins*

Immunohistochemical studies in adult rat and mouse brain have shown PSD-95, SAP97, SAP102 and chapsyn-110 to have predominantly overlapping distributions, all being expressed in cortex, hippocampus, olfactory bulb, caudate putamen and cerebellum (Muller *et al.* 1995; Fukaya and Watanabe 2000). However, differences were observed in the thalamic nuclei, where immunohistochemical reactivity was strong for SAP102, weak for PSD-95 and not detected for chapsyn-110 and SAP97. In addition, PSD-95 immunoreactivity was intense in the pinceau formation around the Purkinje cell axon hillock in the cerebellum. Only chapsyn-110 stained Purkinje cells (Fukaya and Watanabe 2000).

#### *1.2.2.3 Subcellular Localisation*

Immunofluorescent staining of the MAGUKs occurs as bright puncta, indicative of an enrichment at synapses. PSD-95 immunofluorescent staining in cultured neurons (Kornau *et al.* 1995) and brain slices (Cho *et al.* 1992; Fukaya and Watanabe 2000) was enriched at dendritic spines and, exhibited co-localisation with NMDA receptors (Kornau *et al.* 1995; Fukaya and Watanabe 2000) and synaptophysin (Fukaya and Watanabe 2000), although fainter, diffuse staining was also observed throughout dendrites consistent with extrasynaptic PSD-95. Despite their synaptic enrichment, electron microscopy studies of PSD-95, chapsyn-110, SAP97 and SAP102 localisation indicates their presence at both pre- and postsynaptic sites, and at extrasynaptic locations, predominantly dendritic shafts (Brenman *et al.* 1998; El-Husseini *et al.* 2000; Aoki *et al.* 2001; Sans *et al.* 2001). Earlier reports described a much more restricted distribution of the MAGUKs (Muller *et al.* 1995; Brenman *et al.* 1996a; Kim *et al.* 1996; Muller *et al.* 1996), a result likely explained by the lower resolution of the techniques utilized. The later studies reported cytoplasmic PSD-95, chapsyn-110 and SAP97 staining associated with the endoplasmic reticulum (El-Husseini *et al.* 2000;

Aoki *et al.* 2001; Sans *et al.* 2001), raising the possibility that MAGUKs regulate processing or membrane delivery of associated receptors. Indeed, SAP97 has already been shown to preferentially associate with immature, endoplasmic reticulum localised AMPA receptors (Sans *et al.* 2001).

In summary, PSD-95, SAP97, SAP102 and chapsyn-110 are enriched at synapses where they cluster synaptic proteins, but their presence in other cellular compartments implies a more diverse role including processes such as protein trafficking (Sans *et al.* 2001).

## 1.3 PSD-95

The abundance of PSD-95 at the PSD suggested that PSD-95 might have a key role in the organisation and colocalisation of the numerous classes of proteins present at the synapse.

### 1.3.1 Structure of Binding Domains

Sequences within the protein domains of MAGUKs are relatively well conserved and therefore are likely to employ similar binding mechanisms. The 724 amino acids comprising PSD-95 contain three PDZ domains (amino acids 65-151; 160-246; 313-393), an SH3 domain (amino acids 428-498) and a GK domain (amino acids 534-724). The structures of all PSD-95 domains have been determined, the PDZ domains as individual units while the SH3 and GK domain structure was solved as a single module.

#### *1.3.1.1 PDZ Domains*

The structures of the PSD-95 PDZ domains have been resolved in complex with ligands (Doyle *et al.* 1996; Tochio *et al.* 2000; Piserchio *et al.* 2002). These structures, in concert with the structures of related PDZ domains (Morais-Cabral *et al.* 1996; Hillier *et al.* 1999), provided an insight into how ligand selectivity between PDZ domains was achieved. The PDZ domain was found to be globular and compact, made up of two α helices (αA-B) and a beta sandwich consisting of 5 β sheets (βA-E). Ligands occupied a groove on the surface of the PDZ domain and a hydrophobic pocket (Fig. 1.3A). The groove was formed between strand βB and helix αB while the hydrophobic pocket was

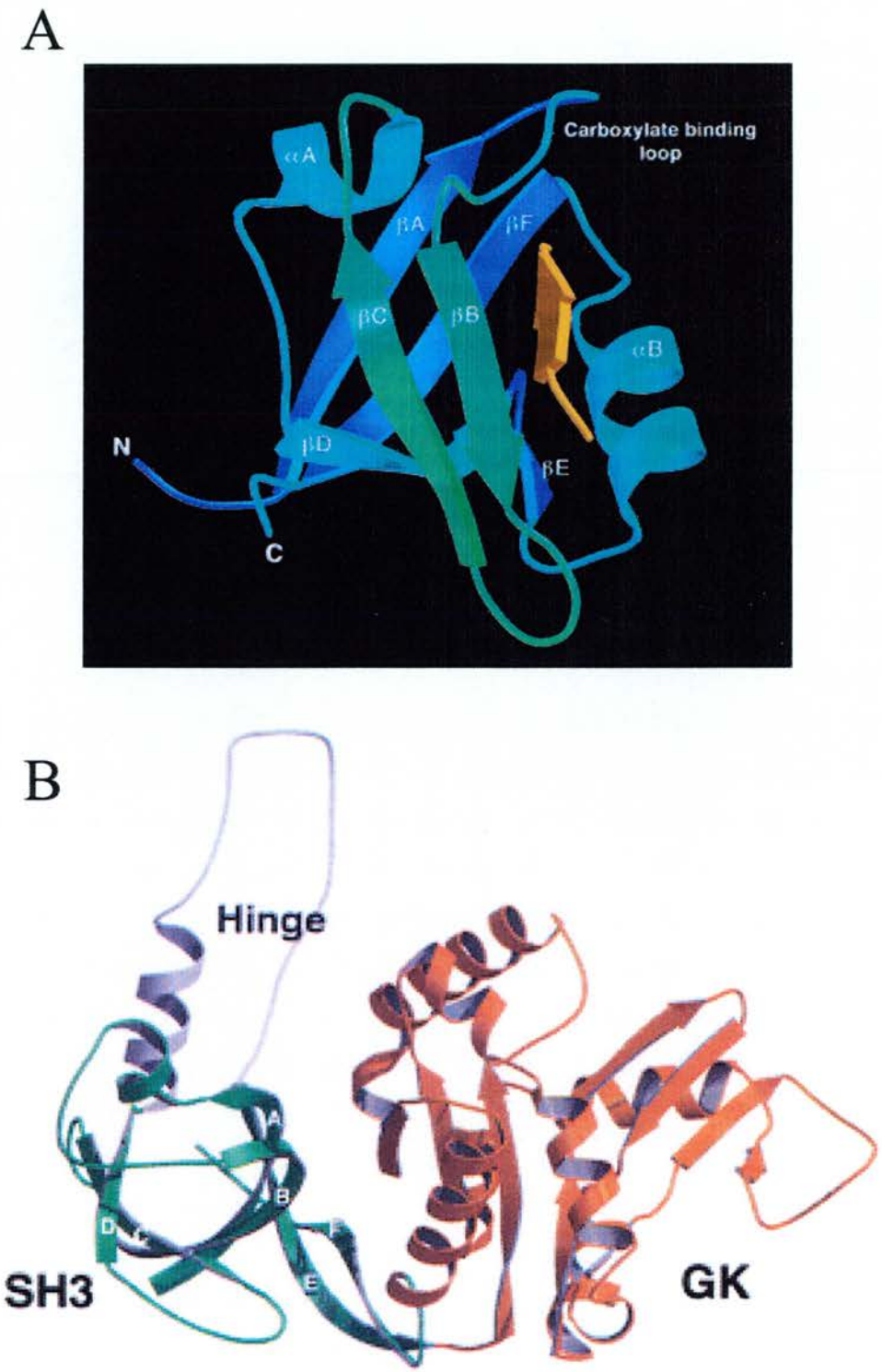


**Figure 1.3 Structure of PSD-95 domains.** ***A.*** Ribbon diagram of PSD-95 PDZ3 complexed with a peptide ligand (yellow). The peptide ligand occupies a groove between strand βB and helix αB and the hydrophobic pocket (or carboxylate binding loop) formed by the βA-βB loop. Diagram from Doyle *et al.*, 1996. ***B.*** Ribbon diagram of the SH3 (green), GK domain (orange) and hinge (or hook) region (grey) that links the SH3 and GK domains. Diagram from McGee *et al.*, 2001.

formed by the βA-βB loop that contains the signature GLGF motif of PDZ domains and side chains from the β2 strand and α2 helix.

Two types of ligand have been identified for PDZ domains. By far the most common ligand type, the C-terminal ligand, interacted via the final residues of the extreme C-terminus and required the interaction of the terminal carboxylate group with the PDZ domain. The second ligand type, the internal ligand, involved the binding of an antiparallel β finger to the PDZ domain (Fig. 1.4). This ligand did not involve interaction of C-terminal sequences.

For C-terminal ligand binding, the terminal hydrophobic side chain (valine/isoleucine) occupied the hydrophobic pocket with the terminal carboxyl group forming hydrogen bonds with main chain amides of the GLGF sequence and a water molecule associated with a conserved arginine, also in the βA-βB loop (Doyle *et al.* 1996; Tochio *et al.* 2000; Piserchio *et al.* 2002). The rest of the C-terminal ligand lay in the groove in a highly ordered state, stabilised by interactions between the ligand main chain and residues forming the groove (Doyle *et al.* 1996), although these interactions would not contribute to specificity.

The last three residues of the ligand appear the most important in binding PDZ domains and not surprisingly, they form clear interactions with PDZ domains in X-ray and NMR studies. In PSD-95 PDZ1, a smaller hydrophobic domain was noted (Piserchio *et al.* 2002), consistent with its preference for a terminal valine instead of larger leucine or isoleucine side chains. Preferences at the –1 position are determined by the second residue in βB. A serine at this position in PDZ1 and PDZ2 (Tochio *et al.* 2000; Piserchio *et al.* 2002) requires negatively charged ligand side chains (aspartate or glutamate) while an asparagine in PDZ3 prefers serine or threonine side chains at –1 (Doyle *et al.* 1996). The permitted residues at the –2 position are conserved across PDZ domains, however different mechanisms for binding the –2 residue appear to be employed between the three PDZ domains of PSD-95. The threonine side chain at the –2 position of the peptide used by Doyle and co-workers (Doyle *et al.* 1996), formed a

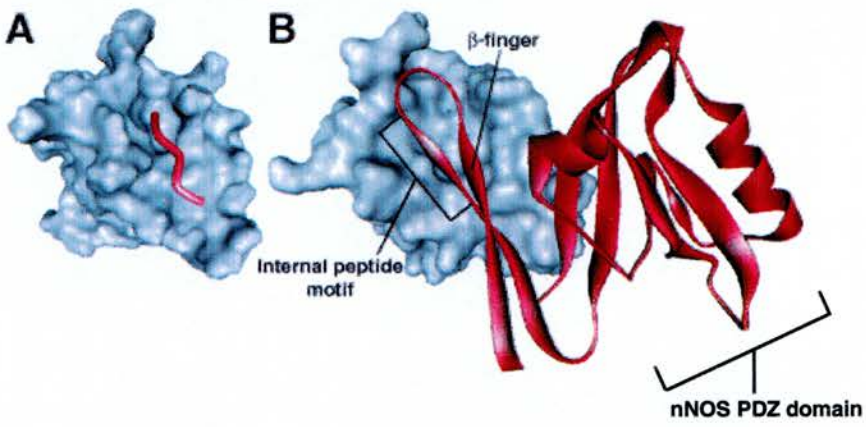


**Figure 1.4 Comparison of C-terminal and internal ligand binding to PDZ domains**. ***A.*** Space-filling diagram of the α1-syntrophin PDZ domain (grey) showing a complexed C-terminal ligand (red). ***B.*** The α1-syntrophin PDZ domain complexed with an internal ligand. The β finger internal ligand and PDZ domain of nNOS is shown in red. The catalytic domain of nNOS, C-terminal to the β finger, is omitted. Diagram adapted from Harris and Lim, 2001.

hydrogen bond with a conserved histidine at the N-terminal end of αB in PDZ3. In contrast, Piserchio and colleagues (Piserchio *et al.* 2002) described the –2 serine present in three C-terminal ligands, derived from Kv1.4, CRIPT and GluR6, to bind an asparagine in the βB-βC loop of PDZ1, close in space to the conserved histidine. However, binding of the –2 residue in PDZ2 may involve both asparagine and histidine residues (Tochio *et al.* 2000; Piserchio *et al.* 2002) and interestingly, the asparagine is contained in a 6aa insertion between βB and βC, present in PDZ1/2 but absent from PDZ3. Differences observed between PDZ1/2 and PDZ3 ligand specificities can therefore be explained to some extent by the substitutions of specific residues, however these studies have been unable to address the preferences observed at more N-terminal residues of the ligand.

In addition to binding C-terminal ligands, the PDZ domains of PSD-95, chapsyn-110, syntrophin and InaD are capable of binding internal ligands (Brenman *et al.* 1996a; Brenman *et al.* 1996b; van Huizen *et al.* 1998; Xu *et al.* 1998), although only the structure of the nNOS-syntrophin interaction has been studied (Hillier *et al.* 1999; Fig. 1.4). The key question was how an internal sequence could overcome the requirements for C-terminal binding. In nNOS, a 30aa sequence just C-terminal to the PDZ domain, but N-terminal to its catalytic domain, made up the internal PDZ binding motif and formed a β-hairpin 'finger' (βG-H). The β finger demonstrated remarkable stability, adopting the same structure in both bound and unbound forms, and crucial to this stability was the interaction between an arginine in βH of theβ finger and an aspartate in the nNOS PDZ domain that pinned the two β strands into a hairpin (Hillier *et al.* 1999). The ...LETTF... sequence within the β finger mimicked the ...S/TXV/I PDZ recognition motif and on invasion of the binding groove, appropriate interactions were formed and the phenylalanine side chain occupied the hydrophobic pocket (Hillier *et al.* 1999).

These structure studies have therefore provided useful information for explaining the mechanisms of binding and the variable specificity of both ligands and PDZ domains.

In particular, how an internal motif can utilise a binding domain that appears to specialise in binding C-termini.

#### *1.3.1.2 SH3-GK Module*

Crystal structures of the PSD-95 SH3-GK module (Fig. 1.3B) were published independently by two groups (McGee *et al.* 2001; Tavares *et al.* 2001) and displayed a surprising topology. Although the SH3 and GK domains showed similar organisation to their homologues, a number of differences in both domains explained their divergence in function from canonical SH3 and GK domains.

Conventional SH3 domains are made up of 5 contiguous antiparallel β strands (reviewed by Cohen *et al.* 1995) whereas the PSD-95 SH3 domain was found to consist of six non-contiguous β strands (βA-F). Strands βA-D were contained in the SH3 homologous sequence, while βE was separated from βA-D by the HOOK domain and from βF, contained in the C-terminus, by the GK domain. The C-terminal βF thus emerged from the GK domain to form an anti-parallel β sheet with βE, which, in concert with βA-D, formed the SH3 hydrophobic core. The PSD-95 SH3 domain therefore differed from conventional SH3 domains by the use of non-contiguous sequences, the presence of an extra β strand and the replacement of the crucial polyproline recognition site, usually between βD and βE, by the HOOK domain (McGee *et al.* 2001; Tavares *et al.* 2001). In addition, certain residues important for polyproline binding are missing from the PSD-95 SH3 domain, however, polyproline-mediated binding of KA2 and MLK is still observed (Garcia *et al.* 1998; Savinainen *et al.* 2001).

The PSD-95 GK domain, like conventional guanylate kinases, consisted of three structural components: a CORE made up of five parallel β strands (β6, β7, β12, β13 and β14) and six α helices (α2, α4, α5, α6, α7 and α8); a GMP binding domain composed of β8, β9, α3, β10 and β11; and a LID that was formed by the α6-α7 loop (Tavares *et al.* 2001). The lack of kinase activity in PSD-95 can be explained by sequence analysis that shows the absence of residues critical for ATP binding (Kistner *et al.* 1995). In

| PDZ1 | PDZ2 | PDZ3 | SH3 | GK |
|---|---|---|---|---|
| GluR6 [#] (Garcia *et al.* 1998) | NR2A, NR2D [*] (Kornau *et al.* 1995) | Neuroligin [*] (Irie *et al.* 1997) | KA2 [+] (Garcia *et al.* 1998) | KA2 [+] (Garcia *et al.* 1998) |
| | NR2B [* #] (Kornau *et al.* 1995) | CRIPT [* @] (Neithammer *et al.* 1998) | Huntingtin [#] (Sun *et al.* 2001) | BEGAIN [#] (Deguchi *et al.* 1998) |
| Cypin [$] (Firestein *et al.* 1999) | Cypin [$] (Firestein *et al.* 1999) | β1 Adrenergic receptor [@] (Hu *et al.* 2000) | AKAP 79 [+] (Colledge *et al.* 2000) | AKAP 79 [+] (Colledge *et al.* 2000) |
| ErbB4 [*] (Huang *et al.* 2000) | ErbB4 [*] (Huang *et al.* 2000) | Citron [*] (Zhang *et al.* 1999) | AKAP 150 [$] (Colledge *et al.* 2000) | AKAP 150 [$] (Colledge *et al.* 2000) |
| KIF1Bα [*] (Mok *et al.* 2002) | KIF1Bα [*] (Mok *et al.* 2002) | α2 Guanylyl cyclase [$] (Russwurm *et al.* 2001) | MLK2 & MLK3 [* #] (Savinainen *et al.* 2001) | GKAP [* @] (Kim *et al.* 1997) |
| | Kir3.2c [#] (Hibino *et al.* 2000) | | | SPAR [*] (Pak *et al.* 2001) |
| | nNOS [*] (Brenman *et al.* 1996b) | | | |

**Table 1.1 PSD-95 domain binding preferences.** For each domain of PSD-95, the name of the preferentially interacting protein and the reference in which preferential binding was demonstrated is shown. Superscript notes appended to references document the methods used in determining protein interactions ([*] = yeast two-hybrid, + = binding of recombinant proteins, @ = blot overlay binding, # = IP or fusion protein binding on affinity column using protein expressed in heterologous cells, [$] = protein from brain homogenate binding to fusion protein on affinity column).

addition, Tavares and co-workers failed to observe a large conformational change upon binding of GMP to the GK domain (Tavares *et al.* 2001), which in yeast guanylate kinase moves the GMP binding site towards the active site of the enzyme and enables the access of ATP (Blaszczyk *et al.* 2001).

### 1.3.2 Binding Partners

Experiments interfering with PSD-95 production have demonstrated its importance in diverse neuronal processes such as synaptic plasticity, learning and memory (Migaud *et al.* 1998), thermal hyperalgesia (Tao *et al.* 2000; Garry *et al.* 2001) and excitotoxicity (Sattler *et al.* 1999; McCulloch *et al.* 2001). A central function of this adaptor molecule is the protein interactions it forms. The five protein-protein interaction domains of PSD-95 enable it to bind a large variety of molecules, presumably in various combinations. For a number of proteins, their exact domain preferences have been documented (Table 1.1).

| Binding protein | PSD-95 | Chapsyn-110 | SAP102 | SAP97 | references |
|---|---|---|---|---|---|
| Kir2.3 | + | + | - | - | Inanobe *et al.*, 2002 $^{\$}$ |
| Kv1.4 | + | + | - | + | Inanobe *et al.*, 2002 $^{\$}$ |
| GluR1 | - | - | - | + | Cai *et al.*, 2002 $^{\$}$ |
| KA2 | + | n/d | + | - | Garcia *et al.*, 1998 $^{IP}$ |
| BAI1 | + | n/d | - | n/d | Lim *et al.*, 2002 $^{IP}$ |
| Kir5.1 | + | n/d | n/d | - | Tanemoto *et al.*, 2002 $^{IP}$ |

**Table 1.2 MAGUK binding preferences for associated proteins.** Binding is designated by +, absence of binding is designated -, and n/d signifies that the interaction was not tested. Brain-specific angiogenesis inhibitor 1 is abbreviated BAI1. Superscript notes appended to references document the methods used in determining protein interactions ( $^{\$}$ = protein from brain homogenate binding to fusion protein on affinity column, $^{IP}$ = immunoprecipitation from brain homogenate).

As all MAGUKs contain these protein binding domains, how specific interactions are determined is an important question. Differential interactions between ligands and MAGUKs (Table 1.2) can be determined by binding specificity, but also by differential distributions of MAGUK and ligand. This is exemplified by the NMDA receptor, which binds all MAGUKs *in vitro* (Inanobe *et al.* 2002), yet SAP97 could not be co-

immunoprecipitated with NMDA receptor subunits from brain preparations (Wyszynski *et al.* 1997), consistent with the preferential intracellular localisation of SAP97 (Sans *et al.* 2001). However, binding preferences must certainly influence associations.

#### *1.3.2.1 PDZ Domain Binding Preferences*

Although the three PDZ domains share considerable homology, it is clear they differ in their binding preferences which, to some extent, have been defined. Binding to PDZ domains is generally mediated by the extreme C-terminus of ligands, nNOS being the exception, which utilises an internal peptide motif. The basic PDZ binding motif (...S/TXV/I where X is any amino acid) requires a hydrophobic C-terminal residue (position 0), such as valine or isoleucine, and either a serine or threonine two positions N-terminal (position -2) to the hydrophobic residue (Table 1.3). Using the yeast two-hybrid system, Niethammer and colleagues (1998) investigated how specificity between PDZ domains within PSD-95 was generated by studying the binding activity of two C-termini, that of the voltage-gated potassium channel, Kv1.4, which binds PSD-95 PDZ1/2, and the C-terminus of CRIPT (cysteine-rich interactor of PDZ3), which binds PSD-95 PDZ3. Systematic mutation of Kv1.4 to CRIPT residues showed that changing binding activity from PDZ3 to PDZ1/2, required only the mutation of residues at the –1 and –3 positions: CRIPT ...QTSV to Kv1.4 ...ETDV. Surprisingly, changing PDZ1/2 to PDZ3 binding required more manipulation, Kv1.4 sequence being exchanged for CRIPT sequence to position –7: ...SNAKAVETDV to ...SNKNYKQTSV (Niethammer *et al.* 1998). Thus, in addition to the basic ...S/TXV/I motif, specificity for distinct PDZ domains requires the use of residues as N-terminal as –7, although more N-terminal residues may engender even greater specificity *in vivo*.

#### *1.3.2.2 SH3 Domain Interactions*

Prototypic SH3 domains (reviewed by Mayer 2001) were first identified as small modules present in divergent signalling molecules that could mediate protein-protein interactions (Cicchetti *et al.* 1992). SH3 domains bind proline-rich regions and require a motif generally described as PXXP, where X is any amino acid (Ren *et al.* 1993; reviewed by Kay *et al.* 2000).

| PSD-95 binding protein | C-terminal sequence | | | | | | | | | | | PDZ domain preference |
|---|---|---|---|---|---|---|---|---|---|---|---|---|
| | -10 | -9 | -8 | -7 | -6 | -5 | -4 | -3 | -2 | -1 | 0 | |
| GluR6 | D | R | R | L | P | G | K | E | T | M | A | 1 |
| Cypin | G | K | Q | V | V | P | F | S | S | S | V | 1 or 2 |
| ErbB4 | P | P | P | Y | R | H | R | N | T | V | V | 1 or 2 |
| KIF1Bα | | | | | A | G | R | E | T | T | V | 1 or 2 |
| Kv1.4 | C | S | N | A | K | A | V | E | T | D | V | 1 or 2 |
| NR2A | Y | K | K | M | P | S | I | E | S | D | V | 2 |
| NR2B | Y | E | K | L | S | S | I | E | S | D | V | 2 |
| NR2D | S | A | H | F | S | S | L | E | S | E | V | 2 |
| Citron | Q | V | N | K | V | W | D | Q | S | S | V | 2 or 3 |
| β1 Adrenergic receptor | G | R | Q | G | F | S | S | E | S | K | V | 3 |
| CRIPT | L | D | T | K | N | Y | K | Q | T | S | V | 3 |
| α2 Guanylyl cyclase | I | G | T | M | F | L | R | E | T | S | L | 3 |
| Neuroligin-1 | P | H | P | H | S | H | S | T | T | R | V | 3 |
| Neuroligin-2 | T | L | P | H | P | H | S | T | T | R | V | 3 |
| Neuroligin-3 | G | L | P | N | S | H | S | T | T | R | V | 3 |

**Table 1.3 C-terminal sequences of PSD-95 PDZ interacting proteins.** Proteins are grouped according to their PDZ binding preference. References demonstrating preferences: GluR6 (Garcia 1998); cypin (Firestein 1999); ErbB4 (Huang 2000); KIF1Bα (Mok 2002); Kv1.4 (Lim 2002); NR2A, B and D (Kornau 1995); citron (Zhang 1999); β1 adrenergic receptor (Hu 2000); CRIPT (Niethammer 1998); α2 guanylyl cyclase (Russwurm 2001); Neuroligin-1, -2 and –3 (Irie 1997).

The PSD-95 SH3 domain binds proteins that contain proline-rich sequences such as mixed lineage kinase (MLK; (Savinainen *et al.* 2001) and the kainate receptor KA2 subunit (Garcia *et al.* 1998), but in addition, it binds protein kinase A (PKA) anchoring proteins 79 and 150 (AKAP 79/150; (Colledge *et al.* 2000), which do not contain the typical SH3 binding motif (...PXXP...). The different binding motifs employed by KA2 and AKAP79 were further highlighted by mutation studies in which a tryptophan required for polyproline binding was mutated to alanine (W470A). This mutation reduced binding of KA2 but had little effect on AKAP79 binding whereas a point mutation (L460P) analogous to the recessive lethal $dlg^{m30}$ *Drosophila* SH3 mutation did ablate AKAP79 binding. The atypical activity of the PSD-95 SH3 domain was clarified when its crystal structure was solved (McGee *et al.* 2001; Tavares *et al.* 2001), described earlier.

#### 1.3.2.3 GK Domain

The MAGUK GK domain is enzymatically inactive (Kistner *et al.* 1995; Kuhlendahl *et al.* 1998) and acts as a protein interaction domain. However, the binding mechanism of the GK domain remains elusive, even though its crystal structure has also been determined (McGee *et al.* 2001; Tavares *et al.* 2001). The only potential binding mechanism, described by Kim and co-workers, required cooperative binding of 14aa repeats in GKAP to the PSD-95 GK domain (Kim *et al.* 1997). GKAP was found to contain 5 of these 14aa repeats and although a single repeat could bind PSD-95, two repeats were required for strong binding activity in a yeast two-hybrid assay. Unfortunately, these repeats have not been identified in other GK ligands.

#### 1.3.2.4 Regulation of Binding

The association of Kir2.3 with PSD-95 can be regulated by PKA, a kinase that is recruited to PSD-95 by AKAP79/150 binding (Colledge *et al.* 2000). PKA phosphorylates the –2 serine of the Kir2.3 C-terminal PDZ binding motif (...RRESAI) and in HEK cells, forskolin stimulation of PKA via adenyl cyclase disrupted the association of co-transfected PSD-95 and a Kir2.3 C-terminal protein (Cohen *et al.* 1996). Therefore, PSD-95 may colocalise the channel with a kinase that regulates its interaction with PSD-95. Such regulated binding has also been observed for stargazin, an AMPA-binding protein that also binds PSD-95 PDZ domains (Chen *et al.* 2000). PKA phosphorylated the –2 threonine (T321) in the C-terminal PDZ recognition motif of stargazin (...RRTTPV) and disrupted its association with PSD-95 (Chetkovich *et al.* 2002; Choi *et al.* 2002). Moreover, a GFP-tagged stargazin phosphorylation mimic (T321E) exhibited a diffuse distribution when transfected into cultured neurons, while a mutant (R318,319A) that disrupted the PKA consensus sequence for T321, exhibited normal synaptic clustering and was not dispersed by PKA (Chetkovich *et al.* 2002). Significantly, the T321E mutant also had a physiological effect, reducing AMPA receptor mEPSC amplitude and frequency, while R318, 319A had no effect (Chetkovich *et al.* 2002). These results are important because synaptic strength depends on the number of AMPA receptors at the synapse, so regulating the association of stargazin with PSD-95 or the localisation of PSD-95 may alter synaptic strength.

### 1.3.3 Dimerisation

A number of MAGUKs, including PSD-95, chapsyn-110, SAP97, SAP102 and CASK can either hetero- or homodimerise (Kim *et al.* 1996; Masuko *et al.* 1999; McGee and Bredt 1999; Nix *et al.* 2000). When co-expressed in heterologous cells with other MAGUKs, or with PSD-95 fusion proteins, PSD-95 was found to bind chapsyn-110, CASK, and SAP97, as well as forming homodimers (Kim *et al.* 1996; Chetkovich *et al.* 2002). To associate with MAGUK proteins, PSD-95 employed three different mechanisms, two of which required the distinct N-terminal sequences encoded by the two PSD-95 variants, while the third utilised SH3-GK interactions.

N-terminal-mediated dimer formation in PSD-95α required the two N-terminal cysteines and these were initially proposed to form intermolecular disulphide bridges (Hsueh and Sheng 1999). However, palmitoylation of the N-terminal cysteines was shown to be required for membrane localisation (El-Husseini *et al.* 2000), hence dimerisation is presumably mediated by another N-terminal sequence. N-terminal dimerisation has been demonstrated in SAP97 (Marfatia *et al.* 2000) and a short region of homology was observed between the PSD-95α and SAP97 N-termini, although the involvement of this sequence in mediating dimerisation in either protein has yet to be determined. However, the distinct N-termini of PSD-95 variants make this form of dimerisation specific to PSD-95α.

Another mechanism of dimerisation is PSD-95β -specific. The PSD-95β N-terminus contains an L27 motif, named after Lin-2 and Lin-7, the two proteins in which this motif was first demonstrated to mediate heterodimerisation. The L27 motif in PSD-95β facilitates heterodimerisation with the mammalian homologue of Lin-2, CASK, and is absent from the more abundant PSD-95α variant, which is unable to interact with CASK (Chetkovich *et al.* 2002). Thus both PSD-95 variants are able to dimerise, utilising distinct sequences and mechanisms that determine the specificity of these interactions.

The third mechanism involves interactions between MAGUK SH3 and GK domains, and is presumably not specific to a particular PSD-95 variant. McGee and Bredt (1999) showed a preference for intra- over intermolecular interactions in PSD-95 SH3-GK interactions *in vitro*, while human CASK and SAP97 could be co-immmunoprecipitated from a human colon carcinoma-derived cell line (Caco-2 cells), an interaction shown to require SH3-GK interactions in transfected HEK cells (Nix *et al.* 2000). Interestingly, the PSD-95 SH3-GK interaction could be abolished by a L460P point mutation in the SH3 domain (McGee and Bredt 1999), analogous to the $dlg^{m30}$ lethal *Drosophila* mutation (Woods *et al.* 1996). The L460P mutation did not involve a residue required for conventional polyproline binding, consistent with the absence of any such motif in the GK domain, however, L460 did form extensive hydrophobic interactions within the core of the β sandwich. Mutation of lysine to proline may alter the orientation of surrounding residues involved in stabilising the structure, particularly V459 in βC, which faces W717 in the C-terminal β strand. McGee and colleagues (2001) proposed that intermolecular SH3-GK interactions involved domain complementation, that is, the C-terminal β strand from one molecule contributes to the SH3 domain of the other and *visa versa*, so maintaining the ability of SH3 and GK domains to bind ligands while forming dimers (McGee *et al.* 2001). The L460P mutation in both SH3 domains would destabilise interactions with the C-terminal β strands and ablate dimerisation, whereas mutation of only one domain would still allow the C-terminal β strand from the mutated molecule to interact with the SH3 domain of the unmutated molecule. This mechanism is supported by genetic complementation experiments in which a number of recessive lethal *dlg* mutations that truncate the GK domain ($dlg^{X1-2}$, $dlg^{v59}$ and $dlg^{IP20}$) are viable as compound heterozygotes with $dlg^{m30}$, which contains the SH3 point mutation (Woods *et al.* 1996). The GK and C-terminal β strand from the $dlg^{m30}$ allele thus presumably binds and complements the GK deletion mutants.

If PSD-95 intermolecular binding occurs *in vivo*, it must be regulated since intramolecular interactions are clearly preferred *in vitro* (McGee and Bredt 1999). Regulation may be imparted by ligands binding the HOOK domain, disturbing intra- in favour of intermolecular interaction. $Ca^{2+}$/calmodulin has been shown to bind the

HOOK region of SAP102, utilising a consensus sequence that is conserved in a number of MAGUKs, including PSD-95. Moreover, heterodimerisation between PSD-95 and SAP102 required the presence of $Ca^{2+}$/calmodulin in the yeast two-hybrid system (Masuko *et al.* 1999). Dimer formation would be advantageous by significantly increasing the binding sites available for co-localisation, enhancing the formation of signalling complexes. This is seen in *Drosophila*, where phototransduction requires the formation of a signalling complex that is coordinated by the inactivation no after-potential D (INAD) protein (Montell 1998). INAD contains five PDZ domains, and dimer formation enables the formation of a functional signalling complex that, with the known binding preferences of INAD ligands, would be unable to form with monomeric INAD (Xu *et al.* 1998).

### 1.3.4 Synaptic Targeting of PSD-95

To isolate the determinants required for PSD-95 synaptic localisation, an array of GFP-tagged PSD-95 constructs expressed in neurons have been used by a number of groups. The N-terminus is critical for PSD-95 synaptic localisation, specifically two cysteines (C3,5) that are palmitoylated (Topinka and Bredt 1998; Craven *et al.* 1999; El-Husseini *et al.* 2000). Abolition of palmitoylation can both prevent PSD-95 targeting to synapses and disperse PSD-95 already clustered at synapses (El-Husseini *et al.* 2002), indicating that palmitoylation is absolutely required for synaptic localisation, even when PSD-95 has presumably bound synaptic membrane proteins.

Despite the importance of palmitoylation, protein interaction domains are also necessary. For example, at least one PDZ domain is required, in addition to palmitoylation, for any synaptic localisation of GFP tagged PSD-95 in cultured hippocampal neurons or cortical slices (Arnold and Clapham 1999; Craven *et al.* 1999), however, differences were observed in the effect of deleting a single PDZ domain. Arnold and Clapham (1999) saw no effect of deleting a single PDZ domain while Craven and colleagues (1999) showed deletion of PDZ1 or 2, but not PDZ3, to reduce synaptic clustering. The only obvious difference that might explain this disparity is the choice of cultures used by the two groups: Craven and co-workers (1999) used dispersed hippocampal cultures while Arnold and Clapham (1999) used cultured rat cortical slices.

A PDZ3 ligand may therefore be absent from dispersed cultures that is able to contribute to PSD-95 localisation in slice cultures.

Another study using GFP-tagged mutants expressed in primary neurons identified a C-terminal tyrosine-based motif important for PSD-95 synaptic targeting (Craven and Bredt 2000). Mutating tyrosine 701 to serine or alanine, or mutating valine 704 to a charged residue impaired PSD-95 synaptic clustering, whereas mutating valine 704 to other hydrophobic residues had no effect. In addition, two hydrophobic residues at 707 and 708 were found to influence clustering if mutated to charged residues, thus defining a YXXΦXXΦΦ motif where X is any amino acid and Φ is a hydrophobic residue (Craven and Bredt 2000). It is noteworthy that this motif is conserved across MAGUKs, also being found in chapsyn-110, SAP97, SAP102 and *Drosophila* DLG.

Localisation of PSD-95 at synapses can also be influenced by cytoplasmic PSD-95 interactor (cypin), which reduced PSD-95 clustering when over expressed in cultured neurons (Firestein *et al.* 1999). Cypin binds PSD-95 PDZ1 and 2 and its C-terminal PDZ interaction motif was required to reduce the number of PSD-95 clusters and abolish SAP102 clustering in neurons (Firestein *et al.* 1999). However, competitive binding to PDZ domains 1 and 2 could not adequately explain the redistribution of MAGUKs since cyan fluorescent protein fused to another C-terminal PDZ-binding motif did not affect PSD-95 or SAP102 clustering (Firestein *et al.* 1999), thus cypin may mediate the active redistribution of PSD-95.

### 1.3.5 Roles for PSD-95

The binding of PSD-95 to its numerous ligands should not be considered a static and inert association, but one in which binding can be regulated and PSD-95 can influence the behaviour of bound proteins.

#### *1.3.5.1 Receptor Localisation*

One of the more striking properties of PSD-95 is its ability to induce clustering of ion channels when expressed in heterologous cells, which was first observed when PSD-95 was coexpressed with the Kv1.4 (Kim *et al.* 1995). In neurons, Kv1.4 preferentially

localises to axons while PSD-95 is enriched in dendrites and PSD-95 exhibited a similar distribution when biolystically transfected into neurons (Arnold and Clapham 1999). Transfected Kv1.4 showed no specific localisation but when PSD-95 and Kv1.4 were cotransfected, Kv1.4 was localised to axons and PSD-95 localised to both axons and dendrites (Arnold and Clapham 1999). Kv1.4 and PSD-95 also colocalise in the optic nerve, however in *PSD-95* deletion mutant mice, Kv1.4 localisation in the optic nerve is unaffected (Rasband *et al.* 2002). It therefore appears that although PSD-95 may be involved in localisation of Kv1.4, it is not required, perhaps because other MAGUKs that bind Kv1.4 can also influence its localisation. The experiments of Arnold and Clapham (1999) might be explained in terms of Kv1.4 transfection saturating the available MAGUK binding sites such that it was not localised. Only by cotransfecting PSD-95 could sufficient binding sites be made available for correct localisation.

PSD-95 is also associated with AMPA receptors, not through direct interaction, but via the stargazin family (Chen *et al.* 2000) and this interaction appears to regulate AMPA receptor synaptic localisation. Palmitoylation, essential for PSD-95 synaptic localisation, is a transient (t½ ~2hr) lipid modification, the stability of which can be modulated by synaptic activity (El-Husseini *et al.* 2002). Blocking palmitoylation by application of 2-bromo palmitate caused a reduction in both PSD-95 and AMPA receptor synaptic localisation, measured by both immunofluorescence and electrophysiology. Surprisingly, no changes were observed in the synaptic localisation of NMDA receptors (El-Husseini *et al.* 2002), an unexpected result since PSD-95 and NMDA receptors directly interact while AMPA receptors are indirectly associated.

#### *1.3.5.2 Modulation of Channels and Receptors*

*In vitro*, the binding of PSD-95 appears to modulate the behaviour of receptors and channels. Coexpression of PSD-95 with Kir2.3 in HEK cells halves single unit conductances (Nehring *et al.* 2000) while transfection of HEK or COS cells with PSD-95 and GluR6/KA2 kainate receptors changed the receptor's response to agonist from rapid desensitisation to incomplete desensitisation, maintaining a steady state current at approximately a third of peak level current (Garcia *et al.* 1998). Furthermore, such incomplete desensitisation of kainate currents has been observed in dispersed

hippocampal cultures (Wilding and Huettner 1997) and slow inward currents were found in mossy fibre synapses (Castillo *et al.* 1997; Vignes and Collingridge 1997). PSD-95 binding has also been reported to reduce NMDA receptor sensitivity to its agonist, glutamate (Yamada *et al.* 1999; Rutter and Stephenson 2000), and inhibit protein kinase C (PKC)-mediated enhancement of NMDA receptor currents (Yamada *et al.* 1999).

PSD-95 can also stabilise cell surface channels and receptors at the cell membrane. Internalisation rates of Kv1.4, Kir5.1, β1-adrenergic receptor and the NMDA receptor were reduced by coexpression with PSD-95 in heterologous cells (Hu *et al.* 2000; Jugloff *et al.* 2000; Roche *et al.* 2001; Tanemoto *et al.* 2002). It is therefore apparent that PSD-95 can both positively and negatively regulate channels or receptors by either directly influencing their behaviour or stabilising them at the plasma membrane, although there has not yet been a clear demonstration of these effects *in vivo*.

#### *1.3.5.3 Signal Transduction*

The promiscuous binding of PSD-95 brings various proteins into close apposition, so coupling components of signalling pathways. nNOS, when activated by $Ca^{2+}$ influx from the NMDA receptor, generates nitric oxide which can inhibit NMDA currents (Manzoni *et al.* 1992), is involved in synaptic plasticity (reviewed by Holscher 1997) and can mediate neurotoxicity *in vitro* and *in vivo* (Huang *et al.* 1994; Dawson *et al.* 1996 but see Khaldi *et al.* 2002). Guanylyl cyclase is stimulated by nitric oxide to produce cyclic guanosine monophosphate (cGMP), which in turn can activates cGMP-dependent kinase. PSD-95 PDZ domains bind three components of this pathway, NMDA receptor NR2 subunits (Kornau *et al.* 1995), nNOS (Brenman *et al.* 1996a; Brenman *et al.* 1996b) and guanylyl cyclase (Russwurm *et al.* 2001), with binding preferences compatible with all three molecules being simultaneously bound by a single PSD-95 molecule. Physiological studies by Sattler and co-workers showed that PSD-95 was required to couple the NMDA receptor to cGMP production; antisense knockdown of PSD-95 in cultured cortical neurons attenuated NMDA-mediated cGMP production by more than 60%. In addition, PSD-95 knockdown attenuated NMDA-mediated

excitotoxicity, potentially by uncoupling nNOS, a mediator of excitotoxicity, from the NMDA receptor (Sattler *et al.* 1999).

PSD-95 therefore displays multiple functions and has been shown to influence cellular processes such as receptor cycling and intracellular signalling. PSD-95 has also been implicated in more complex phenomena that influence neuronal networks and behaviour; synaptic plasticity and memory are two such systems.

## 1.4 Synaptic Plasticity

Hebb proposed the neural basis of memory formation to require an increase in synaptic strength that is induced by the coincident activity of both pre- and postsynaptic neurons (Hebb 1949). Although findings such as the weakening of synaptic strengths have required this theory to be refined, Hebb's postulate remains the basis for many theories concerning the underlying processes of learning and memory.

Hebb's predictions proved correct with the discovery that trains of stimuli can induce increased synaptic strength in hippocampal slices (Bliss and Lomo 1973). Changes in synaptic strength were termed synaptic plasticity, with persistent increases in synaptic strength described as long term potentiation (LTP) while persistent decreases in synaptic strength called long term depression (LTD). Altering synaptic strength required specific frequencies of stimulation, sufficient to result in coincident pre- and postsynaptic activation; in the hippocampus, low frequencies (1 Hz) induced LTD (Dudek and Bear 1992; Mulkey and Malenka 1992) while higher frequencies (5-100 Hz) induced LTP (Bliss and Lomo 1973; Thomas *et al.* 1998).

The mechanisms by which synaptic plasticity is generated became the focus of extensive research and it became apparent that the NMDA receptor was required for some forms of synaptic plasticity. While basic moment-to-moment neurotransmission is mediated by AMPA receptors that depolarise the postsynaptic cell in response to glutamate, NMDA receptors require depolarisation of the postsynaptic cell coincident with presynaptic activation. This property of the NMDA receptor has made it an attractive

candidate for mediating Hebbian synaptic plasticity. In the hippocampal CA1 region both pharmacological and genetic inactivation of the NMDA receptor has been shown to impair synaptic plasticity (Collingridge *et al.* 1983; Coan *et al.* 1987; Dudek and Bear 1992; Mulkey and Malenka 1992; Kutsuwada *et al.* 1996; Tsien *et al.* 1996). The NMDA receptor is also required for some forms of learning (see below) and NMDA receptor-dependent plasticity represents a feasible model for the synaptic changes that occur during learning

## 1.4.1 Mechanisms of NMDA Receptor-Dependent Plasticity

NMDA receptors flux $Ca^{2+}$ ions producing a rise in intracellular $Ca^{2+}$ concentration that can activate a number of signalling molecules. Determining the relevant molecules downstream of the NMDA receptor that are responsible for generating synaptic plasticity has therefore been a focus for considerable research.

### *1.4.1.1 Kinases*

It was recognised that LTP required transient elevations in the intracellular $Ca^{2+}$ concentration (Lynch *et al.* 1983) but a long term alteration in synapse function. Protein kinase C (PKC) and CaMKII were therefore early candidates in mediating long term modifications in synapse function and inhibitor studies showed both to be necessary for the generation of LTP (Lovinger *et al.* 1987; Malinow *et al.* 1988; Reymann *et al.* 1988; Malenka *et al.* 1989; Malinow *et al.* 1989; Ito *et al.* 1991). Further studies using various kinase inhibitors identified other kinases required for LTP including src family tyrosine kinases (O'Dell *et al.* 1991; Abe and Saito 1993; Lu *et al.* 1998), PKA (Frey *et al.* 1993; Matthies and Reymann 1993; Weisskopf *et al.* 1994) and the mitogen-activated protein kinase (MAPK) pathway (English and Sweatt 1997).

Gene targeting technology was also utilised to determine the signalling pathways necessary for LTP production. Knocking out the αCaMKII subunit or mutating its autophosphorylation site in mice resulted in reduced hippocampal LTP (Silva *et al.* 1992; Giese *et al.* 1998), as did mutation of the src family tyrosine kinase, *fyn*, although this mutant also exhibited aberrant hippocampal morphology (Grant *et al.* 1992). Other mutations that impaired synaptic plasticity include PKA Rlβ and Cβ1 subunit

knockouts (Brandon *et al.* 1995; Huang *et al.* 1995; Qi *et al.* 1996) and PKCγ isoform knockouts (Abeliovich *et al.* 1993).

The importance of the MAPK pathway in synaptic plasticity has not yet been clearly demonstrated using gene targeting. Mice lacking extracellular signal-regulated kinase (ERK) 2, the ERK isoform that is preferentially activated by high frequency stimulation (English and Sweatt 1996), die during embryonic development (Adams and Sweatt 2002), precluding analysis of synaptic plasticity. ERK1 is less strongly activated than ERK2 by high frequency stimulation and mice lacking ERK1 demonstrated this isoform, to be required for only theta burst (3 trains of 10 bursts of 4 pulses at 100 Hz, 5 Hz burst frequency) induced hippocampal (Mazzucchelli *et al.* 2002).

#### *1.4.1.2 NMDA Receptor Signalling Complexes*

The various interactions of MAGUK proteins and their association with the NMDA receptor facilitate the physical organisation of signalling pathways downstream of the NMDA receptor to form NMDA receptor associated complexes (NRCs). One example of a signalling pathway organised in such a manner is the colocalisation of nNOS and guanylyl cyclase with the NMDA receptor via PSD-95, mentioned earlier. Another example is the MAPK pathway. Multiple members of the MAPK pathway, including MAPK/extracellular signal-regulated kinase kinase (MEK), ERK and ribosomal protein S6 kinase (RSK), are found in the PSD (Suzuki *et al.* 2001) and are associated with the NMDA receptor (Husi *et al.* 2000). Additionally, a regulator of Ras, synGAP, directly binds PSD-95 (Chen *et al.* 1998).

Further evidence of the association of the MAPK pathway with the NMDA receptor was generated in an experiment that utilised intracellular EGTA. The relatively slow binding kinetics of EGTA allow local increases in $Ca^{2+}$ concentration, for instance at the pore of an ion channel, while preventing global $Ca^{2+}$ increases. Under such conditions, NMDA receptor activation of the MAPK pathway was still observed (Hardingham *et al.* 2001), implying that activation of MAPK components must occur very close to the NMDA receptor.

Many signalling proteins found in the NRC (Husi *et al.* 2000) are implicated in synaptic plasticity, including nNOS (Holscher 1997), the MAPK pathway, CaMKII, PKCγ and PKA, which interacts with PSD-95 via AKAP79/150. However, in addition to the activity of these signalling molecules, gene transcription and protein synthesis, upregulating immediate early gene (IEG) expression, are also required for long term synaptic plasticity (Tischmeyer and Grimm 1999; Platenik *et al.* 2000; Smith *et al.* 2001). Activity-regulated gene 3.1 (arg3.1) / activity-regulated cytoskeleton-associated protein (arc) is an IEG product of particular interest because its expression is induced by LTP, it is the only IEG whose mRNA is rapidly distributed through dendritic processes (Link *et al.* 1995; Lyford *et al.* 1995) and arg3.1/arc antisense impairs the maintenance of *in vivo* LTP and learning in the rat (Guzowski *et al.* 2000). Furthermore, arg3.1/arc induction has been shown to require PKA and MEK activity (Waltereit *et al.* 2001) and it is found in the NRC (Husi *et al.* 2000). The NRC may therefore not only have a role in clustering signalling molecules to facilitate their activation, but may also recruit proteins such as arg3.1/arc that are involved in later phases of synaptic plasticity.

Disrupting interactions within the NRC may allow its importance in synaptic plasticity to be assessed. The intracellular C-terminal tail of NR2 NMDA receptor subunits is the site of interaction of many NMDA receptor associated proteins, including MAGUKs. NR2A and NR2B are the most abundantly expressed NR2 subunits in the adult forebrain (Monyer *et al.* 1994), while NR2B expression dominates the embryonic and early postnatal forebrain (Monyer *et al.* 1994; Sans *et al.* 2000). Mutant mice lacking the NR2 C-termini demonstrated the importance of this region, and by implication, the NRC.

Mice lacking the NR2B C-terminus (NR2BΔC) died perinatally, however some analyses were possible. NMDA receptor currents were reduced in NR2BΔC mutants, corresponding to reduced NR2BΔC expression, while expression of other NMDA and AMPA receptor subunits were unaffected (Mori *et al.* 1998; Sprengel *et al.* 1998). Interestingly, the number of NR2B immunofluorescent puncta was reduced and some clusters did not localised to synapses, determined by colocalisation with synaptophysin

(Mori *et al.* 1998). NR2BΔC protein and NMDA receptor currents were reduced by about half, however this may not have caused the lethality since *NR2B* knockout heterozygotes have a similar reduction in NR2B expression and are viable (Kutsuwada *et al.* 1996), so lethality was proposed to result from a loss of associated proteins and intracellular signalling (Sprengel *et al.* 1998).

In contrast to the NR2BΔC mutants, NR2AΔC mice were viable, although LTP in the hippocampal CA1 region was abolished (Sprengel *et al.* 1998). However, interpretation of these data is complicated due to controversy about NMDA receptor expression levels in NR2AΔC mutants. Sprengle and coworkers (1998) reported normal NR2AΔC expression and NMDA receptor currents while Steigerwald and colleagues observed reduced synaptic NMDA receptors by both immunofluorescent and electrophysiological analyses (Steigerwald *et al.* 2000). Whether abolition of LTP was due to reduced NMDA receptor activation or impaired signalling downstream of the NMDA receptor therefore remains to be clarified.

## 1.5 Learning and Memory

### 1.5.1 Hippocampal-Dependent Learning

The hippocampus is required for the formation of certain types of memories, for example, episodic (e.g. knowledge of personal events) memory in humans (Scoville and Milner 1957; Zola-Morgan *et al.* 1986) and spatial memory in rodents (Morris *et al.* 1982; Moser *et al.* 1993). Bilateral lesions of the hippocampus prevent the formation of new memories (anterograde anaesthesia) and also result in an often temporally graded loss of existing memories (retrograde amnesia). These phenomena imply the involvement of the hippocampus in initially encoding memories, but also in consolidating those memories to generate a more permanent record. The time-scale over which the hippocampus is required for the retrieval of memories is still, however, controversial. Many studies in humans, primates and rodents have shown the hippocampus to be required for the retrieval of recent memories, and that this requirement decreased with progressively older memories producing temporally graded retrograde amnesia (Scoville and Milner 1957; Winocur 1990; Zola-Morgan and Squire

1990; Kim and Fanselow 1992; Winocur *et al.* 2001). However, other studies reported either little retrograde amnesia (Zola-Morgan *et al.* 1986) or profound retrograde amnesia with little temporal grading. Cipolotti and colleagues reported an example of the latter in a detailed study of a patient with restricted bilateral hippocampal dysfunction and revealed a profound retrograde amnesia that extended over 40 years (Cipolotti *et al.* 2001). The question of the extent of involvement of the hippocampus in recall therefore remains to be resolved (reviewed by Rosenbaum *et al.* 2001; Spiers *et al.* 2001).

### 1.5.2 NMDA Receptor Dependence of Learning

The pharmacological requirements for hippocampal function have also been studied using a number of receptor antagonists. Intracerebroventricular injections of NMDA receptor antagonist inactivate the receptor in various brain regions, generating sensorimotor deficits that may interfere with learning paradigms, confounding interpretation. To circumvent these side effects, Morris used intrahippocampal injections of the NMDA receptor antagonist AP5, which prevented spatial learning in rodents tested in the Morris water maze (Morris *et al.* 1986; Morris 1989). The hippocampus, and specifically AMPA receptor activity, is required for the recall of spatial information (Morris *et al.* 1990; Riedel *et al.* 1999), yet the NMDA receptor is not required for recall (Morris 1989), despite its requirement at the time of learning.

### 1.5.3 Kinases and Learning

Many studies utilising knockout mice have investigated the role of signalling cascades in learning and memory with varying success. Initial studies provided promising evidence of the utility of this technology with mice lacking Fyn and αCaMKII that showed profound learning deficits, which correlated with impaired LTP (Grant *et al.* 1992; Silva *et al.* 1992; Silva *et al.* 1992). Interpretations of these phenotypes were, however, accompanied by caveats: Mice lacking fyn exhibited abnormal hippocampal morphology that could have influenced learning, although field EPSPs and NMDA receptor contribution to EPSCs were normal (Grant *et al.* 1992), while the αCaMKII knockout mice were reported as epileptic (Butler *et al.* 1995), which may also affect learning. However, subsequent mutant and transgenic animals established the role of

αCaMKII in both synaptic plasticity and learning (Bach *et al.* 1995; Mayford *et al.* 1995; Mayford *et al.* 1996; Giese *et al.* 1998). The role of PKC in learning appears more peripheral, perhaps acting in a modulatory role, despite early interest from inhibitor studies in LTP induction in slices. Mice lacking PKCγ exhibited impaired LTP but only mild learning deficits, (Abeliovich *et al.* 1993; Abeliovich *et al.* 1993) perhaps as a result of compensatory activity by other PKC isoforms.

PKA consists of a tetrameric holoenzyme, made up of 2 regulatory (R) subunits and 2 catalytic (C) subunits. Mutation of PKA subunits also generated initially confusing results. Mice lacking either Rlβ or Cβ1 subunits exhibited impaired LTP but normal learning (Brandon *et al.* 1995; Huang *et al.* 1995; Qi *et al.* 1996), however, PKA activity was unaffected in mutants and this may explain the dissociation of LTP from learning (Brandon *et al.* 1995; Huang *et al.* 1995). A transgenic mouse expressing R(AB), an inhibitory form of the Rlα that reduced stimulated PKA activity by 25%, later demonstrated a role for PKA in both synaptic plasticity and learning (Abel *et al.* 1997).

The MAPK pathway has been implicated in learning by pharmacological inhibition rather than the use of knockout mice. Infusion of the MEK inhibitor PD098059 into the hippocampus of rats during water maze training impaired memory performance but not acquisition of the task (Blum *et al.* 1999). Unfortunately, mice lacking ERK2 die during embryonic development (Adams and Sweatt 2002) and therefore cannot provide any insight into its importance in learning. ERK1 mice displayed some LTP reduction following strong theta burst (10 bursts of 4 pulses at 100 Hz, 5 Hz burst frequency) stimulation but 100 Hz-induced hippocampal LTP was unaffected (Mazzucchelli *et al.* 2002). Spatial learning was not tested, although the two-way avoidance task revealed improved memory in mice lacking ERK1, which was explained by enhanced ERK2 signalling in the striatum of knockout animals (Mazzucchelli *et al.* 2002). ERK2 is the principle ERK isoform activated following high frequency stimulation and MEK activity (upstream of ERK) is required for LTP induction (English and Sweatt 1996;

English and Sweatt 1997). It therefore appears likely that ERK2 is predominantly involved in generating LTP while ERK1 might play a modulatory role.

### 1.5.4 Limitations of Electrophysiological and Behavioural Paradigms

The use of mutant mice reveal not only associations between LTP and learning, but also the limitations of this technology and the tests for synaptic plasticity and learning. The limitations of mutant mice are discussed later, however electrophysiological and behavioural tests will be briefly discussed here.

A common criticism of LTP induction is the use of unphysiological stimuli such as 1s 100 Hz, particularly when this is the only stimulation protocol tested. Lower frequency stimuli (5-10 Hz) and theta burst stimulation (100 Hz bursts at 5 Hz burst frequency) can also induce NMDA receptor-dependent LTP (Larson *et al.* 1986; Thomas *et al.* 1998) and are similar in frequency to theta rhythms that have been observed in the hippocampus (Bland 1986). Testing only a single stimulation protocol (1s 100 Hz) might not reveal subtle phenotypes and may be assessing events that are less related to the molecular mechanisms of learning than LTP generated by more physiological stimuli. A more rigorous assessment of LTP in mutant animals might therefore test hippocampal slices over a range of stimulation frequencies and include theta burst stimulation.

A number of behavioural tests are used to determine learning and memory deficits, yet often only a single test is used to analyse a new mutant mouse. Again, the use of more than one test would potentially increase the chances of identifying a learning deficit and produce more robust conclusions. One of the more widely used tests of learning ability is the Morris water maze. The Morris water maze was initially designed for the rat, obviously larger but also more at home in the water than the mouse. This task is therefore more physically demanding for the mouse and potentially more stressful, however, with appropriate controls the Morris water maze can be a useful tool in assessing mutant mice. Overtraining can blunt the sensitivity of the water maze such that even NMDA receptor antagonists cannot prevent rats learning the position of a hidden platform (Bannerman *et al.* 1995). Overtraining may therefore explain some of

the mutant phenotypes that dissociate altered LTP from learning deficits such as the inositol-3-phosphate kinase (A) knockout mouse (Jun *et al.* 1998). This mutant exhibited enhanced LTP but learning was normal, however, the animals were trained in the hidden platform task for 40 trials compared to the more common schedule of 20 trials over 5 days. If this mutant were trained over fewer trials, a learning deficit may therefore be revealed.

## 1.6 PSD-95, Plasticity and Memory

The clear importance of the NMDA receptor in synaptic plasticity and learning and memory generated interest in the role of associated proteins such as PSD-95. Could PSD-95 modulate NMDA receptor function *in vivo* and did it influence the downstream effects of NMDA receptor activation?

### 1.6.1 *PSD-95* Deletion Mutant Mouse

To address the role of PSD-95 *in vivo*, a mutant mouse was generated using conventional gene targeting techniques (Migaud *et al.* 1998). An exon encoding part of PDZ3 was interrupted by a drug resistance cassette; the 5' end of the drug resistance cassette contained stop codons in all three reading frames, so truncating PSD-95 at amino acid 346 in PDZ3. Homozygotes were viable and fertile, however, they were obtained at less than the Medelian frequency: 32% wild type, 52% heterozygote and 16% homozygote. The mutation resulted in the production of a truncated PSD-95 protein containing PDZ domains 1 and 2, expressed at <20% levels of wild type protein. However, immunoprecipitation assays did not identify the truncated protein associated with the NMDA receptor (Migaud *et al.* 1998), consistent with studies that demonstrated the SH3 domain and C-terminal sequences were required for correct localisation of PSD-95 (Arnold and Clapham 1999; Craven *et al.* 1999).

Synaptic localisation of the NMDA receptor was reduced in mice in which the intracellular C-termini of NR2A or NR2B had been deleted (Mori *et al.* 1998; Steigerwald *et al.* 2000), implying a role for the NR2A/B C-termini in synaptic targeting and/or stabilising the receptors at the synapse, presumably via proteins binding these regions. The effect of the *PSD-95* mutation on NMDA receptor localisation was

therefore investigated. NMDA receptor localisation appeared normal in *PSD-95* deletion mutants, perhaps because binding of other MAGUKs compensated for the loss of PSD-95, although expression of other neuronal MAGUKs (SAP102, SAP97, chapsyn-110) was unaltered (Migaud *et al.* 1998). Alternatively, PSD-95 binding may have no effect on the localisation of NMDA receptors. For example, loss of synaptic PSD-95 by depalmitoylation did not affect the synaptic localisation of NMDA receptors (El-Husseini *et al.* 2002).

In addition to its localisation, NMDA receptor function was unaffected by the PSD-95 mutation (Migaud *et al.* 1998). It was therefore of great interest that NMDA receptor-dependent synaptic plasticity was profoundly altered in the *PSD-95* deletion mutants. Enhanced LTP was observed at stimulation frequencies from 1-100 Hz, even though 1 Hz stimulation induced LTD in wild type animals (Migaud *et al.* 1998). Increased LTP was not due to impaired inhibition or upregulation of NMDA receptor-independent LTP in *PSD-95* deletion mutants since the $GABA_A$ antagonist picrotoxin was able to further enhance LTP while the NMDA receptor antagonist AP5 completely abolished LTP in mutant mice (Migaud *et al.* 1998).

In the water maze, *PSD-95* deletion mutant mice were found to be profoundly impaired, unable to learn the position of the hidden platform, even when extensively trained (Migaud *et al.* 1998). PSD-95 therefore has a role in NMDA receptor-dependent synaptic plasticity and learning and memory but does not alter NMDA receptor channel properties.

## 1.6.2 The Role of PSD-95 in LTP: CaMKII Competition

PSD-95 may influence NMDA receptor-dependent processes by modulating downstream signalling. Such modulation may take the form of altering the localisation of proteins, particularly those associated with the NMDA receptor.

### *1.6.2.1 PSD-95 and CaMKII Competitively Bind the NMDA receptor*

Multiple proteins bind the NMDA receptor but steric hinderance will limit which proteins can bind concurrently, and thus define the makeup of any one NMDA receptor

complex. Regulation of binding may therefore change the properties of an NMDA receptor complex, influencing the signalling output that results from receptor activation.

CaMKII is a major component of PSDs and is activated by NMDA receptor-mediated $Ca^{2+}$ influx, which stimulates autophosphorylation of its autoregulatory domain (threonine 286 in αCaMKII), conferring $Ca^{2+}$-independent activity on CaMKII. $Ca^{2+}$-independent activity allows CaMKII signalling to continue long after the initial NMDA receptor-meidated $Ca^{2+}$ influx, and in addition, autophosphorylation of CaMKII induces it to translocate to the PSD (Strack *et al.* 1997) where it binds the NMDA receptor NR2A or NR2B subunits (Gardoni *et al.* 1998; Strack and Colbran 1998; Gardoni *et al.* 1999; Leonard *et al.* 1999).

CaMKII and MAGUKs bind distinct sites on NR2A/B subunits, MAGUKs binding the extreme C-termini while CaMKII binds two more N-terminal sites in the intracellular C-terminal tail (Bayer *et al.* 2001). The binding of CaMKII and MAGUKs to the NMDA receptor was predicted to be mutually exclusive due to the considerable steric hindrance conferred by CaMKII (Kennedy 2000; Fig. 1.5) and competitive binding was demonstrated in hippocampal slices (Gardoni *et al.* 2001). It was also shown that glutamate or high frequency stimulation of hippocampal slices resulted in increased CaMKII association with immunoprecipitated NMDA receptors, with concomitant decreases in PSD-95 association and that this activity-stimulated competition could be blocked by the CaMKII inhibitor KN93 (Gardoni *et al.* 2001).

#### *1.6.2.2 CaMKII-Stimulated PSD-95 Dissociation*

What is the role of CaMKII activity in competitive binding with PSD-95? CaMKII can associate with NR2A and NR2B subunits without being autophosphorylated, although autophosphorylation enhances binding (Bayer *et al.* 2001; Gardoni *et al.* 2001) which would presumably shift the binding equilibrium towards CaMKII. However, an alternative explanation might be that CaMKII activity is required to stimulate the dissociation of PSD-95 from the NMDA receptor. PSD-95 has been shown to be phosphorylated by CaMKII *in vitro* (Yoshimura *et al.* 2000) and a potential phosphorylation site exists in the linker region between PDZ2 and PDZ3 that is likely to

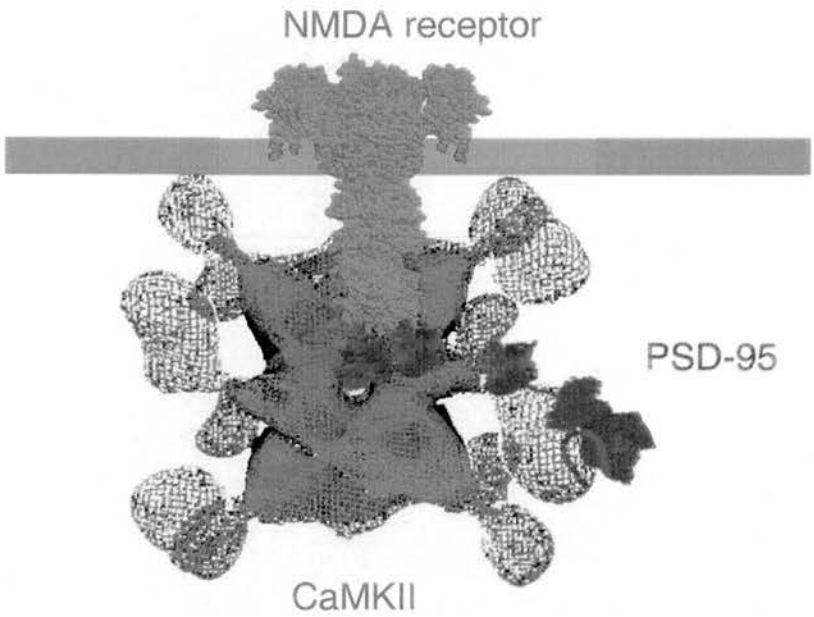


**Figure 1.5 Representation of PSD-95 and CaMKII binding to the NMDA receptor.** Binding of a CaMKII dodecamer and PSD-95 to the NMDA receptor is likely to be mutually exclusive due to steric hindrance. Apart from CaMKII, protein structures have not been determined in their entirety but are based on the structures of individual domains or related domains (the AMPA receptor extracellular domain has been used for the NMDA receptor extracellular domain). No structure information is available for the NMDA receptor cytoplasmic domain, so it is represented by a form depicting its approximate size based on molecular weight. Diagram adapted from Kennedy 2000.

be accessible. The proximity of this phosphorylation site to the PDZ2 domain, which binds NR2 subunits, raises the possibility that CaMKII phosphorylation regulates PSD-95 association with the NMDA receptor. In epithelial cells, another tight junction associated protein, zona ocludens-2 (ZO-2) is a target for PKC. The dispersal of ZO-2 from tight junctions, concomitant with tight junction disassembly, required PKC activity (Avila-Flores *et al.* 2001) that potentially regulated its protein interactions. Thus, a similar mechanism may be present at synaptic junctions, with CaMKII-stimulated dissociation of PSD-95 from the NMDA receptor facilitating the binding CaMKII.

PSD-95 may therefore act as a brake on LTP by competing with CaMKII for NMDA receptor binding. Similar to voltage-gated $Ca^{2+}$ channels (reviewed by Augustine 2001), activation of the NMDA receptor is likely to produce a calcium microdomain around its pore such that only $Ca^{2+}$ -sensitive proteins within the 'activation domain' are activated. PSD-95 may therefore have 2 roles in binding the NMDA receptor: to locate $Ca^{2+}$-sensitive molecules such as nNOS to the NMDA receptor activation domain and to compete with, and therefore limit activation of CaMKII (Fig 1.6A). In *PSD-95* deletion mutants, CaMKII binding to the NMDA receptor, and so localisation in the activation domain may be increased, resulting in enhanced CaMKII activation following NMDA receptor stimulation. Increased CaMKII activation might therefore explain the enhanced LTP observed in the *PSD-95* deletion mutants. However, when $Ca^{2+}$-independent CaMKII is expressed in transgenic mice, 5 Hz or 10 Hz-induced LTP was abolished, although LTP induced by 100 Hz stimulation was unaffected (Mayford *et al.* 1995; Mayford *et al.* 1996).

The level of $Ca^{2+}$-independent CaMKII activity may act as a record of the stimulation to which a synapse has been exposed. Such a molecular record might then influence future outcomes of synaptic activity, for example, previously potentiated synapses can be more easily depressed, or depotentiated, than naive synapses (Staubli and Lynch 1990). The level of $Ca^{2+}$-independent CaMKII activity at the time of stimulation therefore appears critical in determining whether potentiation or depression results. In *PSD-95* deletion mutant mice the $Ca^{2+}$ -independent CaMKII activity is presumably normal at basal

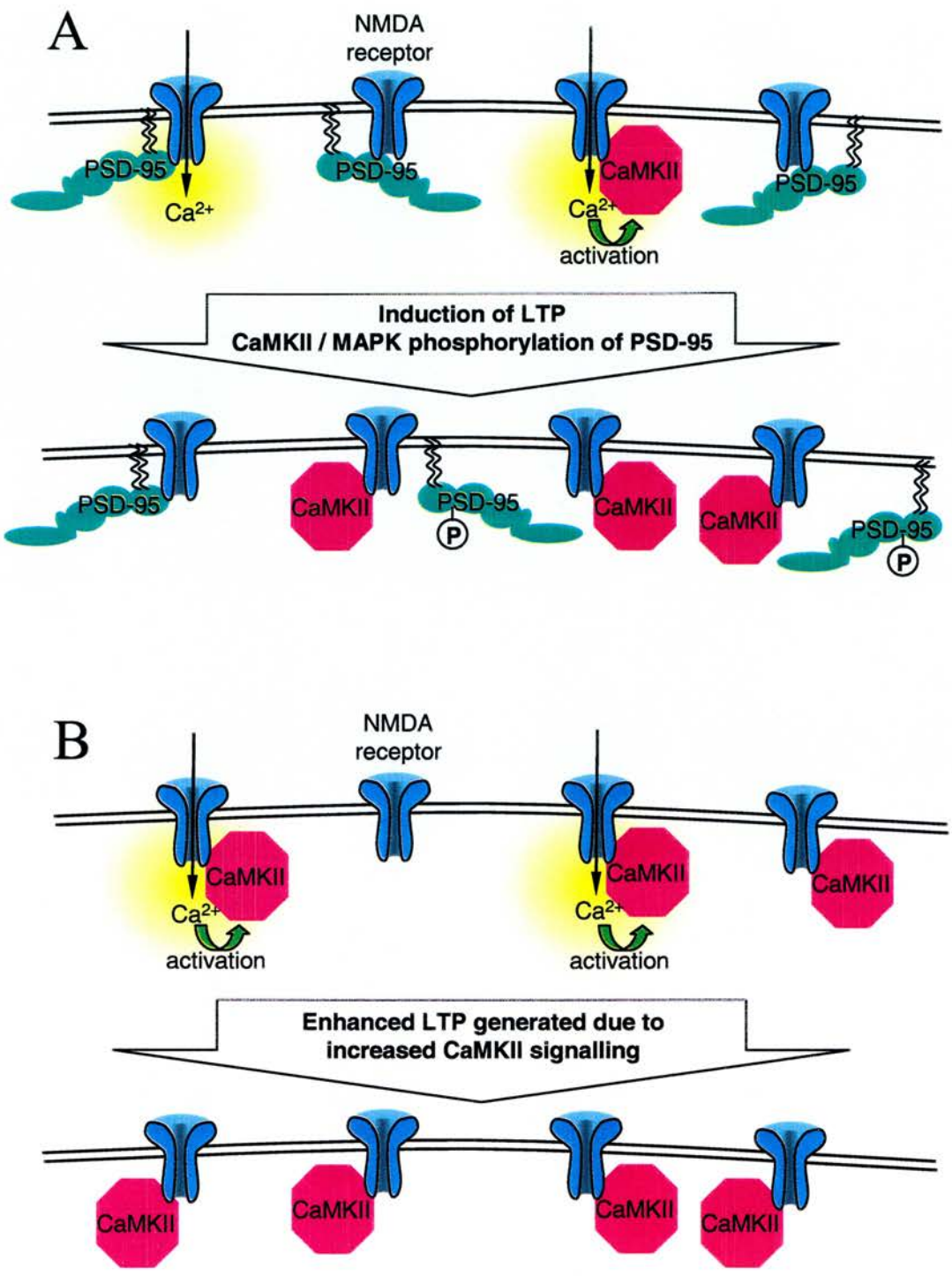


**Figure 1.6 PSD-95 gates LTP induction by competing with CaMKII for NMDA receptor binding.** ***A.*** NMDA receptor stimulation activates associated CaMKII ($Ca^{2+}$ microdomain depicted by yellow circle), producing LTP. LTP may require an increase in the number of CaMKII molecules associated with the NMDA receptor, assisted by CaMKII or MAPK induced dissociation of PSD-95. Wavy lines attaching PSD-95 to plasma membrane represent palmitoylaion. ***B.*** In PSD-95 mutants, increased CaMKII association with the NMDA receptor may result in enhanced CaMKII activation and signalling, generating amplified LTP.

activity but more molecules are stimulated following NMDA receptor activation, resulting in enhanced LTP (Fig 1.6B). Indeed, NMDA stimulation of hippocampal slices taken from *PSD-95* deletion mutants produces an enhanced level of CAMKII activation (T. O'Dell – personal communication).

It should also be noted that increased CaMKII activity caused the *Drosophila* PSD-95 homologue, DLG to disperse from the neuromuscular junction (Koh *et al.* 1999), thus CaMKII-induced PSD-95 dispersal may represent a conserved mechanism important in regulating neuronal function.

#### *1.6.2.3 MAPK-Stimulated PSD-95 Dispersal*

The MAPK pathway might also stimulate PSD-95 dispersal. The activity of the MAPK pathway is stimulated by, and required for LTP induction (English and Sweatt 1996; English and Sweatt 1997). Interestingly, hippocampal slices from *PSD-95* deletion mutants exhibit 5 Hz LTP that is insensitive to MEK inhibitors, yet normal ERK activation is observed when slices are stimulated with glutamate (T. O'Dell – personal communication). This implies the PSD-95 mutation has uncoupled MAPK from its effector. The simplest interpretation of these data is that PSD-95 is a major MAPK target. A mechanism through which MAPK might influence LTP is by stimulating the dissociation of PSD-95 from the NMDA receptor, MAPK-induced PSD-95 dispersal facilitating the association of CaMKII with the NMDA receptor. Such a mechanism would explain why MEK inhibitors have no effect on the enhanced LTP seen in PSD-95 mice.

## 1.7 Inducible/Conditional Gene Regulation in Mice

Advances in gene targeting technology have made available various methods to control gene function or expression in a temporally or spatially restricted manner. Such conditional technologies have already proved powerful tools in neuroscience and are considered below.

### 1.7.1 Gene Targeting

Targeting the murine genome and the establishment of mutant mouse lines is now a widespread technique used to study physiological and behavioural processes *in vivo*. Key to the generation of mutant mice is the *in vitro* manipulation of the endogenous gene locus by homologous recombination. *In vitro* targeting is performed on embryonic stem (ES) cells, which are derived from the inner cell mass of pre-implantation embryos (Evans and Kaufman 1981; Martin 1981) and can be cultured *in vitro* without losing their pluripotency. Indeed, cultured ES cells can be injected into blastocysts, forming chimeras with exogenous ES cell contribution to all somatic tissues, including the germ line (Bradley *et al.* 1984). This feature of ES cells is critical for the generation of mutant mouse lines, since chimeras containing mutated cells are capable of transmitting the mutation through the germline to their offspring (Gossler *et al.* 1986; Robertson *et al.* 1986).

The targeting of endogenous loci by homologous recombination is a rare event and therefore the use of drug resistance cassettes increases efficiency considerably. Insertion of the cassette into the genome can therefore be selected for by the addition of the relevant drug to the cell media. However, this method does not distinguish between random and correct insertion of the targeting vector, the drug-resistant clones must therefore be screened by either polymerase chain reaction (PCR) or Southern blotting to identify clones with integration of the targeting vector into the correct locus (Vega 1995).

### 1.7.2 Conditional Control of Gene Expression

The importance of temporal and spatial control is also evident in the study of brain function, and particularly memory formation. Learning and memory requires the involvement and interaction of multiple brain regions, however, conventional gene targeting is unable to address protein function in distinct brain regions. Conditional techniques allow elegant studies to be performed that can investigate the function of a protein not only in specific brain regions, but also in different phases of memory, for example encoding versus retrieval. A conditional approach is therefore desirable and

two methods are proven in their usefulness, conditional gene inactivation and inducible gene expression.

#### *1.7.2.1 Inducible Gene Expression*

A major system for controlling gene expression exploits the tetracycline (Tet) resistance operon (tetO). The tetracycline-controlled transcriptional activator (tTA) drives expression via tetO, but in the presence of the tetracycline analogue, doxycycline, transcription is repressed (Gossen and Bujard 1992). However, doxycycline is stored in muscle and bone and so not rapidly eliminated from the body. tTA was therefore mutated and a reverse tTA (rtTA) identified in which doxycycline stimulates transcription instead of repressing it (Gossen *et al.* 1995). Thus, initiation of transcription follows doxycycline distribution kinetics as opposed to the slower rate of elimination.

The Tet system therefore consists of 2 elements: a tTA or rtTA transcriptional activator and a tetO-driven transgene of interest. Regional expression of the transcriptional activator transgene can be achieved by the use of an appropriate promotor, for instance, the *αCaMKII* promotor can drive expression in the forebrain (Mansuy *et al.* 1998). However, randomly inserted transgenes, such as those that constitute the Tet system, can be influenced by chromosomal position effects and copy-number independence (reviewed by Bishop 1999). Integration into different chromosomal sites can influence the expression level of the transgene and can affect the tissue distribution and time of onset of expression. Copy-number independence is observed when the expression level of a transgene does not correspond to the number of copies of the transgene integrated; indeed, a high copy-number can result in silencing of the transgene. Another possible consequence of random transgene integration is mosaic expression, which is observed as patchy expression of a transgene through a tissue. Inserting transgenes into the genome at defined loci by homologous recombination can circumvent the problems associated with random integration of trangenes. The *rosa26* locus is well characterised, drives ubiquitous expression of transgenes (Zambrowicz *et al.* 1997) but is apparently dispensable and therefore represents an excellent target for this kind of approach.

Despite the problems associated with random integration of trangenes, the utility of the Tet system for the study of learning and memory has been well demonstrated. A $Ca^{2+}$-independent αCaMKII mutant or a calcineurin inhibitor peptide have both been expression under the control of the tetO promotor and both animals exhibited phenotypes that were entirely reversible with the addition or removal of doxycyclin (Mayford *et al.* 1996; Malleret *et al.* 2001).

#### *1.7.2.2 Conditional Gene Inactivation*

For conditional gene inactivation to be useful, the function of the gene of interest must remain intact until inactivation is desired and inactivation should be complete. Conditional gene inactivation utilises the bacteriophage recombinase Cre or the yeast recombinase Flp, which catalyse recombination between short (34 bp) recognition sequences, Cre recognising loxP sites and Flp recognising FRT sites respectively. Recombination of two recognition sites in series excises the intervening DNA, producing a site-specific deletion.

Homologous recombination can deliver loxP or FRT sites into specific loci, and by placing the recombination sites in introns, gene function is maintained in the absence of the relevant recombinase. This method has allowed genes such as the NMDA receptor NR1 subunit to be targeted (Tsien *et al.* 1996), mutation of which is lethal if inactivated by conventional vectors (Forrest *et al.* 1994). Addition of recombinase results in excision of the DNA flanked by loxP or FRT sites, and a loss of gene product, assuming essential exons have been flanked. The Cre-loxP system has been more widely used than Flp-FRT, so studies using Cre-loxP will be focussed on for discussion.

The key to this type of conditional system is the control of the recombinase. Cre can be delivered to mice containing genes flanked by loxP sites (or floxed) by either crossing targeted mice with *Cre*-expressing mice, or by injecting the mice with *Cre*-expressing vectors, such as adenoviruses.

##### *1.7.2.2.1 Cre-Expressing Transgenics*

*Cre* expression can be limited to specific tissues or regions through the use of tissue-specific promotors. For example, transgenic mice in which Cre expression was driven by the CNS-specific Thy-1 promotor exhibited expression in the brain but not liver (Kellendonk *et al.* 1999) while αCaMKII promotor-driven *Cre* was restricted to the forebrain (Tsien *et al.* 1996). Different transgenic lines may exhibit a range of expression patterns, although the same promotor may drive expression of *Cre*. This was observed for the αCaMKII-driven *Cre* lines where *Cre* expression in the T29-2 line was broadly distributed, with significant expression across the forebrain, while the T29-1 line exhibited enriched expression in the CA1 region of the hippocampus with little expression seen outside the hippocampus (Tsien 1996a). The serendipitous expression pattern of the T29-1 line proved particularly useful for the study of CA1 function in synaptic plasticity and learning and memory (Tsien *et al.* 1996). Hippocampal or CA1-enriched expression of *Cre* therefore allows the involvement of proteins in discrete brain regions to be examined.

In addition to limiting *Cre* expression in a regional manner, it is possible to limit either its activity or expression in a temporal fashion. The Tet system can be used to regulate *Cre* expression (St-Onge *et al.* 1996), however a Tet-driven *Cre* transgenic exhibiting suitably restricted brain expression has not yet been developed. Alternatively, the activity of Cre can be controlled in a hormone-dependent manner by fusing Cre to a mutated steroid hormone binding domain. The resulting fusion protein requires the presence of a synthetic ligand for Cre activity, but is not activated by endogenous steroids. Hence, Cre fused to a mutant progesterone binding domain (Cre-Pr) is activated by RU486 but not progesterone while Cre fused to mutant oestrogen binding domain is activated by 4-hydroxy-tamoxifen but not endogenous estrogens (Kellendonk *et al.* 1996; Zhang *et al.* 1996; Schwenk *et al.* 1998; Kellendonk *et al.* 1999). Initially, control of Cre activity in these systems was poor and Cre activity was observed in the absence of ligand, although further mutation of the ligand binding domain has considerably reduced background recombination (Indra *et al.* 1999; Wunderlich *et al.* 2001).

#### *1.7.2.2.2 Adenoviral Delivery of Cre*

To maximise the benefits of the Cre-loxP system, both spatial and temporal control are desirable. The direct injection of *Cre*-expressing vectors such as the adenoviral system provides one with reasonable control over when and where *Cre* is expressed. Systemic injection of *Cre*-expressing adenovirus resulted in a wide tissue distribution, although preferential expression in some organs was observed while expression was absent from the brain (Akagi *et al.* 1997). Harding and coworkers demonstrated transfection of hippocampal neurons *in vivo* by injection of green fluorescent protein-expressing adenovirus directly into the brains of rats (Harding *et al.* 1998). The stereotactic surgery used in this study allows injections to be accurately directed to specific brain regions, thus not only the time, but also the location of *Cre* expression can be dictated. Another major benefit of this system is that one is not constrained by the availability of *Cre* transgenics when choosing to target a specific brain region.

## 1.8 Aims and Objectives

The *PSD-95* deletion mutant mouse has enhanced our understanding of the role of PSD-95 in synaptic plasticity and learning, however, the utility of this mutant is limited due to the ubiquitous nature of the mutation and the presence of the truncated protein containing PDZ domain 1 and 2. While the truncated protein was not found in synaptosomal fractions and did not associate with the NMDA receptor, it remains possible that the truncated protein acted in a dominant negative fashion. Binding of the mislocalised, truncated PSD-95 protein with PDZ1 or PDZ2 ligands may result in the mislocalisation of the associated proteins, altering neuronal physiology. To counter this argument, a null allele is clearly necessary.

This thesis will describe the generation of a conditional *PSD-95* null allele that will enable the role of PSD-95 to be explored in greater detail. Such a conditional system will allow PSD-95 function to be modulated in a spatially and/or temporally restricted manner *in vivo* to address questions such as the dependence of hippocampal *PSD-95* expression for learning. Another interesting question that could be addressed using this conditional *PSD-95* allele is whether PSD-95 is required for encoding and/or retrieval of memories.

To target *PSD-95* and ensure the production of a null allele, the gene has been fully characterised, including the identification of intron-exon boundaries and splice variants. The study of mouse *PSD-95* yielded interesting data about the organisation and variation of the gene and its transcripts in addition to providing information for designing the targeting strategy.

PSD-95 may also have a role in anaesthesia since antisense knockdown of PSD-95 in the spinal cord results in an enhanced sensitivity to isoflurane. The mechanism of action of volatile anaesthetics such as isoflurance is still under debate, however, NMDA receptors do not appear to be major targets for volatile anaesthetics. To further study the role of PSD-95 in anaesthesia, the sensitivity of *PSD-95* deletion mutants to volatile anaesthetics has been tested.

# Chapter 2: MATERIALS & METHODS

All general reagents were analytical grade or better from BDH, Fischer, Fluka or Sigma.

## 2.1 General Molecular Biology Methods and Techniques

Basic molecular biology techniques were performed as described in Sambrook and Russell (2001).

### 2.1.1 Cloning

#### *2.1.1.1 DNA Cloning from Conventional Plasmids*

Following restriction enzyme digest, DNA plasmids and fragments were separated by gel electrophoresis and the desired DNA fragments purified using the Geneclean Spin kit (Anachem).

Purified plasmids and inserts were ligated at a ratio of 1:1 overnight at 16°C using 1U T4 DNA ligase (Roche) and the accompanying ligation buffer in a final volume of between 10 and 20µl.

#### *2.1.1.2 DNA Cloning from PAC Plasmids*

1µg PAC plasmid DNA was cut with 60U restriction enzyme at 37°C overnight. Cut PAC plasmid DNA was then purified by phenol/chloroform extraction and ethanol precipitation. pBluescript KSII (Invitrogen) was prepared by restriction enzyme digest and Geneclean purification and subsequently phosphatased for 30 min at 37°C using 1U shrimp alkaline phosphatase (Roche) and the accompanying phosphatase buffer.

1µg digested PAC plasmid was ligated with 5ng phosphatased pBluescript overnight at 16°C using 1U T4 DNA ligase (Roche) and the accompanying ligation buffer in a final volume of 10µl.

### 2.1.1.3 TA Cloning of PCR Products

PCR products were either purified by gel electrophoresis followed by GeneClean Spin purification or used directly for subsequent steps. If a proofreading polymerase had been used for PCR, adenosine overhangs were added by 1 hour incubation at 72°C of product with 1.5mM $MgCl_2$, 0.2mM dATP, 1U Taq polymerase (Promega) and the PCR reaction buffer (Promega) in a final volume of 10 to 20µl. Products ready for cloning were TA cloned using either pGEM-T Easy (Promega) or TOPO XL (Invitrogen) kits using the supplier's instructions.

### 2.1.1.4 Generation and Transformation of Competent E. Coli

5mls of LB was inoculated with a single colony of bacteria (DH-5α or DH-10B) and grown overnight in a shaking incubator at 37°C. 250mls of LB was inoculated with 5mls of the stationary overnight culture and grown in a shaking incubator at 37°C until $OD_{600}$ had reached ~0.5. The culture was transferred to 50ml falcon tubes, chilled on ice, spun down at 4°C and the supernatant discarded.

#### *2.1.1.4.1 $CaCl_2$-Competent Bacteria*

Following centrifugation, the bacteria were resuspended in ½ volume (25ml per tube) ice-cold 50mM $CaCl_2$ and left on ice for 15min. They were then centrifuged as before, the supernatant discarded and bacteria taken up in $^1/_{10}$ volume (5ml per tube) ice-cold freezing mix (100mM KCl, 50mM $CaCl_2$, 10% glycerol, 10mM KAc pH 7.5). The bacterial suspension was aliquoted into eppendorf tubes on dry ice and the aliquots stored at -70°C.

To transform, up to 5µl of ligation was added to 200µl bacteria on ice and the mixture then transferred to a 15ml snap cap falcon tube on ice. The bacteria were incubated on ice for 30min and then heat shocked at 42°C for 90seconds after which they were chilled on ice for a further 2-3min. 800µl of SOC medium was added to the bacteria and the cultures incubated at 37°C for 30-60min in a shaking incubator (225rpm). The transformed bacteria were spread onto agar plates containing the appropriate antibiotic and incubated overnight at 37°C.

#### *2.1.1.4.2 Electrocompetent bacteria*

Following centrifugation, the bacteria were resuspended in the 50ml of ice-cold 10% glycerol. They were centrifuged at 4°C, the supernatant discarded and the ice-cold 10% glycerol wash repeated. The bacteria were centrifuged a third time, resuspended in 120µl 10% glycerol per tube and 40µl aliquots made in eppendorf tubes, snap frozen in liquid $N_2$ and stored at -70°C.

1µl of ligation was added to a 40µl aliquot on ice and the mixture transferred to a pre-chilled 0.2ml electroporation cuvette. The bacteria were electrotransformed in a Gene Pulser (BioRad) set at 25µF, 200Ω, 2.5 kV. 1ml of SOC medium was immediately added to the cuvette, the bacteria transferred to 15ml snap cap falcon tubes and incubated at 37°C for 30-60min in a shaking incubator (225rpm). The transformed bacteria were spread onto agar plates containing the appropriate antibiotic and incubated overnight at 37°C.

### *2.1.1.5 Screening Transformants*

LB containing the appropriate antibiotic was inoculated with a single colony and incubated overnight at 37°C in a shaking incubator. Plasmid was purified from the stationary culture (see Plasmid Preparation below) and analysed by restriction enzyme digest and/or PCR.

## 2.1.2 Isolation of Nucleic Acids

### *2.1.2.1 Plasmid Preparation*

Small-scale plasmid purification was performed using QIAprep miniprep spin kits (Qiagen), Wizard plus miniprep kits (Promega) or the lysozyme miniprep method (see below). Large-scale plasmid purification was performed using Midi or Maxi kits (Qiagen).

#### *2.1.2.1.1 Lysozyme Miniprep*

1.5ml stationary culture was spun down in a bench top microfuge. All supernatant was removed and the bacteria resuspended in 120µl STET buffer (8% sucrose, 0.5% Triton

X-100, 50mM EDTA, 10mM Tris pH 7.4). 20µl lysozyme solution (20mg/ml) was added and the tube incubated at 100°C for 50 s. The tube was immediately spun in a microfuge for 10 min at 14000 rpm at room temperature (RT). The glutinous precipitate was removed and 120µl isopropanol added to the supertnatant. Samples were then placed at -20°C for 20 min, after which the precipitated DNA was recovered by centrifugation at 14000 rpm for 10 min at RT. The DNA pellet was washed with 70% ethanol, air dried and resuspended in 35µl of $dH_2O$ containing 34µg/ml RNase A.

### *2.1.2.2 PAC Plasmid Preparation*

PAC clones were delivered as *E. coli* smeared on agar containing kanamycin selection. Each clone was restreaked onto fresh kanamycin agar plates before use. High quality PAC plasmid was purified using Qiagen Large Contruct kits. High yield PAC plasmid purification was performed using a protocol from the University of Oxford Bioinformatics wed page:
(www.molbiol.ox.ac.uk/~jmejia/more_protocols.html).

#### *2.1.2.2.1 Large-scale Preparation of PAC or BAC DNA*

500ml of 2xTY medium containing 0.2 % glycerol and 25µg kanamycin was inoculated with 5 ml of an overnight culture and shaken at 37°C for 5-6 hours or overnight. The culture was transferred into three 250-ml polypropylene centrifuge bottles, spun at 5500 rpm for 7 min, 4°C, in the GSA rotor of a Sorval centrifuge and the supernantant discarded. Each bacterial pellet was resuspended in 20 ml of buffer (50 mM Tris-HCl, pH 8.5, 10 mM EDTA). 40 ml of 1 % SDS, 0.2 M NaOH solution was added to each bottle and gently mixed. 30 ml of 7.5 M ammonium acetate was immediately added, the bottle capped and inverted. The bottles were chilled on ice for 15 min then centrifuged at 10 000 rpm for 15 min at 4°C. The supernatants were poured into 2 fresh bottles through a layer of gauze (each of the new bottles will thus hold the contents of 1½ original bottles) that were then centrifuged at 10 000 rpm for 15min at 4°C. The supernatants were decanted through gauze, 0.5 vol. of isopropanol added and centrifuged at 10 000 rpm for 10 min at room temperature. Supernatants were discarded, each pellet resuspended in 1.5 ml of buffer (50 mM Tris-HCl, pH 8.5, 10 mM EDTA) containing 50 µg/ml RNase A and incubated at 37°C for 1 hour. 0.1 volume of

10 % SDS was added and mixed. Proteinase K was added (final concentration of 0.2 mg/ml) and incubated at 50-60°C for 3-4 hours. DNA was extracted with buffered phenol (pH 8), buffered phenol-chloroform (1:1) and chloroform, successively with centrifugations at 2000 rpm in a swinging bucket rotor for 10 min. 7.5 M ammonium acetate was added to a final concentration of 2.5 M and the DNA precipitated with 0.5 volume isopropanol at room temperature. DNA was spun down in glass Sorval tubes in a SS34 rotor at 12000 rpm, 5 min. The DNA pellet was washed with 1 ml 70 % ethanol and resuspended in 300 $\mu$l of TE buffer.

#### *2.1.2.3 Isolation of Genomic DNA*

Cells were incubated at 55°C overnight in Laird buffer (100mM Tris.HCl pH8.5, 200mM NaCl, 5mM EDTA, 0.2% SDS) containing 20mg/ml proteinase K. DNA was extracted with buffered phenol (pH 8) and buffered phenol-chloroform-isoamylalcohol (25:24:1) then precipitated with 1 volume isopropanol. DNA was washed with 70% ethanol and resuspended in TE.

#### *2.1.2.4 Isolation of RNA*

RNA was prepared from tissues using Trizol reagent (Sigma). Brains were homogenised using 1 ml Trizol reagent per 50-100mg of tissue. Homogenates were centrifuged at 12000 x g for 10 min at 4°C to remove insoluble material. The supernatant was collected, 0.2 ml $CHCL_3$/ml Trizol was added and mixed vigorously and then centrifuged at 12000 x g for 10 min at 4°C. The supernatant was transferred to a new tube and 0.5 ml isoproanol/ml Trizol was added and incubated at RT for 10 min and centrifuge at 12000 x g for 10 min at 4°C. Remove supernatant, wash RNA pellet with 75% ethanol, briefly air dry and resuspend RNA in DEPC $H_2O$.

### 2.1.3 Nucleic Acid Transfer to Membranes

#### *2.1.3.1 Colony Lifts*

Nylon filters were laid onto agar plates containing the relevant antibiotic. Transformed bacteria were then spread onto the filters and incubated overnight at 37°C; these are the master filters. Duplicate filters were laid on fresh agar plates to wet. A master filter was peeled off an agar plate and laid, colony side up, onto Whatman 3M papers. A duplicate

filter was removed from its agar plate and laid, agar side up, on top of the master filter. The filters were marked for orientation by puncturing 3 holes around their edges with a needle. Whatman 3M paper was laid on top of the filters and gentle, even pressure applied to the stack. The filters were carefully separated and replaced to their respective agar plates. The duplicate filter was then incubated at 37°C for 3-4 hours until the duplicate colonies had grown. To lyse the bacteria, the duplicate filter were peeled off the agar plate and placed onto Whatman 3M paper wetted with a 2×SSC, 5%SDS solution. To bake the DNA onto the filters, they were microwaved at full power for 30-90 seconds until the colonies looked glassy.

### *2.1.3.2 Southern Blotting*

#### *2.1.3.2.1 Restriction Enzyme Digest of Genomic DNA*

For digests using a single restriction enzyme: To approximately 10µg of genomic DNA was added 120U of restriction enzyme and 5µl of 10x digestion buffer, the volume adjusted to 50µl with sterile $H_2O$. For digests using 2 restriction enzymes: To approximately 10µg of genomic DNA was added 120U of each restriction enzyme and 9µl of 10x digestion buffer, the volume adjusted to 90µl with sterile $H_2O$. Reactions were incubated overnight at 37°C.

#### *2.1.3.2.2 Restriction Enzyme Digest of PAC DNA*

To 1-2µg of PAC DNA was added 50-60U of restriction enzyme and 5µl of 10x digestion buffer, the volume adjusted to 50µl with sterile $H_2O$. Reactions were incubated overnight at 37°C.

#### *2.1.3.2.3 Alkali Blotting*

Restriction enzyme-digested genomic DNA was run on a 0.6% agarose gel overnight. The gel was photographed and treated with depurination solution (0.25M HCl) for 15 min. The gel was then treated with denaturation solution (0.5M NaOH, 1.5M NaCl) for 20 min before being placed onto a Whatman 3M filter wick dipped into the transfer solution (0.4M NaOH). A Hybond N+ nylon membrane, pre-wetted in transfer solution, was placed onto the gel followed by 4 pieces of Whatman 3M filter paper. A stack of

paper towels were paced on top of the Whatman filters and finally a weight was added. Gels were blotted for at least 12 hours. After blotting, the nylon membrane was washed in 2x SSC.

## 2.1.4 Hybridisation of Nucleic Acids Bound to Membrane

### *2.1.4.1 Probes*

#### *2.1.4.1.1 PDZ1+2 Probe (nucleotide 1-983)*

A PSD-95 PDZ1+2-specific probe was generated by restriction enzyme digest of a rat PSD-95 cDNA plasmid (gift from M. Sheng). SmaI-EcoRI restriction enzyme digest produced a cDNA fragment encompassed the PSD-95α N-terminal sequence and the first 2 PDZ domains, terminating with the SmaI site at nucleotide 983.

#### *2.1.4.1.2 PDZ1, PDZ3 and Exons 1-4 Probes*

All probes were generated by PCR (see PCR section below).

#### *2.1.4.1.3 5' Probe for Screening Targeted Clones*

Subclone SacI (LR) was cut with EcoRI restriction enzymes and an ~500bp fragment was purified and used as the 5' probe. This fragment contained sequence between the 2 EcoRI sites in *PSD-95* intron 1, which was external to the targeting vector.

#### *2.1.4.1.4 3' Probe for Screening Targeted Clones*

A subclone (subclone D) derived from the mouse genomic lambda clone (Migaud *et al.* 1998) was cut with BamHI and EcoRI restriction enzymes and an ~1735bp fragment was purified and used as the 3' probe. This fragment contained genomic sequence from the BamHI site in *PSD-95* intron 16 to the EcoRI site in intron 18, which was external to the targeting vector.

### *2.1.4.2 $^{32}$P Labelled Probes*

Probes were $^{32}$P labelled using the Megaprime DNA labelling system (Amersham). 25ng of probe and random nonomer primers were denatured in 33µl at 95°C for 5min and allowed to cool to room temperature. Labelling buffer (dATP, dGTP, dTTP in

Tris/HCl pH7.5, 2-mercaptoethanol, $MgCl_2$), 2U klenow and 50μCi [$^{32}P$] dCTP was added to a final volume of 50μl. This mix was incubated at 37°C for 30-45min. The labelled probe was separated from unincorporated nucleotide by passing through Micro Bio-Spin 30 chromatography columns (BioRad) at 1000×g for 4 min.

### 2.1.4.3 Hybridisation of Mouse Genomic PAC Library

The PAC library, obtained from the UK HGMP resource centre, was constructed using female 129/SvEvTACfBr mouse spleen genomic DNA partially digested with MboI. PAC clones were gridded onto nylon hybridisation filters such that each filter contained over 18,000 distinct mouse PAC clones per filter with each clone arrayed in duplicate to allow correct identification of specific versus non-specific signals. The high density filters were hybridised as per the manufacturer's instructions. Filters were pre-hybridised in Church buffer (10mg/ml BSA, 1mM EDTA, 0.5M $NaPO_4$ (pH7.2), 7% SDS) for 1 hour at 65°C. The PDZ1+2 probe was $^{32}P$ labelled (as above) and incubated with the filters in Church buffer overnight at 65°C. The filters were washed to moderate stringency (40mM $NaPO_4$ (pH7.2), 1mM EDTA, 1% SDS) and exposed to film overnight.

### 2.1.4.4 Hybridisation of Southern Blots

Hybridisations were performed in Techne hybridisation bottles rotating in a Techne HB-1 oven using approximately 25mls of hybridisation buffer (0.5M $Na_2HPO_4$ (pH7.2), 7% SDS, 0.1mg/ml salmon testes DNA). Prehybirdisation, hybridisation and washes were carried out at 65°C.

Southern blots were prehybridised for 10 min to 1 hour in hybridisation buffer. Radiolabelled probe was denatured at 100°C, snap cooled on ice and added to the hybridisation buffer. Filters were hybridised overnight. Following hybridisation, filters were washed at least 2x 10 min in wash buffer (2x SSC, 0.5% SDS). If required, higher stringency washes were performed: 2x 10 min using 0.5x SSC, 0.1% SDS. After washes, filters were wrapped in Saran wrap and exposed either to autoradiographic film at -70°C for up to 4 days or to phosphorimaging plates for up to 3 days.

#### 2.1.4.5 Hybridisation of Colony Lifts

Hybridisations were performed in 15cm petri dishes in an Innova 4000 shaking oven (New Brunswick Scientific). 25mls of formamide hybridisation solution was used (50% formamide, 0.025% sodium pyrophosphate, 5x SSC, 5x Denhardts). Filters were wetted with 2x SSC and placed into hybridisation solution. No prehybridisation was performed; hybridisation was carried out overnight at 42°C. Washes were performed using Techne hybridisation bottles in a Techne-HB1 oven at 65°C as described above.

### 2.1.5 PCR

PCR reactions were carried out on Omnigene (Hybaid), MJ Research DNA Engine Tetrad (GRI), GeneAmp 9700 (Applied Biosystems) or Mastercycler gradient (Eppendorf) PCR machines. dNTPs were supplied by Roche and the Taq polymerase used is indicated in each protocol. Primer sequences are listed in appendix 4.

#### 2.1.5.1 PAC Diagnostic PCRs

##### *2.1.5.1.1 Determination of Regions of PSD-95 Contained in PAC*

To approximately 500ng of PAC DNA was added 5µl of 10x system 1 PCR buffer (Roche), 1.75µl 10mM dNTPs and 1µl of each 20µM forward and reverse primer (M8144 and M8145; A8643 and SH3 Spe Bot; GK For and RPD; GK Spe Top and 3N). The volume was adjusted to 49.25µl with sterile $H_2O$ and the tube heated to 93°C for 2 min. 0.75µl of Expand Long Range PCR enzyme mix (Roche) was added and the PCR continued as follows: 10x (93°C for 10 sec, 59°C for 30 sec, 68°C for 1 min); 20x (93°C for 10 sec, 59°C for 30 sec, 68°C for 1 min + 20 sec/cycle) followed by 68°C for 8 min.

##### *2.1.5.1.2 Comparison of PSD-95 Gene Structure in PAC and Genomic DNA*

To 250µg mouse genomic DNA or 80ng of Qiagen-prepared PAC DNA was added 5µl of 10x system 3 PCR buffer (Roche), 2.5µl dNTPs, 1µl of each 20mM forward and reverse primer (5' start and PDZ1 Rev; Exon 2 For and PDZ1 Rev; PDZ1 For and A8646; A8643 and B7524) and the volume made up to 49.25µl with sterile water. The

reaction mix was heated to 94°C for 10min after which 0.75µl of Expand long range PCR enzyme mix (Roche) was added and the PCR continued as follows:

**5' start / PDZ1 Rev**

10x 94°C for 10 sec
60°C for 30 sec
68°C for 15 min

20x 94°C for 10 sec
60°C for 30 sec
68°C for 15 min + 20 sec/cycle

1x 68°C for 7 min

**Exon 2 For / PDZ1 Rev**

10x 94°C for 10 sec
66°C for 30 sec
68°C for 3 min

20x 94°C for 10 sec
66°C for 30 sec
68°C for 3 min + 20 sec/cycle

1x 68°C for 7 min

**PDZ1 For / A8646**

10x 94°C for 10 sec
60°C for 30 sec
68°C for 8 min

20x 94°C for 10 sec
60°C for 30 sec
68°C for 8 min + 20 sec/cycle

1x 68°C for 7 min

**A8643 / B5724**

10x 94°C for 10 sec
58°C for 30 sec
68 °C for 4 min

20x 94°C for 10 sec
58°C for 30 sec
68 °C for 4 min + 20 sec/cycle

1x 68°C for 7 min

### *2.1.5.1.3 Exon Orientation in Subclones*

Hotstar Taq (Qiagen) was used for PCRs involving BamHI (9): To 1µl of miniprep (approximately 250ng) was added 5µl 10x PCR buffer (Qiagen), 1 µl 10mM dNTPs, 1µl of 20mM reverse primer (PDZ1 Rev; PDZ2 Rev), 1µl 20mM t3 or t7 primer, 0.25µl Hotstart Taq polymerase (Qiagen) and the volume adjusted to 50µl using sterile $H_2O$. The reaction mix was cycled as follows: 1x (95°C for 15 min); 30x (94°C for 10 sec, 59°C for 30 sec, 72°C for 3 min).

Expand Long Range PCR system 3 was used for PCRs involving SacI (1), SacI (20) and KpnI (4): To 1µl of miniprep (approximately 250ng) was added 5µl 10x PCR buffer (Roche), 2.5 µl 10mM dNTPs, 1µl of 20mM forward primer (Exon 2 For; PDZ1 For; 5' start) and 1µl 20mM t3 or t7 primer. The volume was adjusted to 49.25µl, the reaction mix heated to 94°C for 10 min after which 0.75µl enzyme mix (Roche) was added and the PCR continued as follows: 10x (94°C for 10 sec, 55°C for 30 sec, 68°C for 3 min);

20x (94°C for 10 sec, 55°C for 30 sec, 68°C for 3 min + 20 sec/cycle) followed by 68°C for 7 min.

#### 2.1.5.2 Southern Probe PCRs

PCR protocols to generate probes are listed below. Subsequent to PCR, products were ran out on an agar gel and purified using either QIAEX II (Qiagen) or Geneclean (Anachem) gel extraction kits.

##### *2.1.5.2.1 PDZ1 Probe (nucleotides 5-503)*

To 200ng *PSDS-95* cDNA was added 5µl 10x PCR buffer (Qiagen), 1µl 10mM dNTPs, 1µl 20mM 5' start, 1µl 20mM PDZ1 Rev and 0.25µl Hotastar Taq polymerase (Qiagen). The volume was adjusted to 50µl with sterile $H_2O$. PCR conditions were as follows: 1x (95°C for 15 min); 30x (94°C for 30 s, 60°C for 1 min, 72 °C for 1 min).

##### *2.1.5.2.2 PDZ3 Probe (nucleotides 986-1572)*

To 200ng *PSDS-95* cDNA was added 5µl 10x PCR buffer (Qiagen), 1µl 10mM dNTPs, 1µl 20mM A8643, 1µl 20mM GK Spe Bot and 0.25µl Hotastar Taq polymerase (Qiagen). The volume was adjusted to 50µl with sterile $H_2O$. PCR conditions were as follows: 1x (95°C for 15 min); 30x (94°C for 30 s, 63°C for 1 min, 72 °C for 1 min).

##### *2.1.5.2.3 Exon 1-4 Probe (nucleotides 5-280)*

To 50ng *PSD-95* cDNA was added 5µl 10x PCR buffer (Qiagen), 1µl 10mM dNTPs, 1µl 20mM 5' start, 1µl 20mM M8145 and 0.25µl Hotastar Taq polymerase (Qiagen). The volume was adjusted to 50µl with sterile $H_2O$. PCR conditions were as follows: 1x (95°C for 15 min); 35x (94°C for 30 s, 60°C for 1 min, 72 °C for 30 s).

#### 2.1.5.3 RT-PCR

##### *2.1.5.3.1 First Strand Synthesis*

First strand cDNA was generated from 2 to 5µg mouse brain total RNA using oligo dT with Superscript II (Invitrogen) as per the suppliers directions. For 5' RACE, the SMART cDNA kit (Clonetech) was used for first strand synthesis as per the suppliers

instructions using 0.9µg total RNA, the SMART IV oligo and Exon 2 Rev reverse primer with Powerscript reverse transcriptase (Clonetech).

#### *2.1.5.3.2 Exon 2 Splice Variant PCR*

To 10% of first strand cDNA was added 10µl of PCR buffer (Promega), 6µl of 1.5mM $MgCl_2$, 2µl of 10mM dNTPs, 1µl of 5' start and 1µl of PDZ1 Rev. The volume was adjusted to 49µl with sterile $H_2O$ and the reaction mix heated to 94°C for 3 min after which 1µl of Taq polymerase (Promega) was added and the PCR continued as follows: 35x (94°C for 15 s, 59°C for 45 s, 72°C for 45 s).

#### *2.1.5.3.3 5'RACE*

To 20% of first strand cDNA was added 5µl of Expand Long Range PCR kit 10x PCR buffer (Roche), 1µl 10mM dNTPs, 2µl 10mM 5' PCR primer (Clonetech) and 1µl 20mM 5' Start Rev. The volume was adjusted to 49µl and the reaction mix heated to 94°C for 1 min after which 1µl enzyme mix (Roche) was added and the PCR continued as follows: 10x (94°C for 10 s, 60°C for 30 s, 68°C for 6 min); 20x (94°C for 10 s, 60°C for 30 s, 68°C for 6 min + 20 s/cycle).

### *2.1.5.4 Screening Targeted ES Cell Clones*

#### *2.1.5.4.1 Screening for Selection Cassette Excision*

To 1µl of genomic DNA (~500ng) was added 5µl 10x PCR buffer (Qiagen), 1µl 10mM dNTPs, 1µl 20mM Sac 1 For 2, 1µl 20mM M3 Rev, 1µl 20mM LP3 Rev and 0.25µl Hotastar Taq polymerase (Qiagen). The volume was adjusted to 50µl with sterile $H_2O$. PCR conditions were as follows: 1x (95°C for 15 min); 30x (94°C for 10 s, 60°C for 30 s, 72 °C for 1 min 25 s).

#### *2.1.5.4.2 Screening for Presence of loxP Sites*

To 1µl of genomic DNA (~500ng) was added 5µl 10x PCR buffer (Qiagen), 1µl 10mM dNTPs and 0.25µl Hotastar Taq polymerase (Qiagen). To PCR across the 5' loxP site, 1µl 20mM Sac 1 For 3 and 1µl 20mM M4 Rev was added. To PCR across the 3' loxP site, 1µl 20mM 631-9 For and 1µl 20mM LP3 Rev was added. The volume was adjusted

to 50µl with sterile $H_2O$. PCR conditions were as follows: 1x (95°C for 15 min); 30x (94°C for 10 s, 60°C for 30 s, 72 °C for 1 min). Products generated to screen for the 3' loxP site were digested with the EcoRI restriction enzyme to determine the presence of the EcoRI site that was included in the loxP site oligo: To 10µl PCR product was added 3µl buffer H (Roche), 1U EcoRI and the volume adjusted to 30µl with sterile $H_2O$. The reaction was incubated at 37°C for 1 hour.

## 2.1.6 DNA Sequencing

To 500ng of template was added 3.2 pmoles of primer, 4µl Big Dye Terminator reaction mix (ABI) and the volume adjusted to 10µl with sterile $H_2O$. PCR conditions were as follows: 25x (96°C for 30 s, 50°C for 15 s, 60°C for 4 min). Following PCR, reaction products were precipitated and then ran out by the Centre for Genome Research sequencing service. All sequences were analysed using GeneJockey 2 (Biosoft).

### *2.1.6.1 Online Sequence Analysis*

#### *2.1.6.1.1 NCBI BLAST*

The National Centre for Biotechnology Information (NCBI) basic local alignment search tool (BLAST; http://www.ncbi.nlm.nih.gov/BLAST) was used to identify local regions of sequence similarity between a candidate sequence and sequences in the GenBank sequence database.

#### *2.1.6.1.2 Translate*

The Translate tool (http://ca.expasy.org/tools/dna.html) was used to translate all 3 cDNA reading frames of cDNA sequence to protein sequence.

#### *2.1.6.1.3 ScanProsite*

ScanProsite (http://ca.expasy.org/tools/scanprosite) was used to scan protein sequences for patterns in the Prosite database.

#### *2.1.6.1.4 Grail 1.3*

The gene recognition and assembly internet link (Grail) version 1.3 (http://compbio.ornl.gov/Grail-1.3) was used to screen genomic sequence for CpG islands.

#### *2.1.6.1.5 NNPP*

Neural network promotor prediction (NNPP; http://www.fruitfly.org/seq_tools/promoter.html) was used to screen genomic sequences for possible transcription promoters.

#### *2.1.6.1.6 Proscan 1.7*

Proscan 1.7 (http://bimas.dcrt.nih.gov/molbio/proscan) was used to screen genomic sequences for transcription promoters and to identify transcription factor binding sites.

#### *2.1.6.1.7 UTR Scan*

UTR scan (http://bighost.area.ba.cnr.it/BIG/UTRScan) was used screen for untranslated region (UTR) functional elements defined in UTRsite.

#### *2.1.6.1.8 EMBOSS*

EMBOSS (http://www.ebi.ac.uk/emboss/align) was used to perform global pairwise alignments of sequences and calculate the percentage homology between the 2 sequences.

### 2.1.7 Protein Analysis

#### *2.1.7.1 Sample Preparation*

Mice were killed by cervical dislocation (Schedual 1 procedure in accordance with UK Home Office regulations), their brains quickly removed and rapidly cooled in ice cold PBS. All subsequent steps were performed on ice. The brain was hemisected, one hemisphere being snap frozen in a methanol/dry ice bath while the other hemisphere was weighed and placed in ice cold deoxycholate (DOC) buffer (1% DOC, 50mM Tris.Cl pH9, 50mM NaF, 200μM $ZnCl_2$, 0.5mg/ml phenylmethylsulfonyl fluoride (PMSF), 1mM Na vandate, 1.125× Complete protease inhibitors (Roche)) at a ratio of 0.38g wet weight to 7 ml DOC buffer. The hemisphere in DOC buffer was homogenised with 20 strokes of a loose-fitting type S pestle in a Potter-Elvehjem homogeniser. The homogenate was cleared by centrifugation at 25000 rpm for 15 min at 6°C in a MLA-130 rotor using an Optima MAX ultracentrifuge (Beckman Coulter). Protein concentration was determined using the bicinchoninic acid (BCA) method.

If a sample was to be used immediately for SDS-PAGE (see below), it was diluted 1:1 in 2x sample buffer (20mM Tris.Cl pH6.8, 4% SDS, 20% glycerol, 200mM dithiothreitol, 1mg bromophenol blue) and denatured at 100°C for 5 min.

#### *2.1.7.2 Immunoprecipitation*

All steps were performed on ice or at 4°C. Protein samples were diluted to 1mg/ml in RIPA buffer (1% DOC, 10mM Tris.Cl pH8, 140mM NaCl, 0.025% sodium azide, 1% Triton X-100, 0.1% sodium dodecylsulphate, 0.5mg/ml PMSF, 1.125× Complete protease inhibitors (Roche)). To 1ml of protein solution was added 1μg anti-NR2B mouse monoclonal antibody (Transduction Labs), 1.2μg anti-Kv1.4 rabbit polyclonal antibody (Alomone Labs) or 4μg anti-KA2 rabbit polyclonal antibody (Upstate Biotechnology). Proteins were incubated with antibody at 4°C overnight on a rotator. 50μl of protein A (for rabbit antibodies) or protein G (for mouse antibodies) sepharose bead/ phosphate buffered saline (PBS; 10mM phosphate buffered saline, 138mM NaCl, 2.7 mM KCl, pH7.4) slurry was added to the samples and incubated at 4°C for 2 hr on a rotator. The sepharose beads were collected by a 5 s spin at 10 000 rpm at 4°C, the supernatant discarded and the beads washed with 1ml RIPA buffer. Washes were repeated 3 more times. The sepharose beads were resuspended in 25μl of PBS to which 25μl of 2x sample buffer was then added. Samples were then denatured at 100°C for 5 min. Samples were then spun down (5 s spin at 10 000 rpm) and the supernatant loaded onto 8% polyacrylamide gels.

#### *2.1.7.3 SDS-Polyacrylamide Gel Electrophoresis (SDS-PAGE)*

Vertical polyacrylamide gels were prepared using BioRad mini gel protein kits. 30% acrylamide (37.5:1 acrylamide to N,N'-methylene-bis-acrylamide) solution was supplied by BioRad. An 8% acrylamide resolving gel mix, containing 375mM Tris.Cl pH8.8 and 0.1% SDS was made to which ammonium persulphate and N,N,N',N'-tetramethylethylenediamine (TEMED) were added to final concentrations of 0.09% and 0.1%, respectively. The resolving gel was then immediately poured and butan-2-ol layered on top to ensure uniform polymerisation.

After polymerisation, the butan-2-ol was rinsed off with distilled water. A stacking gel (4% acrylamide, 125mM Tris.Cl pH6.8, 0.1% SDS, 0.09% ammonium persulphate, 0.2% TEMED) was prepared in a similar manner to the resolving gel. The stacking gel was poured immediately after ammonium persulphate and TEMED addition and a Teflon comb inserted into the gel to form wells.

Electrophoresis was performed at RT in electrophoresis tank buffer (125mM Tris, 960mM glycine, 0.5% SDS) at 150V until the dye front reached the bottom of the gel (approximately 60 min). BenchMark prestained protein ladder (Invitrogen) was included in all gels.

#### *2.1.7.4 Western Blotting*

Following electrophoresis, polyacrylamide gels were washed in Transfer buffer (10% methanol, 9mM 3-(cyclohexylamino)-1-propanesulphonic acid pH11). Mini trans-blot cells (BioRad) were then set up as follows: Whatman 3M filter paper was placed onto a trans-blot fibre pad, both of which were soaked in Transfer buffer. The washed polyacrylamide gel was placed onto the filter paper and a Hybond-P (Amersham) membrane was activated in methanol then placed on the gel. Another Whatman 3M filter paper and trans-blot filter pad (both soaked in Transfer buffer) were placed onto the membrane. All components were then locked into the cassette which was placed into the Mini trans-blot cell and covered with Transfer buffer. Electrophoretic transfer was performed at 100V for 1 hr.

Following electrophoretic transfer, Western blots were transferred to 50ml Falcon tubes and incubated overnight at 4°C with blocking solution (PBS containing 0.1% TWEEN and 3% skimmed milk powder). The blocking solution was then discarded and replaced with fresh block containing anti-PSD-95 mouse monoclonal antibody (Upstate Biotechnology, clone K28/43) at a dilution of 1:10 000. The anti-PSD-95 antibody was incubated with the Western blot for 2 hrs at RT and then washed with blocking solution 3 times over 30 min. The Western blot was then incubated with blocking solution containing anti-mouse Ig sheep antibody conjugated to horseradish peroxidase (Amersham) at RT for 1 hr. The blot was then washed with PBS containing 0.1%

TWEEN 3 times over 30 min. Horseradish peroxidase activity was detected using enhanced chemiluminescence (ECL) Western blotting detection reagents (Amersham) with Hyperfilm ECL (Amersham). Films were exposed for 5 or 10 s.

## 2.2 Tissue Culture

### 2.2.1 ES Cell Culture

General methods for the manipulation of ES cells are based on Hogan *et al.*, 1994. All ES cell manipulations were performed in laminar flow sterile hoods using a strict sterile technique that included wiping the hood down and spraying all items entering the hood with 70% industrial methylated spirits. Cell culture plasticware was supplied by Iwaki. All cell culture flasks were gelatinised (5 min 0.1% gelatin in PBS) prior to addition of ES cells. E14TG2a ES cells were used for all experiments. ES cells were incubated in 7.5% $CO_2$ at 37°C in a humidified incubator (Scientific Laboratory Supplies Ltd). All solutions were tested for sterility and warmed to 37°C prior to use. ES cells were examined using an inverted microscope (Olympus CK2).

### 2.2.2 Reagents

ES cells were maintained in 1x glasgow minimum essential medium containing: 10% foetal calf serum; 15% sodium bicarbonate; 0.1% nonessential amino acids; 4mM glutamine; 2mM sodium pyruvate; 0.1mM 2-mercaptoethanol. ES cells were maintained in an undifferentiated state by addition of differentiation inhibiting activity/leukaemia inhibitory factor (DIA/LIF). Human DIA/LIF expression plasmids were used to transiently express DIA/LIF in COS-7 cells (Smith 1991). Serial dilutions of the supernatant were tested on ES cells for their ability to maintain pluripotency. Routinely, 100x the minimum concentration required to keep ES cells undifferentiated was used as the working concentration. All stock solutions were prepared by Derek Rout at the Centre for Genome Research. G418 (PAA Laboratories) was at 200μg/ml, ganncyclovir (Roche) was used at 2.5μM.

### 2.2.3 Thawing ES cells

Frozen ES cell vials were taken directly from the liquid nitrogen storage and quickly thawed in a 37°C water bath. The cell suspension was transferred to a 20ml centrifuge tube containing 10ml of pre-warned ES cell medium. The cell suspension was then centrifuged at 1 200 rpm for 4 min (MSE Mistral 2000 benchtop centrifuge). The media was aspirated and the cell pellet was resuspended in 4 or 10ml ES cell medium and transferred to a single well of a 6 well plate or a 25cm$^2$ flask, respectively.

24 well plates containing frozen adherent ES cells were removed from the -80°C storage and thawed by holding between hands. 1ml of pre-warmed ES cell medium was added to the thawed wells and ~80% was then aspirated. Another 1 ml of ES cell medium was then added to the well and the plate placed in an incubator.

### 2.2.4 Passage and Expansion of ES Cells

Cultures were monitored every day to ensure that ES cells had not grown past confluence. Cells were normally passaged every 2 days. Culture medium was aspirated and cells rinsed twice with PBS. Trypsin solution (0.025% trypsin (Gibco); 0.1% chicken serum (Flow Labs); 1.3mM EDTA (Sigma) in PBS) was added to the cells and incubated ay 37°C to ~5 min until the cells detached. The trypsin was quenched with at least 5 ml ES cell medium and the cells dispersed to a single cell suspension with vigorous pipetting. The cell suspension was centrifuged at 1 200 rpm for 4 min (MSE Mistral 2000 benchtop centrifuge), the medium aspirated and the cell pellet resuspended in ES cell medium. Cells were then transferred to fresh well or flasks at dilution ratios of 1:2 to 1:5, depending on their rate of growth.

### 2.2.5 Freezing ES Cells

ES cells were frozen at ~5x10$^6$ cells or directly in 24 well plates.

For freezing in vials, cells were trypsinised into a single cell suspension and centrifuged as above. The cell pellet was resuspended in 0.5ml ice-cold freezing solution (80% ES cell medium; 10% FCS; 10% dimethylsulphoxide) per vial. The cells were transferred to Nunc cryotubes and the tubes rapidly transferred to the -80°C freezer. The next day,

vials were transferred to liquid nitrogen storage. Exposure to dimethylsulphoxide is kept to a minimum as it is toxic to the cells and is an ES cell differentiation agent.

For freezing 24 well plates, ES cells were grown to ~80% confluence. The medium was aspirated, the cells washed twice in PBS and 0.5ml freezing solution added directly to the wells. Plates were transferred immediately to the -40°C freezer. Plates were moved to the -80°C freezer the next day.

### 2.2.6 ES Cell Electroporation

Exogenous DNA was routinely introduced into ES cells by electroporation. A single cell suspension was obtained and the cells pelleted as above. Cells were resuspended in ES cell medium and counted in a haemocytometer. The appropriate volume of cell suspension was centrifuged again and the cell pellet resuspended in 600µl of PBS. The cell suspension was then transferred to an electroporation cuvette.

For gene targeting experiments, ~150µg of linearised targeting vector was added to the cell suspension in 100µl of PBS. For transient transfection of Cre-expressing plasmid, 60µg of circular pMC Cre (kind gift from A. J. H. Smith) was added to the cell suspension in 100µl of PBS.

Cells were electroporated at 0.8kV, 3µF in a BioRad GenePulser, which would normally result in a time constant of 0.1. The cells were left for 10 min after eletroporation before any further manipulations were performed. Cells were then transferred to a fresh 20 ml centrifuge tube containing 9 mls of pre-warmed ES cell medium. Cells were plated in 10cm tissue culture dishes at densities of $5\times10^6$, $10^6$, $5\times10^5$ and $10^5$ cells per plate. The medium was changed the next day to medium containing G418 selection (200µg/ml).

7-9 days after electroporation, drug resistant colonies were isolated and transferred to individual wells of 24 well plates. Individual colonies were sucked off the culture dish using a 20µl pipette with a yellow tip. The yellow tip containing the colony was placed

into a well of a 96 well plate containing ~100µl of trypsin solution and incubated at room temperature for ~5 min. The contents of the well were then transferred to a well of a 24 well plate containing 2 ml ES cell medium. The medium was changed the next day. As wells became confluent they were passaged to generate duplicate plates, one plate to freeze for storage and another plate from which DNA was extracted for analysis by Southern blotting.

## 2.3 Animals

All animals were housed and treated in accordance with the animals (scientific procedures) act 1986. Animals were housed in a 12:12 light dark cycle with food and water provided *ad libitum*. Wild type litter mate controls were used with *PSD-95* deletion mutants.

### 2.3.1 Loss of Righting Reflex Test

A diagram of the apparatus used is shown in figure 2.1. Mice (30.5 to 61.5g) were placed into a Perspex tube (14cm diameter × 80cm) and the ends sealed with Perspex plates containing a single hole at their centre to allow inflow of gas at one end and outflow at the other. To prevent the animals huddling together, the tube was separated into two equal sections by a wire mesh placed across the tube's diameter. 2 strips of rubber tubing were placed along the internal base of the tube to prevent the mice sliding during the loss of righting reflex test. To maintain body temperature during the procedure, the ambient temperature was maintained between 28 and 32°C and the tube heated from above by two 60W lamps. Insulation (bubblewrap) was placed on external underside of the tube. Halothane was supplied in 100% $O_2$ and gas concentrations measured inline at the exhaust with a Datex CapnoMac Ultima (Datex). A rectal temperature probe was fed into the tube via the gas inflow pipe and used to monitor either mouse or tube internal temperature. Lamp height was adjusted to maintain tube internal temperature at 33.5 ±1.0°C.

Usually 4 different halothane concentrations were tested in one experiment. 6 mice of the same genotype were placed into the tube, 3 in either section. The highest concentration to be tested was supplied to the tube first. To record rectal temperatures,

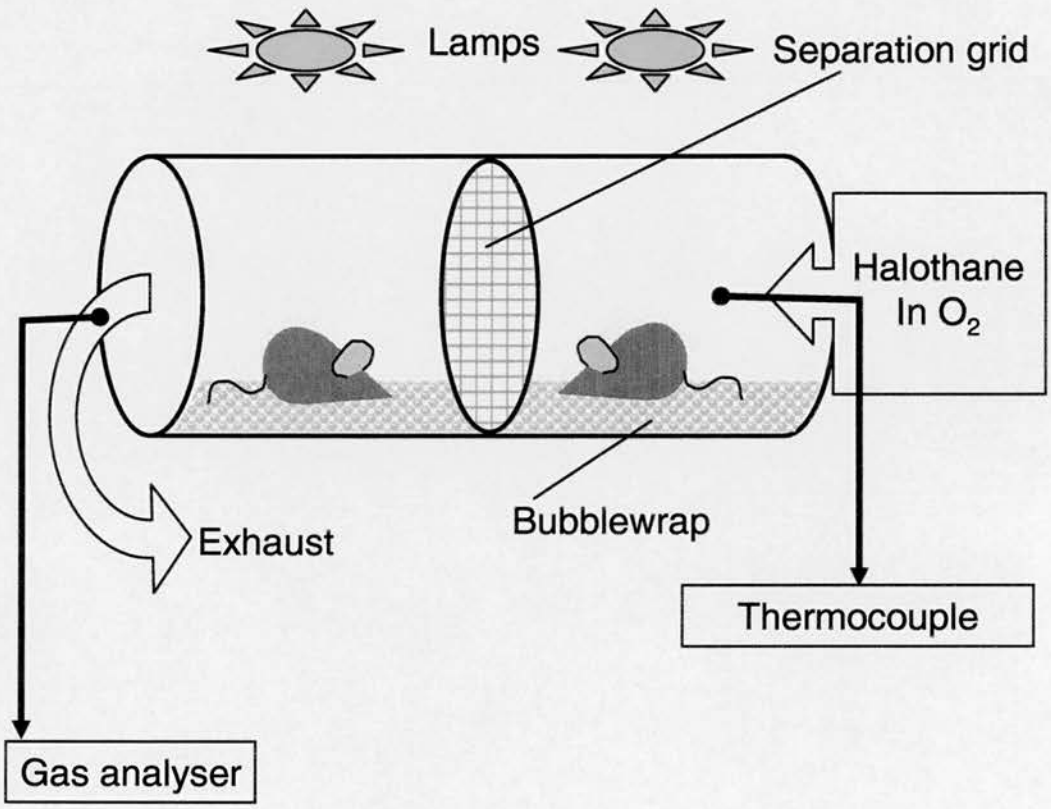


**Figure 2.1 Diagram showing LORR apparatus.** A perspex tube was separated into 2 compartments by wire mesh to prevent mice from huddling together. The tube was heated from above by lamps and bubblewrap was attached to the underside of the tube to provide insulation. Ambient or internal temperature was monitored using a rectal temperature probe fed into the chamber via the gas inlet. The gas outlet was sampled by a gas analyser.

the inflow end of the tube was opened after the halothane concentration within the tube had been stable for at least 7 min. The rectal probe was inserted into one of the mice and the end of the tube was rapidly replaced and mouse internal temperature monitored for at least 10 min. To avoid injuring the animal, the probe was removed from the mouse, but not the tube, prior to performing the loss of righting reflex test. Removing the probe from the mouse could be performed without opening the tube, thus the internal halothane concentration was undisturbed by the process. Tube temperature was monitored for the rest of the experiment.

The loss of righting reflex (or obtunding test) was performed only when the internal halothane concentration had been stable for at least 10 min. The test consisted of rolling the tube sufficiently (<120°) to turn the mice onto their backs. Not all mice were obtunded by a single roll of the tube, so 2-3 rolls were performed to test all mice within the tube. Loss of righting reflex was scored as being unable to right within 5 s of being obtunded.

At the end of each experiment, mice were removed from the tube and allowed to recover under supervision in the warmth of the experiment room. Once recovered, mice were returned to the mouse house.

## 2.4 Data Analysis

Data from halothane-induced LORR experiments was fitted to a dose response curve by nonlinear regression using GraphPad Prism 3.0. Data generated from halothane-induced LORR experiments measured an all-or-nothing response (righting or not righting) across a range of halothane concentrations. Because of the difficulty in dictating halothane concentration delivered to the LORR apparatus, concentrations between genotypes could not be matched. For these reasons, probit analysis was used to analyse the data. 95% confidence intervals were computed and compared at the $EC_{50}$ values of wild type and *PSD-95* deletion mutant animals. This allowed the null hypothesis "the halothane $EC_{50}$ is unaffected by *PSD-95* genotype" to be tested.

# *Chapter 3:* RESULTS Cloning and Characterisation Of Mouse *PSD-95*

## 3.1 Introduction

At the start of this project, there was no information about the genomic structure of the human *PSD-95* gene and detail about the murine gene was limited to the 3' region coding from PDZ3 to the GK domain. PSD-95 isoforms were originally considered species-specific with rodent and human proteins exhibiting distinct N-termini, however, exons encoding 'human' PSD-95 were identified in mouse genomic sequence (described below) . Furthermore, the 'human' transcript and protein was recently identified in rat brain extratcts (Chetkovich *et al.* 2002). In the interest of clarity, I have adopted the nomenclature used by Chetkovich and coworkers to describe the PSD-95 variants and the exons that encode these variants, the rodent variant being designated PSD-95α and the human variant PSD-95β.

As mentioned in the introduction, PSD-95α constitutes the major transcript and has two N-terminal cysteines that, when palmitoylated, mediate synaptic localisation. PSD-95β, which makes up approximately 10% of PSD-95 protein, encodes a longer N-terminus that does not contain cysteines, but does contain an L27 protein interaction domain that mediates synaptic localisation and enables PSD-95β to bind CASK (Chetkovich *et al.* 2002).

The human PSD-95 gene (*DLG4*) corresponding to PSD-95β, was cloned in 1999 and found to span ~30kb of genomic sequence (Stathakis *et al.* 1999). In contrast to studies in rodents, human PSD-95 transcripts were found in a wide range of tissues including brain, mammary gland, pancreas and testes (Stathakis *et al.* 1997) and splice variants distinct from PSD-95α and PSD-95β were found to exhibit tissue-specific distributions (Stathakis *et al.* 1999).

Targeting the exon encoding part of PDZ3 had not generated a null allele (Migaud *et al.* 1998), so to ensure the generation of a conditional null allele, a more 5' region of the gene needed to be targeted. In generating the original *PSD-95* deletion mutant, part of the murine gene had already been characterised from a lambda library clone, identifying exons coding from the third PDZ domain to the end of the open reading frame (Migaud *et al.* 1998). However, exons encoding PDZ domains 1 and 2 and the alternative transcriptional start sites were not contained in the lambda clone and therefore were not characterised (Fig. 3.1). Thus the 5' region of *PSD-95* needed to be cloned and characterised to provide detailed information about the gene structure such as intron-exon boundaries and any alternative splicing events. These properties of *PSD-95* would influence the targeting strategy design and the cloned sequence could then also be used for the generation of a targeting vector.

## 3.2 Identification and Analysis of PAC clones

Since the previously screened lambda library (Migaud *et al.* 1998) did not yield any clones containing 5' sequence of *PSD-95*, I elected to use a different genomic library, a P1 artificial chromosome (PAC) mouse genomic library. PACs are large capacity (up to 250 kb) vectors that generate good quality genomic libraries used for genome mapping and sequencing as well as gene cloning. A 129/SvEvTACfBr mouse genomic PAC library from the human genome mapping project (HGMP) was screened (Osoegawa *et al.* 2000). The library segment used had an average insert size of 147 kb and with 128,899 clones, provided 6.3× genomic coverage (Osoegawa *et al.* 2000), thus the probability of identifying at least one positive clone was >99%.

### 3.2.1 Screening of PAC Library

The project was initiated when only rat and mouse PSD-95 cDNA, corresponding to PSD-95α, had been published, so all PCR primers and cDNA probes were generated using PSD-95α cDNA as a template. The PAC library was constructed using 129/SvEvTACfBr mouse genomic DNA and PAC clones gridded onto nylon hybridisation filters such that each filter contained over 18,000 distinct mouse PAC clones per filter. Each clone was arrayed in duplicate in a pattern that allowed correct identification of specific versus non-specific signals.

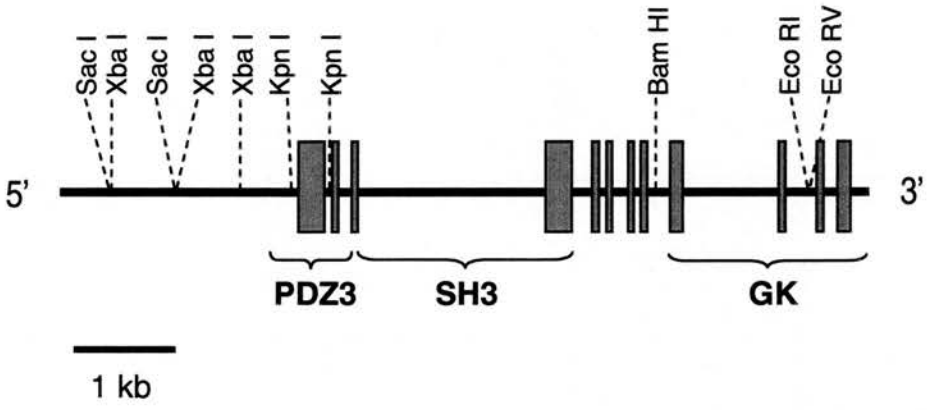


**Figure 3.1 Known *PSD-95* structure at start of project.** Figure shows 3' end of gene containing exons that encode PDZ3, SH3 and GK domains of PSD-95 (Migaud *et al.* 1998). 5' exons encoding the N-terminal region, including PDZ domains 1 and 2. Exons are shown as blue boxes and relevant restriction enzyme sites are labelled.

To identify PAC clones that contained the outstanding 5' *PSD-95* sequence, the PAC library filters were screened with a rat cDNA probe (nucleotides 1-983; GenBank Acc. No. M96853) specific to the 5' sequence of PSD-95α and the first two PDZ domains (PDZ1+2 probe). This probe had previously been demonstrated to hybridise to mouse genomic DNA on a Southern blot. When the PDZ1+2 probe was used to screen the PAC library, strong signals were seen for four clones (456, 534, 612 and 631), while weak signals were observed for another eight clones (377 2C, 377 16E, 390, 431, 460, 484, 500, 507). All twelve clones were ordered from the HGMP resource centre to be used in a second round of screening.

PAC clones were delivered as *E. coli* smeared on agar. Clones were restreaked and grown up as miniprep cultures to provide DNA for secondary screening. A different probe was used to screen the PAC clones by Southern blot for false positive clones. Previous blots of genomic DNA had identified an approximately 12 kb BamHI fragment that positively hybridised to the PDZ1+2 cDNA probe. Following BamHI or EcoRI digestion, Southern blotting, and probing with a PDZ1 probe (nucleotides 5-503), clones 456, 534, 612 and 631 produced positive signals (Fig. 3.2A), these clones having generated strong signals in the original PAC library screen (Table 3.1). Clones 456, 612 and 631 showed positively hybridising BamHI bands of ~12 kb while 534 had a positively hybridising band of much greater than 12 kb. Other clones that had hybridised weakly in the primary screen failed to hybridise when analysed as Southern blots (see Table 3.1).

Finer analysis of the PAC clones was required to ensure that they overlapped with, and contained sequence 5' to the genomic sequence derived from the lambda clone identified by Migaud and coworkers (1998). A PCR strategy was used to assess the regions of the *PSD-95* open reading frame present in clones 456, 534, 612 and 631. Primer pairs (Fig. 3.3) were used that were specific to PDZ1 (M8144, M8145), PDZ3 (A8643, SH3 Spe bot), SH3 (GK for, RPD) and GK domains (GK Spe top, 3N). The PDZ1 reaction failed in all clones, however, M8145 was designed from cDNA sequence and was later found to span an intron-exon boundary and thus was unable to anneal to

**Figure 3.2 Analysis of PAC clones 456, 534, 612 and 631.** ***A***. Southern blot of BamHI and EcoRI digested PAC DNA hybridised with PDZ1 probe. No difference was observed in the size of positively hybridising bands with EcoRI digested DNA, but clone 534 exhibited an anomalous sized band (arrowhead) with BamHI digestion. ***B***. Ethidium-stained gel showing PCR products generated using primer pairs specific to either PDZ1, PDZ3, SH3 or GK coding regions of *PSD-95*. Lanes containing size markers are labelled M. PAC clone 456 was shown to contain partial sequence of *PSD-95*, the GK-coding region being absent. Clone 534 appeared to not contain *PSD-95* sequence while clones 612 and 631 contained regions of the gene encoding the PDZ3, SH3 and GK domains. The PDZ1-specific reaction was later found have failed because one of the primers was intron spanning. ***C.*** Comparison of the *PSD-95* locus in genomic and PAC 631 DNA. Ethidium-stained gel shows overlapping PCR products that span most of the *PSD-95* locus. Genomic and PAC DNA templates generate PCR products of identical sizes.

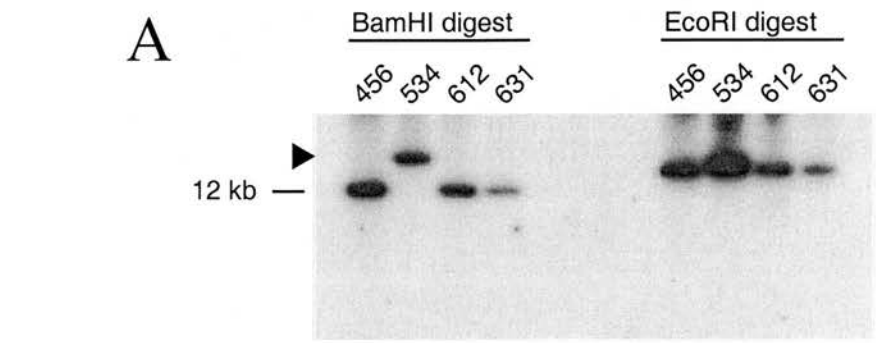
A
BamHI digest
EcoRI digest
456
534
612
631
456
534
612
631
12 kb

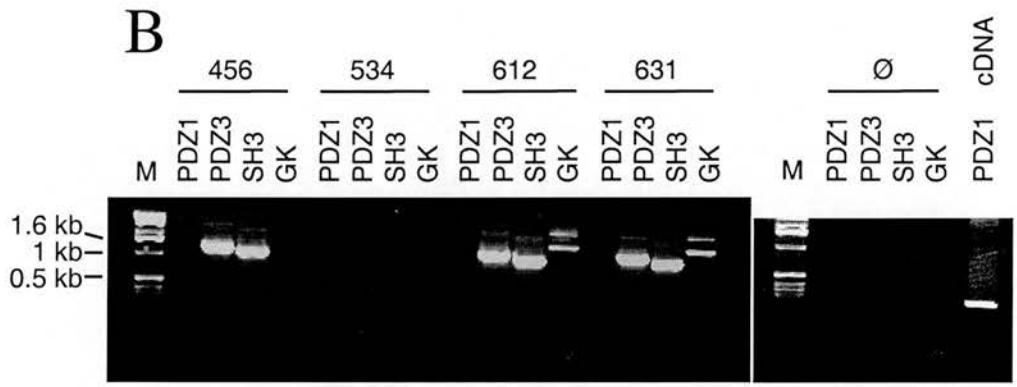
B
456
534
612
631
Ø
cDNA
M
PDZ1
PDZ3
SH3
GK
PDZ1
PDZ3
SH3
GK
PDZ1
PDZ3
SH3
GK
PDZ1
PDZ3
SH3
GK
M
PDZ1
PDZ3
SH3
GK
PDZ1
1.6 kb
1 kb
0.5 kb

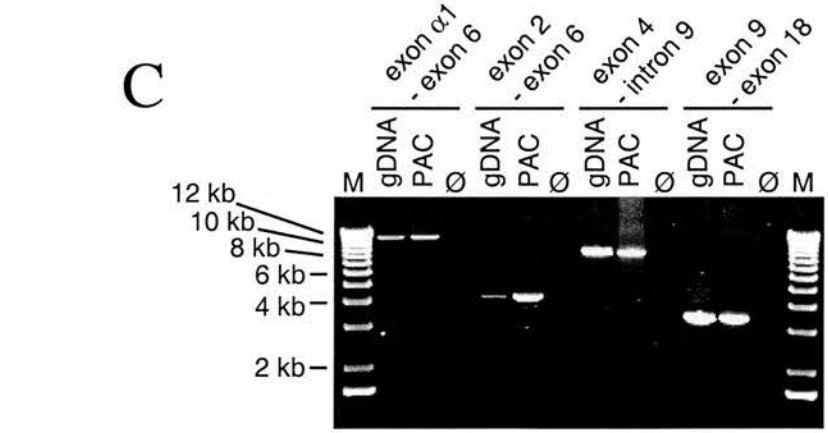
C
exon α1
- exon 6
exon 2
- exon 6
exon 4
- intron 9
exon 9
- exon 18
M
gDNA
PAC
Ø
gDNA
PAC
Ø
gDNA
PAC
Ø
gDNA
PAC
Ø
M
12 kb
10 kb
8 kb
6 kb
4 kb
2 kb

the genomic sequence. The other PCR reactions identified clones 612 and 631 as containing PDZ3, SH3 and GK domains, clone 456 contained PDZ3 and SH3 domains while 534 did not show any amplification using PSD-95 specific primers (Fig. 3.2B), consistent with its aberrant BamHI Southern band. *PSD-95* therefore appears to be represented in this PAC library at a frequency of 3/128 899 clones. Analyses of the PAC clones are summarised in Table 3.1.

| PAC clone no. | Signal strength in library filter screen | Signal in Southern blot screen and comments | PSD-95 domains identified by PCR analysis |
|---|---|---|---|
| 377 2C | weak | no | n/d |
| 377 16E | weak | no | n/d |
| 390 | weak | no | n/d |
| 431 | weak | no | n/d |
| 456 | strong | yes; hybridising fragments correct sizes | PDZ3, SH3 |
| 460 | weak | no | n/d |
| 484 | weak | no | n/d |
| 500 | weak | no | n/d |
| 507 | weak | no | n/d |
| 534 | strong | yes; hybridising BamHI fragment of incorrect size | Ø |
| 612 | strong | yes; hybridising fragments correct sizes | PDZ3, SH3, GK |
| 631 | strong | yes; hybridising fragments correct sizes | PDZ3, SH3, GK |

**Table 3.1 Results of primary and secondary screens for *PSD-95*.** The PACs were screened using a probe (PDZ1+2 probe) specific to the outstanding 5' coding sequence of *PSD-95*. The 12 clones identified in the primary screen of the PAC library are shown. 4 clones (456, 534, 612, 631) positively hybridised to the PDZ1+2 probe in the secondary screen of Southern blots, however clone 534 exhibited an aberrantly sized positively hybridising BamHI fragment. In further analysis by PCR, no *PSD-95* sequence was identified in clone 534. n/d indicates that a clone was not tested.

As clones 612 and 631 were initially identified using the PDZ1+2 cDNA probe, I was confidant that, despite the failure of the PDZ1 PCR, these clones contained sufficient 5' sequence to be useful. Southern blots of PACs 612 and 631 produced identical patterns of positively hybridising bands and clone 631 was chosen for subsequent analysis and cloning of *PSD-95*.

### 3.2.2 Comparison of PAC and Genomic *PSD-95* Structure

Both DNA rearrangement and chimeric clones have been identified in PAC libraries. The library used in this study was analysed for chimerism and rearrangement: ~1% of clones were chimeric; no deletions of >10 kb were identified although smaller rearrangements were identified in <10% of clones (Osoegawa *et al.* 2000). To determine whether rearrangement had occurred in the *PSD-95* locus of PAC 631, comparative Southern blots were performed on PAC and mouse genomic DNA (gDNA). Identical hybridisation fingerprints were observed for both PAC and gDNA, demonstrating the PAC and genomic loci to be grossly similar. Further analyses were performed by long range PCR (LR-PCR) using primer pairs (5' start + PDZ1 Rev; Exon 2 For + PDZ1 Rev; PDZ1 For + 3N; A8643 + B7524) that generated overlapping products spanning from the 5'UTR of PSD-95α to the GK domain. Again, the PAC and genomic loci were shown to be identical by the equally sized products (Fig. 3.2C).

In additional PAC Southerns, a provisional restriction enzyme digest map of *PSD-95* was generated using a panel of restriction enzymes in conjunction with probes specific to either PDZ1 (nucleotides 5-503) or PDZ3 (nucleotides 986-1572). The 12 kb BamHI and larger EcoRI fragment identified in earlier Southern blots (Fig. 3.2A) were found to hybridise to both PDZ1 and PDZ3 probes, implying that the fragments overlapped with the PDZ3 containing lambda fragment. This was supported by the presence of BamHI and EcoRI sites in the lambda clone, 3' to PDZ3 (Fig. 3.1). The 12 kb BamHI fragment was therefore an obvious starting point in subcloning the *PSD-95* gene.

## 3.3 Subcloning PSD-95 Genomic Fragments

Large scale PAC preparations were required to facilitate subcloning, however the ~160 kb PAC proved difficult to grow in Luria Bertani medium and purification using Qiagen midiprep columns failed to generate good yields due to inefficient elution of the PAC from the column matrix. A variety of methods were therefore tested until reasonable yields (500μg DNA from a 500ml culture) were obtained using a protocol obtained from the Oxford University Bioinformatics Centre (see Methods). This method utilised a rich medium (2xTY) and alkaline lysis but resin columns were not used to purify the PAC

DNA. Instead, RNA and protein contaminants were degraded followed by phenol/chloroform extraction to remove degraded proteins and added enzymes.

The PAC's size also complicated the isolation and subcloning of the 12 kb BamHI fragment. Following digest, gel separation and purification, the yield of the correct fragment was low and after extensive optimisation, the fragment could still not be subcloned using standard methods. I therefore performed shotgun cloning: Digested PAC was added directly to ligation reactions to generate a library of PAC fragments in pBluescript KSII that was then transformed into *E. coli*. The resultant colonies were screened by colony hybridisation using the PDZ1 probe to identify correct subclones. This method yielded the correct 12.4 kb BamHI subclone, BamHI (9) and was subsequently used to isolate other useful subclones: SacI (1), SacI (20) and KpnI (4). These subclones are shown in relation to the genomic structure of *PSD-95* in figure 3.3.

BamHI (9), SacI (1) and KpnI (4) were mapped by restriction enzyme digest and confirmed to overlap with each other, and BamHI with the lambda clone. The positions of exons were determined by PCR using exon-specific primers while sequencing identified the intron-exon boundaries.

SacI (20) was also analysed by restriction enzyme digest and PCR but was found not to overlap with KpnI (4), the most 5' of the overlapping subclones. To characterise the intervening region, LR-PCR was performed using a forward primer specific to the PSD-95α 5' UTR (5' start) and a reverse primer specific to PDZ1 (PDZ1 reverse). The LR-PCR product was digest mapped and compared to the Southern digest map of *PSD-95*, allowing a SacI fragment containing the intervening sequence to be identified. However, the genomic sequence that separated SacI (20) from KpnI (4) proved impossible to subclone from the PAC library using the probes available (e.g. exons 1-4 probe), but was subcloned from the 5' start-PDZ1 rev LR-PCR product (SacI (LR)), allowing a more detailed and accurate restriction enzyme map of this area to be made.

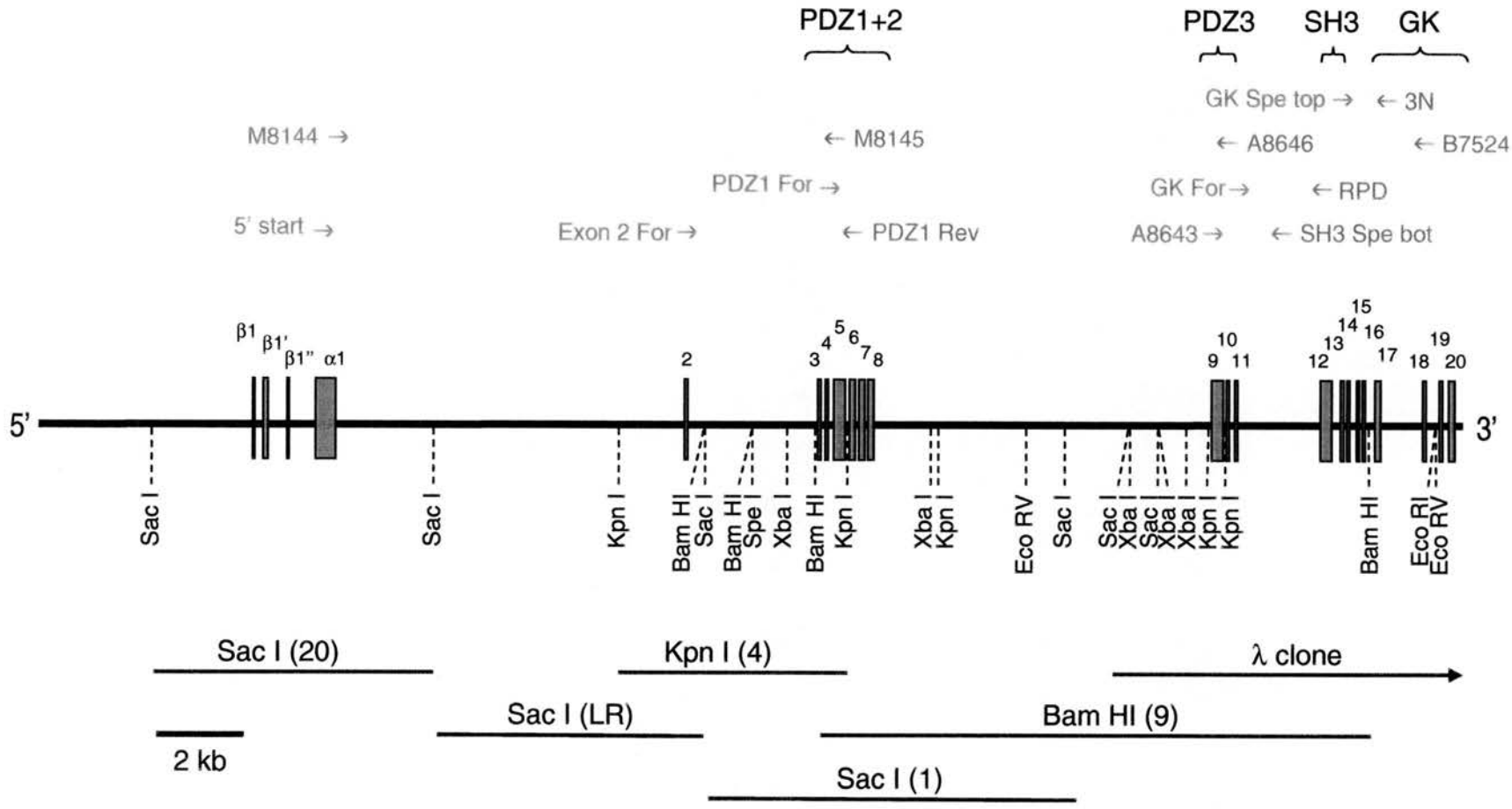


**Figure 3.3 Genomic structure of mouse *PSD-95*.** The *PSD-95* locus is shown as a solid line, exons are depicted as grey boxes and are numbered (above), restriction enzyme sites are labeled below. Subcloned sequences are shown below as lines and labeled with the subclone name. The location of primers is shown above the genomic structure. Forward primers are represented by blue arrows with blue labels. Reverse primers are shown as red arrows and are labeled in red. Domains encoded by exons are indicated top.

## 3.4 Characterisation of PSD-95 Gene Structure

I focussed on characterising the 5' region of mouse *PSD-95* since the 3' region had already characterised and the 5' region was to be the target of any subsequent mutation. I therefore wanted to determine not only the intron-exon boundaries, but also identify alternative splice variants and promotor sequences.

Using the information from the subclones combined with LR-PCR data, the genomic structure of PSD-95 could be clarified and is shown in Fig. 3.3. All sequences were cloned and analysed prior to the publication of PSD-95α and PSD-95β (Chetkovich *et al.* 2002), however I have adopted the nomenclature used by Chetkovich and coworkers in the interest of clarity. SacI (20) was completely sequenced, thus sequence alignment was performed to determine the presence of exons homologous to what was thought at the time to be the human PSD-95 variant, PSD-95β. In concordance with Chetkovich and coworkers (2002), the PSD-95β-specific exons (β1', β1'') were found 5' to the single PSD-95α exon (α1; Fig. 3.4A). Homology in the 5'UTR sequence encoded by exon β1 was weak, however sequence surrounding the translation start codon was reasonably well conserved (Fig. 3.4B). Murine PSD-95 therefore spans over 27kb of genomic sequence.

Comparing mouse *PSD-95* with its human homologue, DLG4 (Stathakis *et al.* 1999), revealed identical intron-exon boundaries (Table 3.2). Intron and exon sizes are shown in table 3.2, as are splice donor and acceptor sequences, which show 53% – 93% homology to consensus sequences. In addition, the human and mouse genes exhibit a remarkably similar exon distribution, in particular, exons 3 – 8 encoding PDZ domains 1 and 2 are clustered, with small introns separating them (Fig. 3.5.).

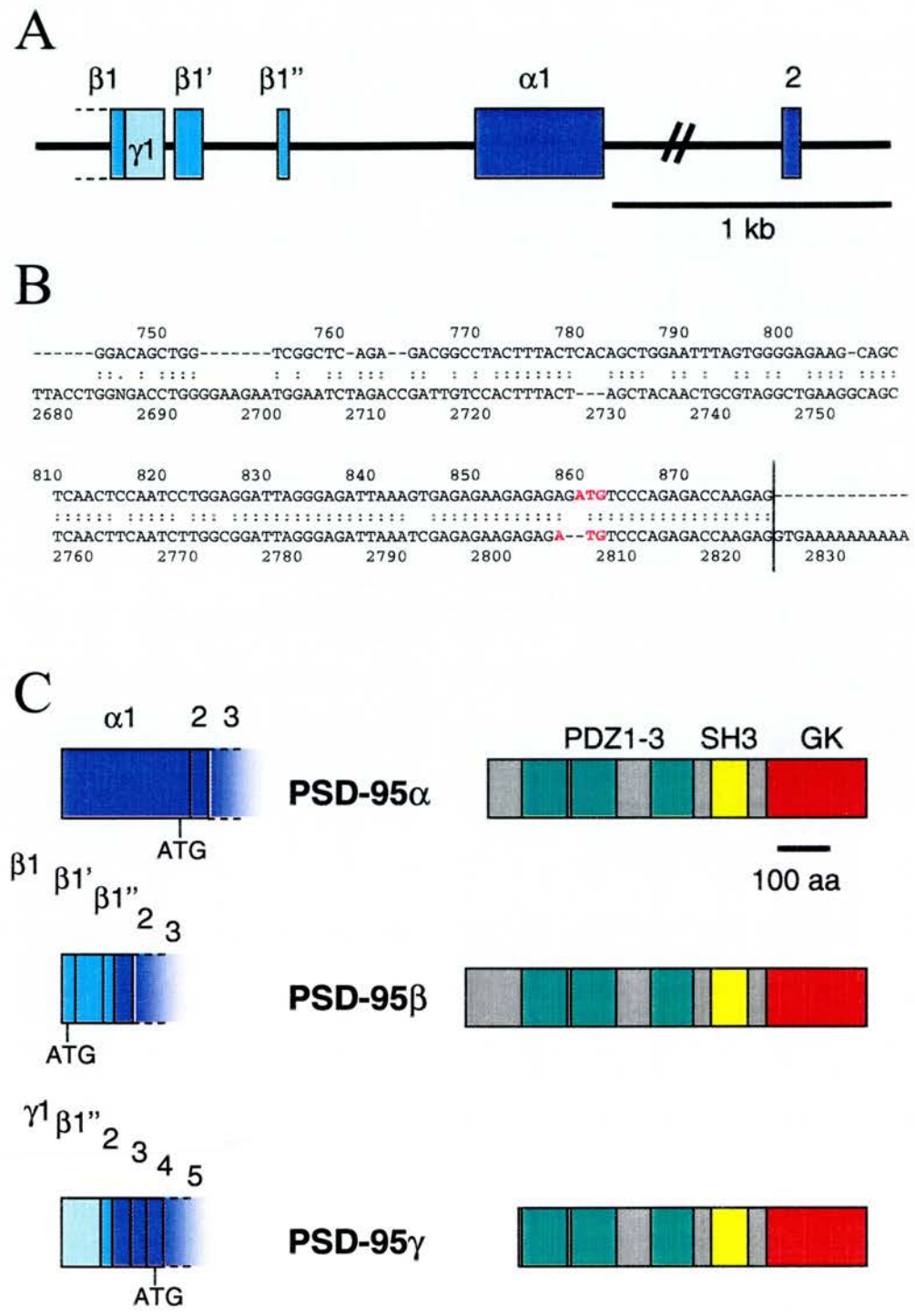


**Figure 3.4 Alternate transcriptional start sites generate N-terminal variety in PSD-95.** ***A:*** Genomic organisation of alternate 5' exons. ***B:*** Homology between mouse and human β1 exons is limited to sequence surrounding the translational start codon (red). Human PSD-95β cDNA (top; GenBank U83198) aligned against mouse genomic sequence from subclone SacI (20) (bottom). Vertical line designates intron-exon boundry. ***C:*** Diagrams on left show partial open reading frames of PSD-95 isoforms. Diagrams on right show translated protein products. Open reading frames and protein products of PSD-95α and PSD-95β are known while those of PSD-95γ are predicted from EST BI731555 .

| exon | exon size (bp) | cDNA position | 5' splice donor junction | intron | intron size (bp) | 3' splice acceptor junction | codon type |
|---|---|---|---|---|---|---|---|
| 1 | 459 | -372 - +87 | ACCAAGgtaagcatgatgggg (8/9) | 1 | n/d | tgtccccatccccagAAATAC (19/28) | 0 (K) |
| 2 | 66 | 88 - 153 | AACCAGgtaaacgcccccnag (7/9) | 2 | 3410 | tgtctcctctcacagGCCAAT (26/28) | 0 (Q) |
| 2b | 165 | 88 - 153 + 99 | CTCAAGgtaggagaccctggc (7/9) | 2 | 3311 | tgtctcctctcacagGCCAAT (26/28) | 0 (K) |
| 3 | 54 | 154 - 207 | GGATATgtgagttgtttagat (7/9) | 3 | 142 | ttctgccccgtgctgGAGTTG (22/28) | 0 (Y) |
| 4 | 60 | 208 - 267 | GAAAGGgtgagtgccagcccc (8/9) | 4 | 212 | tctttttttccccagGGTAAC (26/28) | 0 (R) |
| 5 | 125 | 268 - 392 | CCTCAGgtggggagagaagac (7/9) | 5 | 97 | cgctgctgttcccagGGTCAA (19/28) | 2 (R) |
| 6 | 170 | 393 - 562 | CTAAAGgtagtactcgttcaa (6/9) | 6 | 97 | ctccctcccatccagGACTTG (25/28) | 1 (G) |
| 7 | 137 | 563 - 699 | CTGGCGgtgaggacctcaacc (6/9) | 7 | 153 | tcccctccccccccagGTCAAC (26/28) | 0 (A) |
| 8 | 145 | 700 - 844 | CAACCTgtgagagccctccaa (6/9) | 8 | n/d | cctgtctcccctcagCATATT (24/28) | 1 (S) |
| 9 | 296 | 845 - 1140 | CTGTCGgtgagagagcccgtg (6/9) | 9 | 165 | cttctccctttctagGTCAAT (19/28) | 0 (S) |
| 10 | 103 | 1141 - 1243 | CAGAAGgtaccacgcctaagc (6/9) | 10 | 159 | cttgtccttactcagAGTATA (21/28) | 1 (E) |
| 11 | 115 | 1244 - 1358 | TATCAGgtaagaccgtccttg (8/9) | 11 | n/d | acttgtgttatccagGGCCCT (19/28) | 2 (R) |
| 12 | 177 | 1359 - 1535 | ACGGCGgtgaggctcctgggg (6/9) | 12 | 255 | ctatgtatcccatagGGTCGA (23/28) | 2 (R) |
| 13 | 37 | 1536 - 1572 | GCCAAGgtaggtggaaggtag (8/9) | 13 | 92 | tgctttttcttctagGACTGG (19/28) | 0 (K) |
| 14 | 28 | 1573 - 1600 | CACAGGgtaggtagagttaat (7/9) | 14 | 128 | cctgtctcctaccagGTCGAG (22/28) | 1 (G) |
| 15 | 48 | 1601 - 1648 | TGGAAGgtgagcctctgcccc (8/9) | 15 | 76 | accatttctccccagTGCACT (19/28) | 1 (V) |
| 16 | 102 | 1649 - 1750 | TCCCTCgtgagtacggggtcc (6/9) | 16 | 238 | atgacttcttggcagATACGA (15/28) | 1 (H) |
| 17 | 172 | 1751 - 1923 | GAGCAGgtaagaagctggcag (8/9) | 17 | 879 | cntgcctgcccccagGGGAAG (24/28) | 0 (Q) |
| 18 | 109 | 1924 - 2033 | TGTGCTgtgagtatggtccca (6/9) | 18 | 508 | tctccctcttgacagAGAGAT (23/28) | 1 (A) |
| 19 | 91 | 2034 - 2125 | TCTCAGgtgagaggccangca (8/9) | 19 | 223 | ctgcctgacttgcagCCATCG (21/28) | 2 (L) |
| 20 | 179 | 2126 - 2305 | - | - | - | - | - |

**Table 3.2 Intron-exon splice junctions of mouse *PSD-95*** Negative cDNA position values indicate novel 5'UTR sequence. Positive cDNA position values denote position in published cDNA (GenBank D60621). Uppercase letters denote nucleotides contained in exon, lowercase letters denote nucleotides contained in intron. Number of nucleotides identical to consensus sequence is given in parenthesis. 5' splice donor consensus: MAGgtragt, where M = C/A and R = A/G. 3' splice acceptor consensus: $(y)_{23}$ncagG, where Y = C/T and N is any nucleotide (Penotti 1991). Codon types: 0 = intron located between codons; 1 = intron located between first and second nucleotides within a codon; and 2 = intron located between second and third nucleotides within a codon.

**Figure 3.5 Relationship of mouse *PSD-95* to its human homlogue, mRNA transcript and protein sequence.** The genomic structure of DLG4, the human homologue of PSD-95, is shown top with the genomic structure of mouse PSD-95 shown beneath it. Loci are shown as solid lines with exons depicted as grey boxes. Exons encoding the unique PSD-95α or -β sequences are labeled. Below, the gene structures is shown the PSD-95α mRNA; the 5' UTR is indicated by diagonal blue hatching while the coding sequence is signified by solid blue. The protein structure is shown bottom.

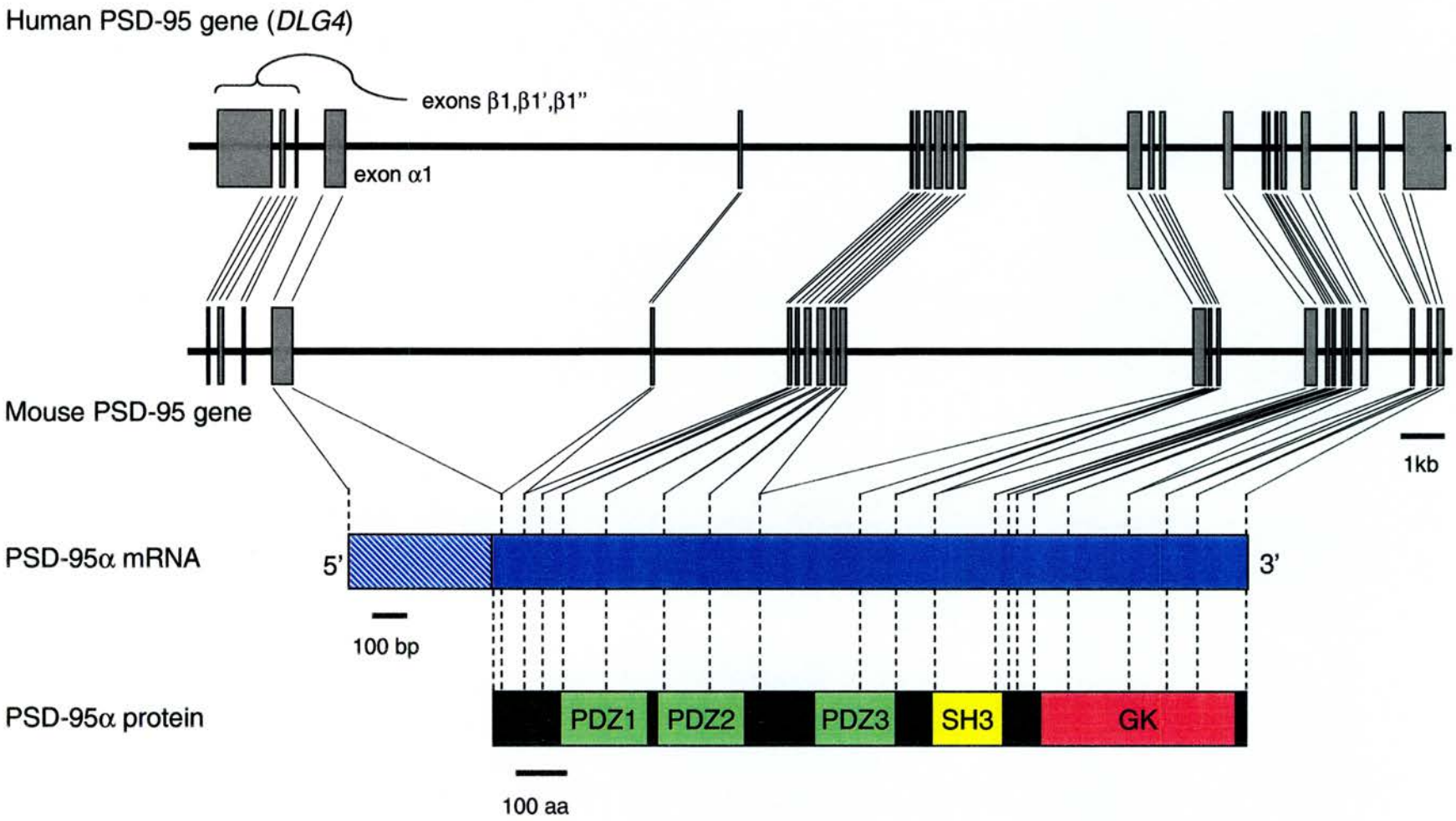
Human PSD-95 gene (*DLG4*)
exons β1,β1',β1"
exon α1
Mouse PSD-95 gene
1kb
PSD-95α mRNA
5'
3'
100 bp
PSD-95α protein
PDZ1
PDZ2
PDZ3
SH3
GK
100 aa

### 3.4.1 PSD-95γ

Sequence analysis identified exons β1, β1' and β1'' in the cloned murine genomic sequence. To determine whether the sequence encoded by these exons was expressed, I screening it against mouse expressed sequence tags (ESTs) using NCBI BLAST. PSD-95β was not identified, which is surprising in light of the findings of Chetkovich and colleagues (2002), however BLAST analysis did identify a mouse EST (GenBank accession number: BI731555) that contained sequence homologous to exon β1''. EST BI731555 is the 5' sequence of a partial cDNA clone identified from a mouse retina cDNA library and contains a unique first exon (γ1), a second exon consisting of exon β1'' followed by sequence homologous to *PSD-95* exons 2 through 5. The unique γ1 exon of BI731555 was identified in SacI (20), between exons β1 and β1' (Fig. 3.4A).

BI731555 is only a partial cDNA sequence and alignment of BI731555 sequence to PSD-95 cDNA revealed some sequencing errors i.e. insertion of incorrect bases. Following correction of BI731555 sequence by removal of these spurious bases, BI731555 cDNA sequence was translated using the Translate programme (see Methods section). Reading frame 1 generated a protein at least 117 amino acids in length, however analysis using ScanProsite failed to identify any potential protein domains. Reading frame 2 produced a 14 amino acid peptide. Reading frame 3, in frame with PSD-95, generated a protein containing part of the first PDZ domain of PSD-95 by utilising a start methionine encoded in *PSD-95* exon 4. Sequence information is limited, preventing the establishment of whether the entire PDZ domain is encoded and thus functional, however, BI731555 could represent another PSD-95 variant, PSD-95γ (Fig. 3.4C), with a novel 5' UTR that is encoded by an alternative start site.

To examine the potential variety of PSD-95 isoforms at the protein level, immunoprecipitations and Western blots were performed on mouse brain homogenate. The blots were probed with an anti-PSD-95 antibody that recognised an epitope between amino acids 77 and 299 (from the middle of PDZ1 to between PDZ2 and PDZ3), a region that is not alternatively spliced. Immunoprecipitations were performed using an

anti-NR2B antibody to determine whether any PSD-95 isoforms identified also bound the NMDA receptor.

The anti-PSD-95 antibody identified 3 immunoreactive bands in mouse brain homogenate: a major band presumably corresponding to PSD-95α, a minor band (band 1) of slightly higher electophoretic mobility and a much smaller band (band 2) of approximately 70 KDa (Fig. 3.6). If PSD-95γ transcribed exons 2 to 20, a protein would be expected that lacked the first 60 amino acids of PSD-95α, with an estimated molecular weight of ~87KDa. Band 1 may represent such an isoform. It is notable that the PSD-95α band and band 1 are both observed in the immunoprecipitant (Fig. 3.6), indicating that the band 1 protein retains the ability to bind the NMDA receptor. No known PSD-95 isoforms are able to generate a protein the size of band 2, therefore it might represent a cross-reacting protein, consistent with its absence from the immunoprecipitant (Fig. 3.6). It therefore appears that at least one smaller PSD-95 isoform is present in the brain that is capable of interacting with the NMDA receptor.

### 3.4.2 5' RACE

The published PSD-95α mouse cDNA has a very short 5' untranslated region (UTR) compared to PSD-95β (1198 nucleotides). To determine the full length of the PSD-95α 5'UTR and to facilitate promotor analysis, rapid amplification of cDNA 5' ends (5'RACE) was performed on mouse brain RNA. Sequences corresponding to PSD-95β and PSD-95γ were not identified by this method, possibly due to their low expression. A prominent product of approximately 500bp was cloned and sequenced, identifing an additional 371bp of PSD-95α 5' UTR (Fig. 3.7A). Thus, all PSD-95 variants have long 5'UTRs (428, 1198 and 333 nucleotides for PSD-95α, β and γ respectively) implying possible translational control of these transcripts. UTR scan (Pesole *et al.* 2002) failed to identify translational control elements in these 5'UTRs, however, upstream open reading frames (uORFs) were identified in the 5' UTRs of all PSD-95 variants: 1 uORF in mouse PSD-95α (Fig. 3.7A), 8 in human PSD-95β and 4 in mouse PSD-95γ. uORFs in the 5' UTR are able to exert translational control via a number of mechanisms, including the stalling of ribosomes or the dissociation of ribosomes following uORF

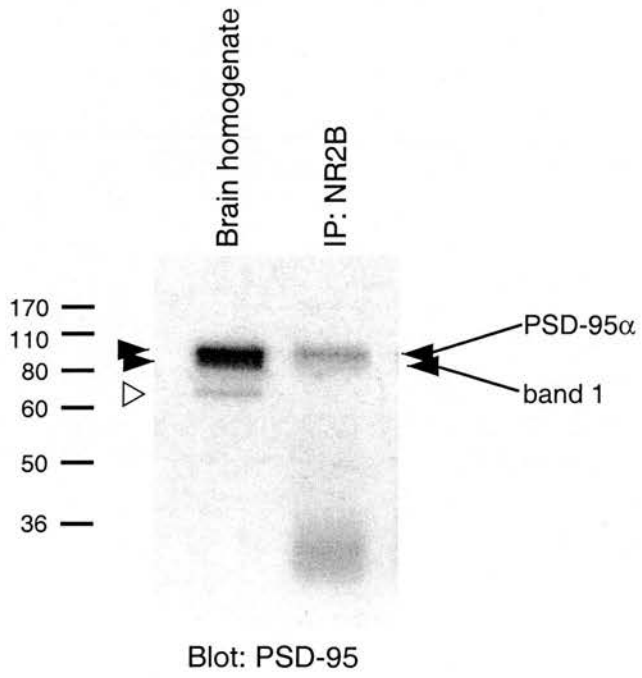


**Figure 3.6 Analysis of PSD-95 isoforms and their ability to interact with the NMDA receptor.** Western blot of mouse brain homogenate and anti-NR2B immunprecipitation. The PSD-95α band is indicated by black arrowheads and can be seen following immunoprecipitation, indicating its interaction with the NMDA receptor. Band 1, possibly corresponding to PSD-95γ, is labelled by grey arrowheads and also associates with the NMDA receptor. A likely cross reactant is labelled with an open arrowhead.

**Figure 3.7 5' UTR and potential promotor sequence of PSD-95α.** ***A:*** cDNA sequence of PSD-95α 5' UTR. Upstream open reading frame is boxed in red. Known PSD-95 cDNA (D50621) is bold, novel sequence is in italic. The translation start codon is in red. ***B:*** Alignment of mouse (top) and human (bottom) genomic sequences reveal potential PSD-95α promotor. Exon α1 is boxed in dark blue. A region of homology (highlighted in yellow) can be seen in the ~200bp 5' to exon α1, potentially revealing the promotor driving the PSD-95α variant.

# A

```
-372 GCCATCTCCA ACCCCCCCCA CCCCACTCCC CCGCCACGGC CCCTAGCCCC TGGCCGTTTG
-312 GCAAGACCCC CGCATACCCC GGGGCTTCCC GAAATCCAGT TCCCCTCCCC CATCCCAGCT
-252 CATGCCCCAG CCCCAGAACT CCGGGGCTGC CAGCCCCCTG TGCCCCTACC CCTCCTGAGA
-192 ATCGGGGTGT GCTCCTCAAG CCCCCTCCCC TCCACTGGGG AGCCCCTTTT AGGGTCCCCC
-132 CTCCCTTCCA CGCTCCCCTA CCCTTCTCTT CTCCAACCTT CTCCTTCCCC TCTCACCCCT
 -72 CCCCCCATCC TGGCCCCCCC TGCAAAAGTG GGGTGCGGAG GGGGGAGGGG TGAGAACCCA
 -12 CCGAGGGGAG GAACAAAACT CCAATGAAGT CAGAGCCCCC TACTCGCCGC CGCGGCCAGG
  48 CCCCCCAACA TGGACTGTCT CTGTATAGTG ACAACCAAG
```

# B

Mouse *PSD-95* sequence top, human *DLG4* sequence bottom

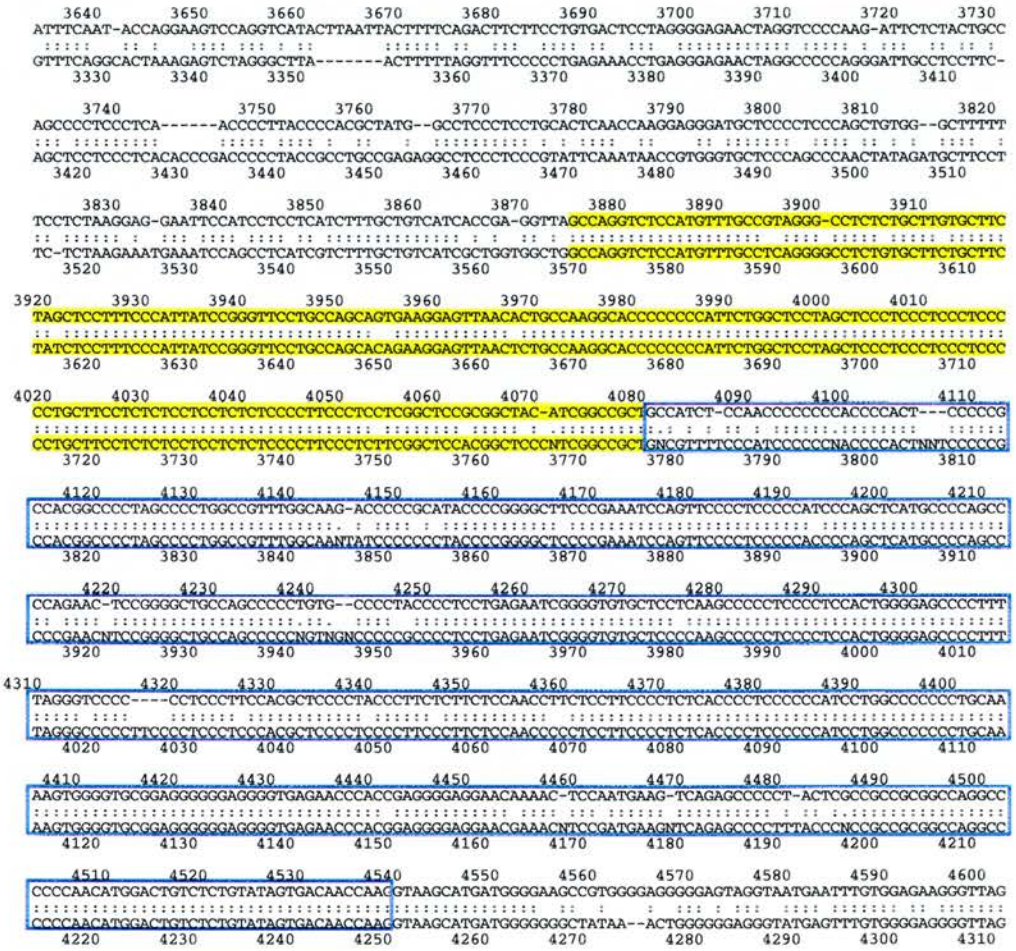

translation (reviewed by Morris and Geballe 2000). Both these methods prevent ribosomes reaching and translating the downstream open reading frame. Translational control of PSD-95 can also be inferred from the abundance of PSD-95 transcripts in embryonic mouse brain as early as 13 days post coitum (Fukaya *et al.* 1999), while the earliest detection of protein, at low levels, is at postnatal day 2 (Cho *et al.* 1992).

### 3.4.3 Promotor Analysis

The apparent use of alternative transcriptional start sites by *PSD-95* prompted me to analyse the cloned genomic sequence for promotor sequences that might drive the various transcripts. Mouse genomic sequence encompassing sequence 5' to γ1, β1, and α1 exons was subjected to a number of analyses including promotor scanning services (Proscan 1.7 and NNPP) and screening for CpG islands (Grail 1.3), which are associated with approximately 50% of mammalian transcriptional start sites (Antequera and Bird 1999). Unfortunately, these programs failed to identify a promotor or an associated CpG island, although it should be noted that *DLG4* is driven by a TATA-less promotor (Stathakis *et al.* 1999). Despite the failure of these analyses, comparison of mouse and human sequences revealed a high level of homology (88%) in the ~200bp of genomic sequence immediately 5' to exon α1 (Fig. 3.7B), potentially exposing a promotor.

### 3.4.4 Alternative Splicing

The considerable conservation between mouse and human genes, both in structure and use of alternate transcriptional start sites, led me to investigate alternate splicing in the mouse. *DLG4* exhibits a number of splice variants: a variant in which exon β1'' is omitted; an exon 18 variant that is not expressed in brain, where PSD-95 is highly expressed; and a variation at exon 2. Since PSD-95β is the minor variant and the exon 18 variant is not expressed in the brain, I focussed on the potential alternative splicing of exon 2 in the mouse. Following RT-PCR, two products were observed (Fig. 3.8A), a major product of the expected size and a less abundant product approximately 100 bp larger than the expected product. Both products were TA cloned and sequenced. Sequence analysis identified the smaller fragment as PSD-95 and revealed the larger product to be a splice variant resulting from a 99 nucleotide extension of exon 2,

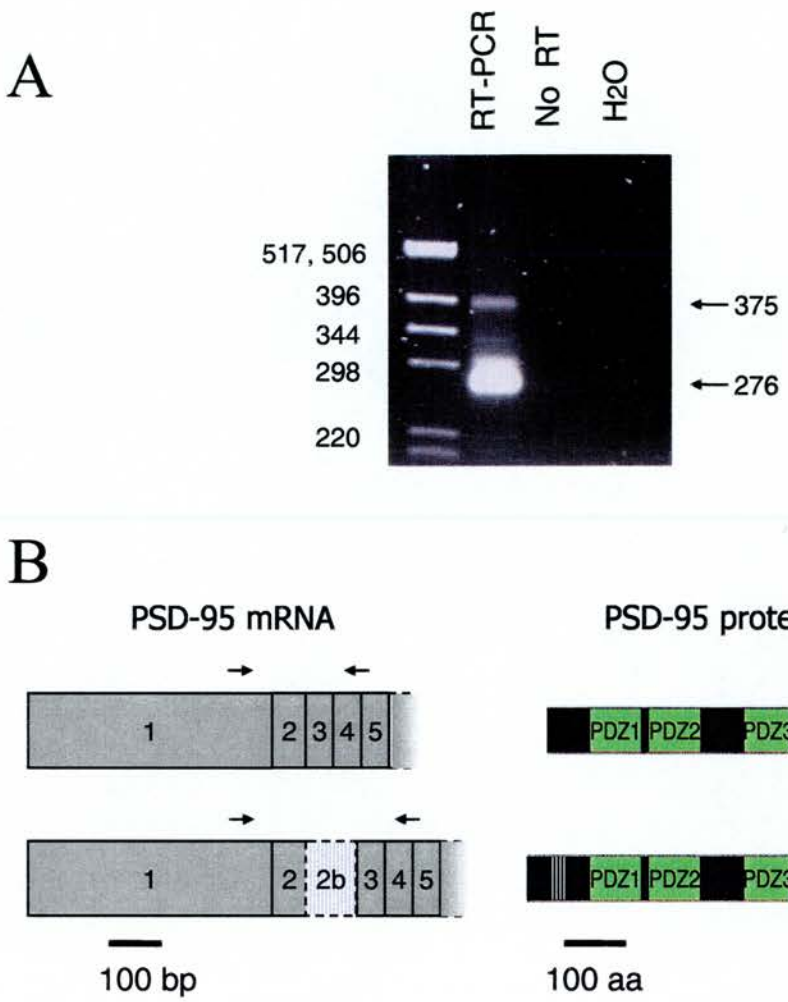


C

| | |
|---|---|
| mPSD-95 | V N A P E L V H V A E R N L S H L E A V H G V V G H A H L S P I K |
| hPSD-95 | V N A P E L V H V A E R N L S H L E A G H G V V G H A H L S P F K |
| hSAP97 | V I G P E L V H V S E K N L S E I E N V H G F V S H S H I S P I K |
| hChapsyn110 | V R G P E L V H V S E K N L S Q I E N V H G Y V L Q S H I S P L K |

**Figure 3.8 Mouse *PSD-95* is alternatively spliced at exon 2.** ***A:*** RT-PCR from mouse brain mRNA generates 2 products, a major product of 276 bp, and a minor product of 375 bp. ***B:*** Cloning and sequencing of the RT-PCR products revealed the minor 375 bp product to result from a 99 bp extension of exon 2, designated exon 2b. On the left, partial open reading frames are shown, indicating the inserted 2b sequence (striped). Positions of primers (arrows) used for RT-PCR are shown above mRNA. The 99 bp extension of exon 2 results in a 33 amino acid insertion, shown right (striped section of protein). ***C:*** Mouse PSD-95 (mPSD-95) insertion is aligned against the protein sequences of the analagous human insertion (hPSD-95) and sequences found constitutively in SAP97 and chapsyn-110. Human sequences of these proteins are shown; hSAP97 and hChapsyn110 respectively.

analogous to that seen in humans (Stathakis *et al.* 1999). The alternative splicing event introduced a 33 amino acid insertion after residue 32 of mouse PSD-95, N-terminal to the first PDZ domain (Fig. 3.8B). The inserted mouse sequence shares 96% homology with the human insertion at the nucleotide level, resulting in two amino acid substitutions between mouse and human (Fig. 3.8C). Sequence homologous to the alternate transcripts is found constitutively in Chapsyn-110 and SAP97 proteins (Fig. 3.8C), however, when analysed by ScanProsite the PSD-95 inserted sequence contained only a putative casein kinase II phosphorylation site that has a high probability of random occurrence. Thus a function for this insertion has yet to be determined.

Western blot analysis should have identified the exon 2b splice variant and PSD-95β at higher molecular weights than PSD-95α, however these were not observed (Fig. 3.6). The exon 2b splice variant and PSD-95β may not have been expressed at levels high enough to be seen at the exposure shown (Fig. 3.6), and at higher exposures they may have been masked by the strong PSD-95α signal, which masked weaker nearby signals such as band 1.

## 3.5 Discussion

The cloning of murine *PSD-95* has revealed considerable similarity between the mouse and human homologues, both in the organisation of the gene and the intron-exon boundaries. Further similarity was demonstrated with the identification of the murine exon 2b splice variant, while a novel putative variant, PSD-95γ was found to result from an alternative transcriptional start site. Murine *PSD-95* is a ~27 kb locus containing 24 exons, exons 2-20 being included in the PSD-95α and PSD-95β isoforms, and possibly the PSD-95γ isoform.

### 3.5.1 PSD-95 Variants

Exons α1, β1 and γ1 are utilised by alternative transcriptional start sites, generating protein diversity in the N-terminal region through the use of different translation initiation methionines. This N-terminal variety results in the inclusion of palmitoylation sites in PSD-95α and an L27 domain in PSD-95β, which alter the membrane targeting

mechanisms used by PSD-95 and its protein interactions. It should be noted that the putative translated PSD-95γ lacks both palmitoylation and L27 sites, so another membrane targeting mechanism must used if PSD-95γ interacts with the NMDA receptor.

In addition to generating differences in the protein, however, alternative splice sites also allow greater variety in the control of transcription by the use of different promotors or translation through the generation of distinct 5'UTRs. This is particularly pertinent in light of the developmental expression profile of *PSD-95*, which is observed at the transcript level in embryonic mouse brains (Fukaya *et al.* 1999), but protein is not seen at substantial levels until after birth (Cho *et al.* 1992; Sans *et al.* 2000). Transcriptional and translational control therefore provides considerable potential for variants to be expressed with distinct developmental and/or regional distributions.

### 3.5.2 MAGUK Evolution

MAGUKs are found in species as diverse as *C. elegans* and man. Moreover, a homologue of ZO-1 has been identified in *Hydra* (Fei 2000), a member of the second oldest phylum in the animal kingdom, indicating that MAGUKs arose early in evolution.

A notable feature of the genomic organisation of *PSD-95* is the cluster of exons encoding PDZ domains 1 and 2. The clustered arrangement of exons encoding PDZ domains 1 and 2 and their intron-exon boundries are conserved in the genomic oganisation of another mouse MAGUK, *SAP102* (P. Cuthbert – personal communication). In addition, a similar arrangement of coding sequence is observed in *Drosophila*; sequence encoding PDZ domains 1 and 2 of DLG consists of 2 exons that are separated by a 61 nucleotide intron (Fig 3.9). Interestingly, the close association of PDZ 1 and 2 encoding exons is mirrored by a close association between PDZ 1 and 2 protein domains; PDZ domains 1 and 2 form a single, protein module that is resistant to protease digestion (Marfatia *et al.* 1996). These observations therefore raise interesting questions about the development of the MAGUK genes with evolution. Interesting information about the evolution of the MAGUK genes may be gained from a species

evolutionarily intermediate between *Drosophila* and mouse. Although a PSD-95 related MAGUK has yet to be cloned from zebrafish, this species may yield interesting information once its genome has been fully sequenced.

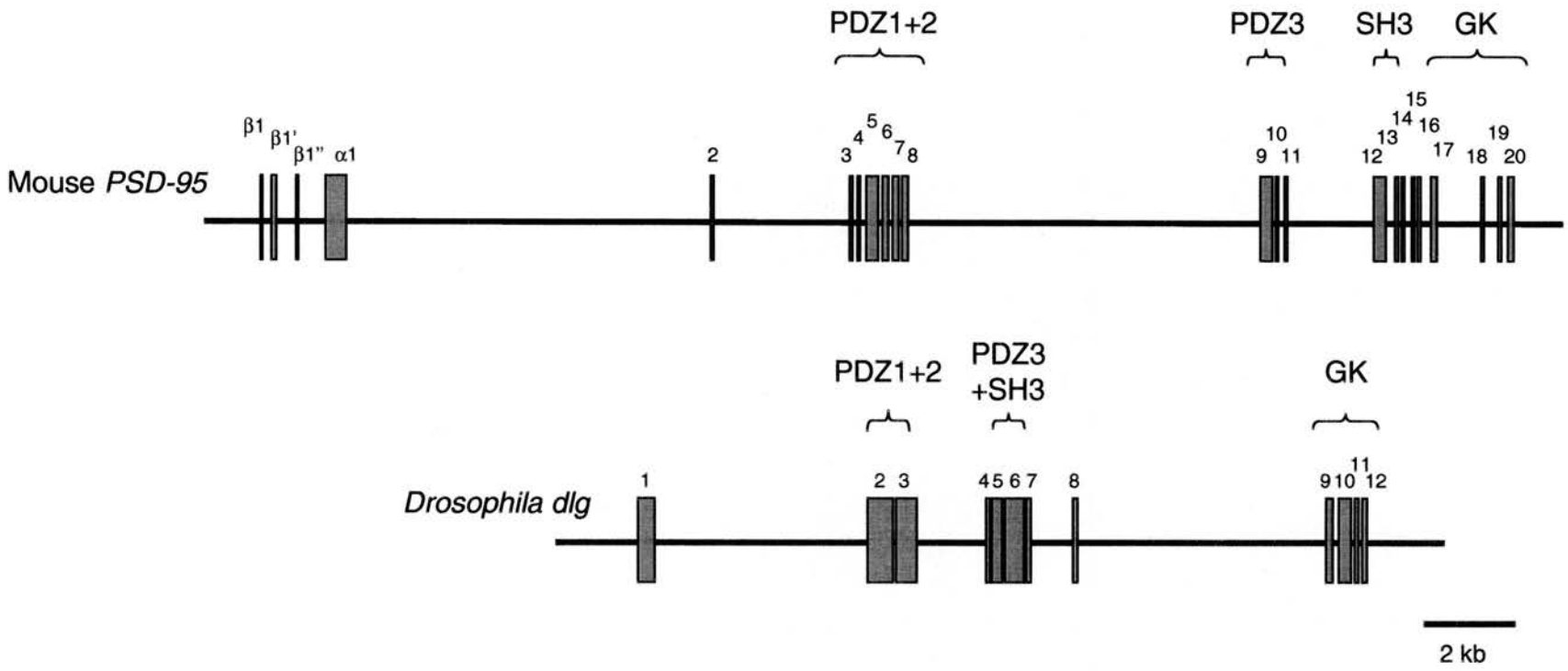


**Figure 3.9 Comparison of mouse *PSD-95* and *Drosophila dlg* genomic structures.** Exons encoding PSD-95 PDZ domains 1 and 2 are separated by small introns, producing a clustering of these exons. Similarly in *Drosophila*, the 2 exons that encode DLG PDZ domains 1 and 2 are separated by a 61 nucleotide intron. Diagrams are drawn to scale with exons depicted as grey boxes, exon number indicated above. Regions encoding the domains of PSD-95 are labelled and bracketed above.

# Chapter 4: RESULTS Generation of a *PSD-95* Conditional Allele

## 4.1 Introduction

The *PSD-95* mutant mouse (Migaud *et al.* 1998) was generated using conventional gene targeting technology; that is, the gene was interrupted by the insertion of a selectable cassette. This technique can be relatively rapid and ablates gene function ubiquitously and constitutively, allowing a first investigation of protein function to be performed. A disadvantage of this form of gene targeting is that it does not provide any control over the timing and distribution of gene inactivation. This may limit the usefulness of a mutation if the mutants are embryonic lethal since limited analyses can be preformed. Alternatively, there may be difficulty in breeding homozygous animals if less than Mendelian numbers of homozygotes are obtained, as is the case with the *PSD-95* deletion mutant. The spatial and temporal control over gene expression that is possible with conditional systems can circumvent deleterious phenotypes.

## 4.2 Assessment of Available Technology

The Tet system is useful for the expression of inhibitor peptides, dominant negative or constitutively active proteins as well as overexpression of wild type protein. These strategies, however, are inappropriate for the study of PSD-95 since the multiple binding activities of PSD-95 cannot be out-competed by a single peptide and dominant negative forms of the protein have not been identified. The best use of the Tet system would be to conditionally induce wild type PSD-95 expression in the *PSD-95* deletion mutant background. However, such a system would operate in the presence of the truncated PSD-95 protein and which would complicate analysis. Furthermore, an extensive breeding strategy would be required to generate a mouse that was homozygous for the *PSD-95* deletion allele and carried both the Tet transcriptional activator and PSD-95 transgene. Such a breeding strategy is particularly daunting when it is considered that *PSD-95* deletion homozygotes do not breed well. Another system, such as conditional gene inactivation, would therefore be preferable.

Compared to conventional gene targeting, conditional gene inactivation using the Cre-loxP system requires a more complex cloning strategy to insert loxP sites either site of the target region and also requires more *in vitro* manipulation of ES cells to excise the selection cassette prior to their injection into blastocysts. However, the Cre-loxP system could improve on the existing *PSD-95* deletion mutant by generating a null *PSD-95* allele with the benefits of conditional inactivation. In addition, Cre-expressing transgenics were already available to the lab, so I elected to use the Cre-loxP system for the study of PSD-95 function.

## 4.3 Vector Design for Cre-loxP Based Mutation

Having decided to use the Cre-loxP system, the design of the targeting vector and cloning strategy was then considered. In an ideal strategy, the expression of a reporter, such as green fluorescent protein (GFP), would be activated upon inactivation of the gene. This might be achieved by flanking critical exons and the polyadenylation signal with loxP sites (or floxing) and inserting a splice acceptor-GFP cassette with the 3' loxP site (Fig. 4.1A). Placing such a cassette 3' to the endogenous polyadenylation site would prevent its transcription in the absence of recombination. However, upon recombination most of the gene, including the stop codon and polyadenylation signal, would be removed allowing upstream exons of the endogenous gene to splice to the reporter cassette, driving transcription of GFP from the endogenous gene's promotor (Fig. 4.1B). Such a system would allow cells in which recombination had occurred to be easily identified and scored. Unfortunately, the efficiency of Cre-mediated recombination declines with increasing distance between loxP sites, thus the size of the *PSD-95* gene precluded the use of such a readout.

Since a truncated protein was generated in the original PSD-95 mutation (Migaud *et al.* 1998), a null allele would require more 5' sequence to be targeted. The cluster of exons encoding PDZ domains 1 and 2 (exons 3-8) appeared a good region of the gene to flank with loxP sites (flox) since there was little coding sequence 5' to these exons, the cluster was compact enough that the distance between loxP sites would be relatively short and recombination would produce a frameshift in all known variants of PSD-95. Cre-

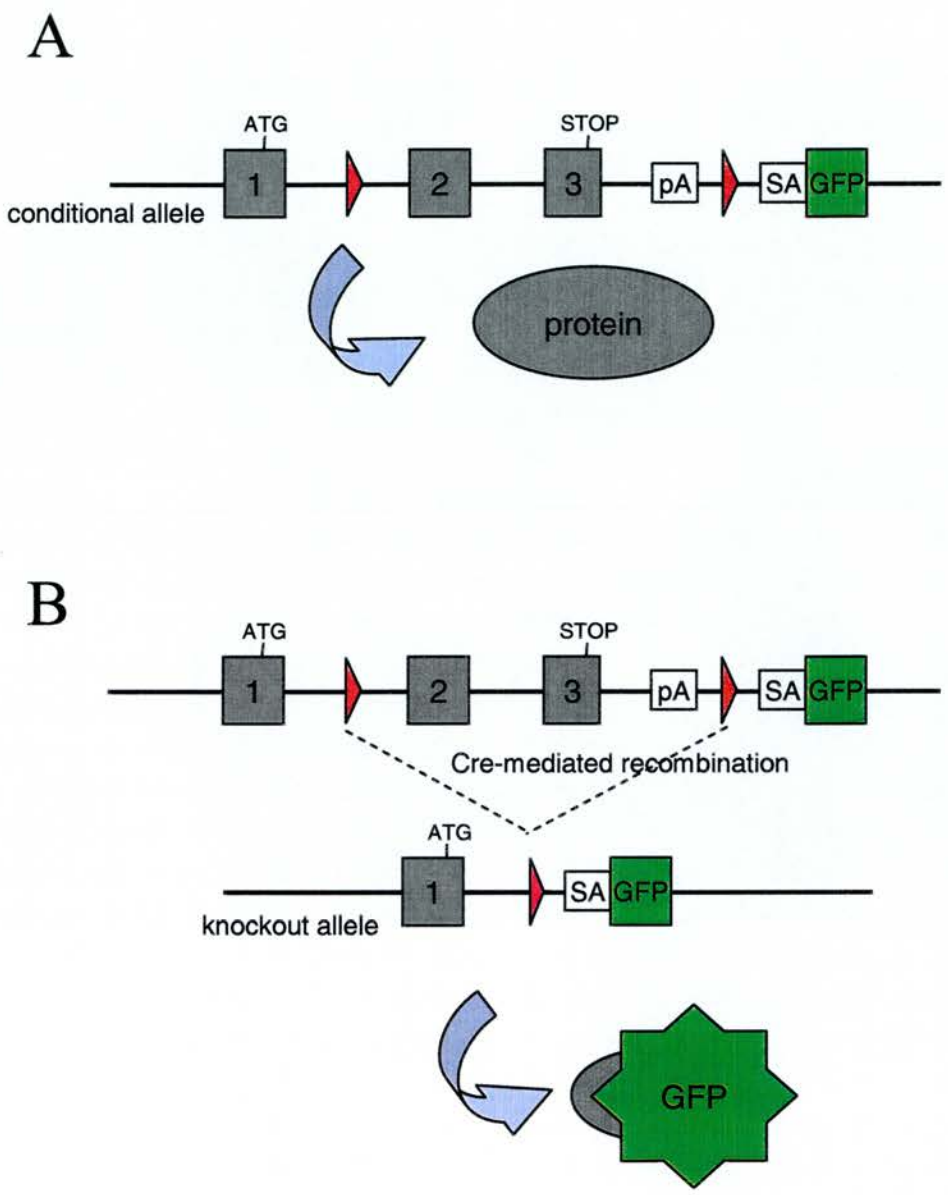


**Figure 4.1 Targeting vector with reporter of recombination.** ***A:*** The conditional allele shows loxP sites (red triangles) flanking 3' exons (grey boxes) of a gene, including the translation stop codon and the polyadenylation (pA) signal. The translation start codon (ATG) is indicated on exon 1. A green fluorescent protein (GFP) reporter gene with a splice acceptor (SA) site is inserted 3' to the endogenous pA signal. In the absence of Cre recombinase this arrangement allows the normal production of protein but not GFP. ***B:*** Cre-mediated recombination removes critical exons such that a functional endogenous gene product is no longer generated. Recombination also removes the endogenous stop codon and pA signal. The first endogenous exon can now splice to the GFP gene, resulting in the generation of a GFP fusion protein that reports recombination.

mediated deletion of exons 3 to 8 would introduce a stop codon 69 nucleotides into exon 9, leaving a potential PSD-95α product of 56 amino acids that may be unstable.

Placing loxP sites in introns should not interfere with normal gene function, although one must ensure that loxP sites do not disrupt splice donor or acceptor sequences. One must also consider the possibility of interrupting an enhancer element, but unfortunately, enhancer sequences are not well conserved and are therefore difficult to identify. To ensure that the loxP sites did not affect splicing sequences, I wanted to place the loxP sites at least 1 kb from the nearest exon. Restriction enzyme sites were available for such a strategy, allowing me to insert a floxed thymidine kinase (*tk*) / neomycin phosphotransferase (*neo*) cassette into the SpeI site in intron 2 and an isolated loxP site into an XbaI site in intron 8. *Neo* would be used during targeting to positively select for ES cell colonies that had integrated the cassette i.e. they would be resistant to the antibiotic G418. *Tk* would be used after transient Cre expression in ES cells *in vitro* as negative selection to screen for ES cell colonies from which the cassette had been deleted, i.e. colonies that were not killed by gancyclovir, which is converted to its toxic form by *tk*. Removal of the selection cassette after targeting is required because it can interfere with gene expression, even if located in an intron. Cryptic splice sites in *neo* cause aberrant splicing of the gene product such that *neo* sequence is spliced into the endogenous transcript, inserting frameshifts and/or stop codons (Wassarman *et al.* 1997; Meyers *et al.* 1998; Nagy *et al.* 1998).

The length of homologous DNA flanking the selection cassette or other non-homologous sequences critically influences targeting efficiency (Thomas and Capecchi 1987; Hasty *et al.* 1991). In targeting the *PSD-95* locus, experiments performed in our lab (M. Arbuckle – personal communication) have shown at least 1.5 kb of sequence is required in a homology arm (Table 4.1).

| Mutation | Homology (kb) | | | Targeting efficiency (%) |
|---|---|---|---|---|
| | 5' | 3' | Total | |
| ΔPDZ3-GK | 1.6 | 4.2 | 5.8 | 6.7 |
| SH3* | 0.9 | 4.5 | 5.4 | No targeting |
| SH3* | 3.8 | 4.5 | 8.3 | 2.7 |
| ΔGK | 1.35 | 4.5 | 5.85 | No targeting |
| ΔGK | 4.8 | 4.5 | 9.3 | 7.8 |

**Table 4.1 Targeting efficiency is dependent on homology arm length at the *PSD-95* locus.** The first PSD-95 mutation (Migaud *et al.,* 1998) is designated ΔPDZ3-GK. Other mutations shown are an SH3 domain point mutation (SH3*) and a deletion of the GK domain (ΔGK).

My final cloning strategy therefore included 3 kb of 5' homology and 10 kb of 3' homology. A floxed *tk/neo* (LTNL) cassette was placed in intron 2, which resolved into a single loxP site following Cre-mediated excision of the cassette *in vitro*. The 3' loxP site was introduced as an oligonucleotide containing an EcoRI site, allowing the presence of the unselectable oligonucleotide to be tracked by restriction enzyme digest. The construction of the targeting vector to produce this allele is described below and summarised in figure 4.2.

## 4.4 Vector Construction

The XbaI site in the pBlueScript KSII multiple cloning site was ablated by a SpeI-XbaI digest followed by religation to form the plasmid pBS KSII (XbaI-). BamHI-EcoRV digestion of BamHI (9) yields two insert fragments, a 4.8 kb BamHI-EcoRV fragment and a 7.6 kb EcoRV-BamHI fragment. The 4.8 kb BamHI-EcoRV fragment genomic fragment containing exons 3 to 8 from BamHI (9) was inserted into pBS KSII (XbaI-) to produce plasmid B-EV. An EcoRI-loxP oligo with XbaI overhangs was then inserted into the XbaI site 3' to exon 8 (step 2 in Fig. 4.2), generating plasmid BlpEV.

Meanwhile, the remainder of the BamHI (9) insert, the 7.6 kb EcoRV-BamHI fragment containing exons 9 to 16, was inserted into a pET29 vector to form plasmid EV-B. To reconstitute the 12.4 kb BamHI fragment following addition of the EcoRI - loxP

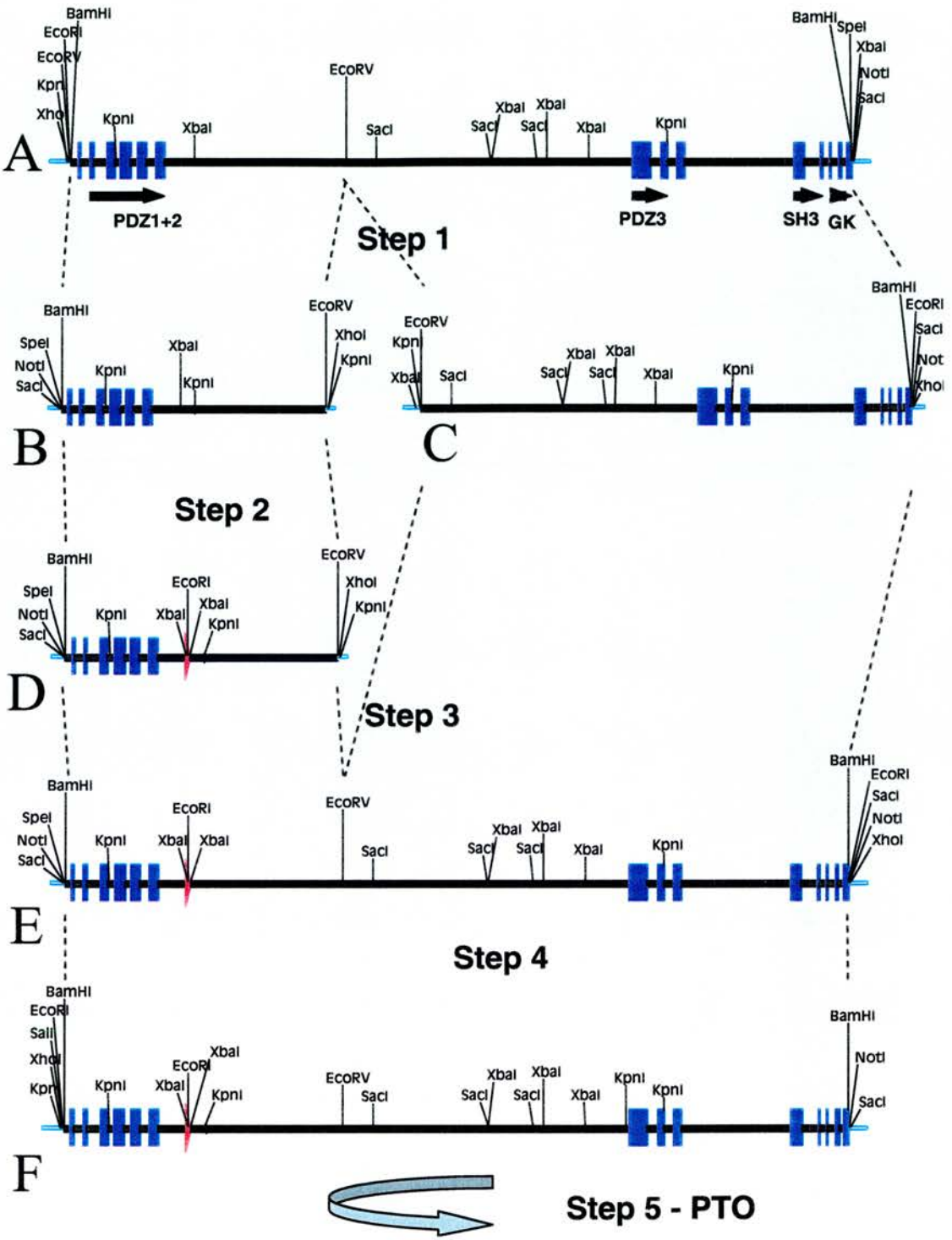


**Figure 4.2 Construction of floxed *PSD-95* targeting vector.** Step 1: BamHI-EcoRV digest of BamHI (9) (A) to clone 5' fragment into pBS KSII (XbaI-) and 3' fragment into pET-29a(+). Step 2: XbaI digest of B-EV (B) to ligate in EcoRI-loxP oligo. LoxP site is shown as red triangle. Step 3: EcoRV-XhoI digest of both BlpEV (D) and EV-B (C) to clone EcoRV-XhoI fragment from EV-B into BlpEV. Step4: BamHI fragment from BlpEVB (E) transferred to pBlue (SalI-NotI). (figure continues on next page) Step 5: BamHI digest of BlpB (F) to insert BamHI fragment from KpnI (4). Step 6: SalI-SpeI digest of BBlpB (G) to ligate in SalI-SpeI fragment from KpnI (4). Step 7: SpeI digest of KBBlpB (H) to insert LTNL cassette as a XbaI fragment. Step8: SalI digest of KLTNLB (I) to insert DTA cassette as a SalI-XhoI fragment to form the final targeting vector, DTA-KLTNL (J).

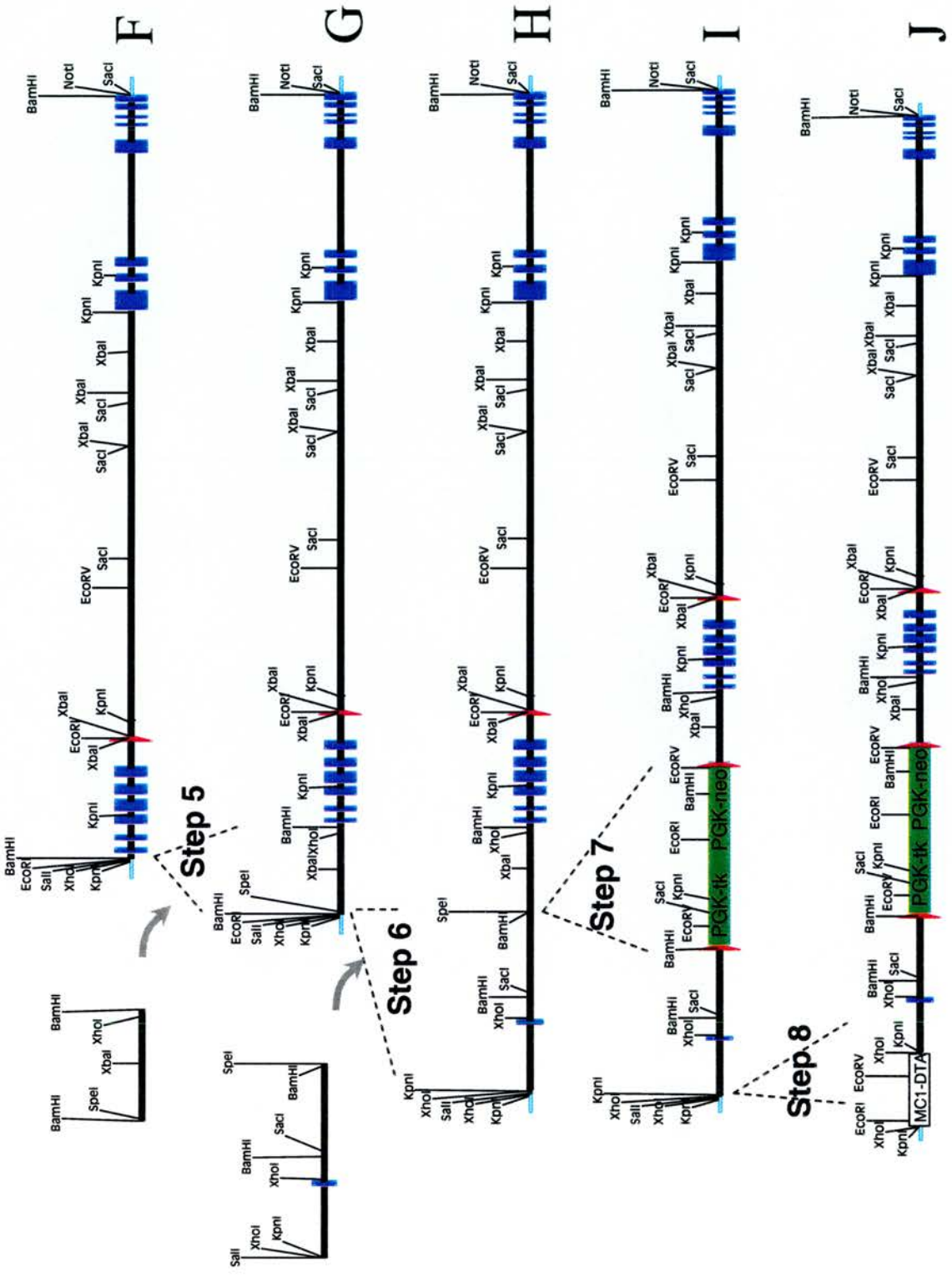
F
G
H
I
J
Step 5
Step 6
Step 7
Step 8
PGK-tk
PGK-neo
MC1-DTA

oligonucleotide, EV-B was cut with EcoRV and XhoI, releasing the 7.6 kb insert and a portion of the pET-29a(+) multiple cloning site. B-EV was digested with EcoRV and XhoI to ligate the EcoRV-XhoI fragment into the EcoRV site forming the 3' end of the B-EV insert and the XhoI site in the multiple cloning site (step 3 in Fig. 4.2), producing plasmid BlpEVB.

To complete the cloning, a new plasmid (pBlue(SalI-NotI)) was generated by inserting a new polylinker into pBlueScript KSII as a SalI-NotI fragment. This replaced ClaI-HindIII-EcoRV-EcoRI-PstI-SmaI-BamHI-SpeI-XbaI with EcoRI-BamHI-BglII. The 12.4 Kb BamHI fragment from BlpEVB containing exons 3 to 16 and the inserted EcoRI-loxP oligo was then inserted into the BamHI-BglII sites of pBlue(SalI-NotI), generating plasmid BlpB (step 4 in Fig 4.2). This cloning step ablated the BamHI site at the 3' end of the BlpB insert, allowing BlpB to be linearised by BamHI. Following BamHI digestion of BlpB, contiguous 5' sequence was added from KpnI (4) in the form of a 1.5 kb BamHI fragment containing a SpeI site (step 5 in Fig 4.2), producing plasmid BBlpB. SalI-SpeI digestion of BBlpB excised a fragment from the SalI site in the BBlpB polylinker to the SpeI site in the genomic sequence. Further 5'sequence was then added by inserting a SalI-SpeI fragment from KpnI (4) into the SalI site in the BBlpB polylinker and the genomic SpeI site (step 6 in Fig 4.2), generating plasmid KBBlpB. The LTNL cassette was then inserted as an XbaI fragment into the SpeI site of KBBlpB (step 7) forming plasmid KLTNLB. Finally, to select against backbone insertion, a diphtheria toxin-A (DTA) cassette was inserted as a SalI-XhoI fragment into the SalI site in the KLTNLB polylinker (step 8). The completed DTA-KLTNLB vector is shown in figure 4.2.

## 4.5 ES Cell Targeting

The DTA-KLTNLB vector was electroporated into E14TG2a ES cells. Neomycin-resistant colonies were picked, expanded and screened by Southern blotting using probes external to the targeting vector. The LTNL cassette contained two EcoRV sites, thus wild type gDNA digested with NotI and EcoRV and hybridised with the 5' probe yielded a 12 kb positively hybridising wild type band while correct insertion of the

cassette into the *PSD-95* locus shortened the positively hybridising band to 5.5 kb (Fig. 4.3).

4 kb separates the LTNL cassette and the isolated loxP site, therefore correct integration of the cassette did not ensure that the unselected, isolated loxP site was also integrated. Indeed, integration of a separated loxP site and the selection cassette is inversely proportional to the distance that separates the two (Torres and Kuhn 1997). Integration of the isolated loxP site was determined by Southern blotting utilising the EcoRI site included in the loxP oligo. When EcoRI digested gDNA was probed with the 3' probe a 19.5 kb wild type band was observed, while correct integration of the 3' loxP site yielded an 11.5 kb band (Fig 4.3). This screening strategy allowed integration of the floxed cassette and the third isolated loxP site to be independently scored: 63 ES cell clones were screened with both 5' and 3' probes, 23 (32%) clones were identified that contained the selection cassette alone while 4 (6%) clones were identified that contained both the cassette and the 3' loxP site.

Having identified correctly targeted clones, the cells then had to be expanded to perform a second round of electroporation in order to transiently transfect a Cre-expressing plasmid to remove the LTNL cassette. Clones 110, 132, 87 and 20 were thawed for expansion, however only clones 110 and 132 recovered and grew well. Clones 87 and 20 failed to thrive, eventually differentiating and dying.

## 4.6 Cre-Mediated Excision of Selection Cassette

Transfection of ES cells with a plasmid encoding Cre results in transient expression of Cre. Cre-mediated recombination of the targeted *PSD-95* allele can generate 3 possible recombined alleles, however, under gancyclovir selection, selecting for LTNL cassette removal, only two recombination events were viable (Fig. 4.4A). If the two most distal loxP sites recombined (complete recombination), both the cassette and exons 3 to 8 were excised generating a null allele. If only the LTNL loxP sites recombined (partial recombination), the cassette was deleted but the flox of exons 3 to 8 was maintained producing the conditional allele.

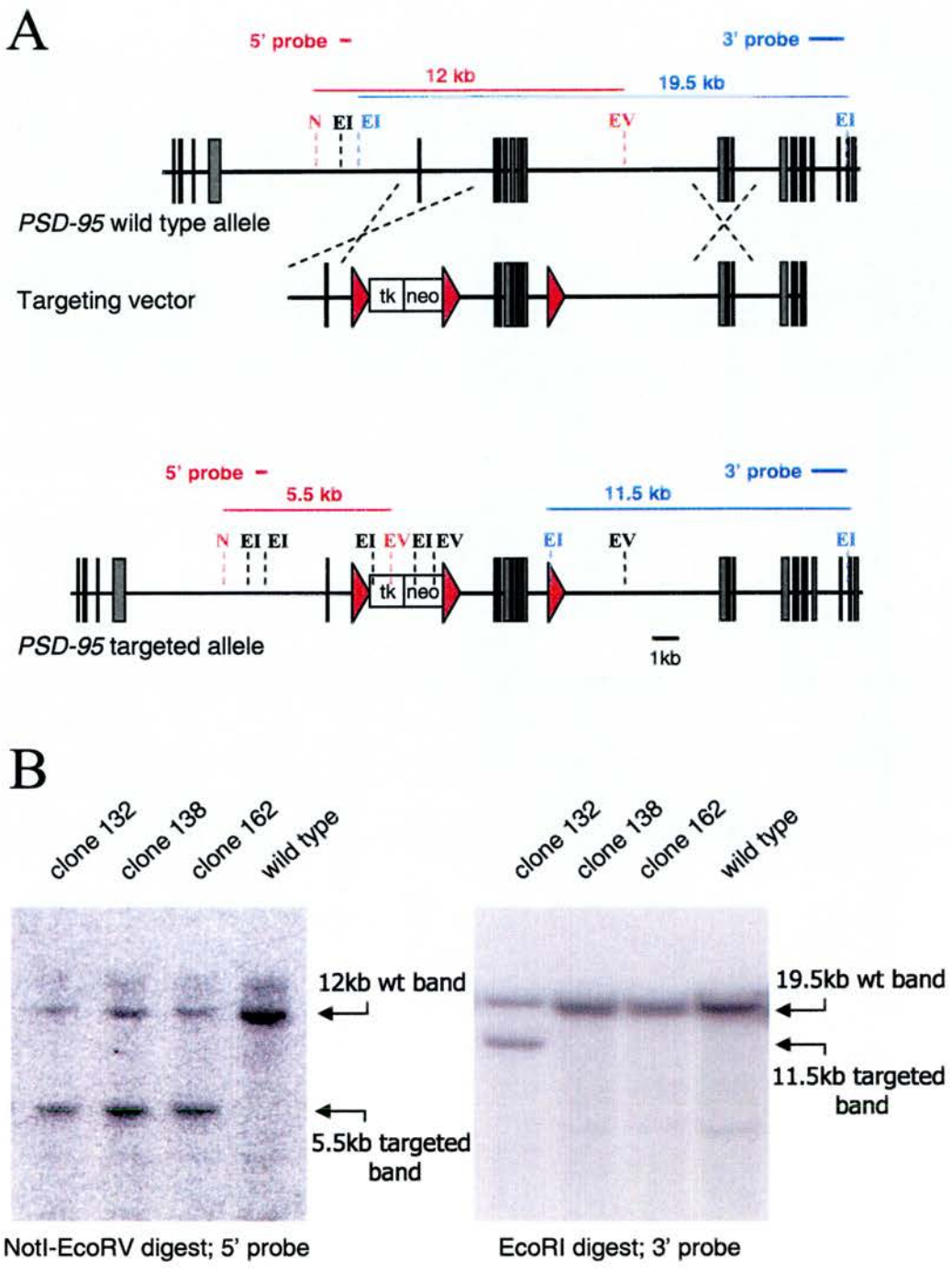


**Figure 4.3 Targeting of *PSD-95*.** ***A:*** Wild type *PSD-95* allele is shown top, the targeting vector is shown middle and the targeted allele is shown bottom. LoxP sites are shown as red triangles. Probes used to screen clones are shown as thick lines above alleles; red for the 5' probe and blue for the 3' probe. Restriction enzyme fragments that hybridise to probes are shown as thin lines; red fragments hybridise to the 5' probe and blue fragments hybridise to the 3' probe. Fragment sizes are labelled. ***B:*** Southern blots using NotI-EcoRV digested DNA with the 5' probe identify integration of the selection cassette into the *PSD-95* locus by the presence of a 5.5 kb band. Southern blots using EcoRI digested DNA with the 3' probe identify integration of the 3' loxP site into the *PSD-95* locus by the presence of an 11.5 kb band. The Southern blots shown identify clone 132 as correctly targeted (far left lane) and clones 138 and 162 as integrating only the selection cassette (middle 2 lanes). Wild type DNA is shown in the far right lane.

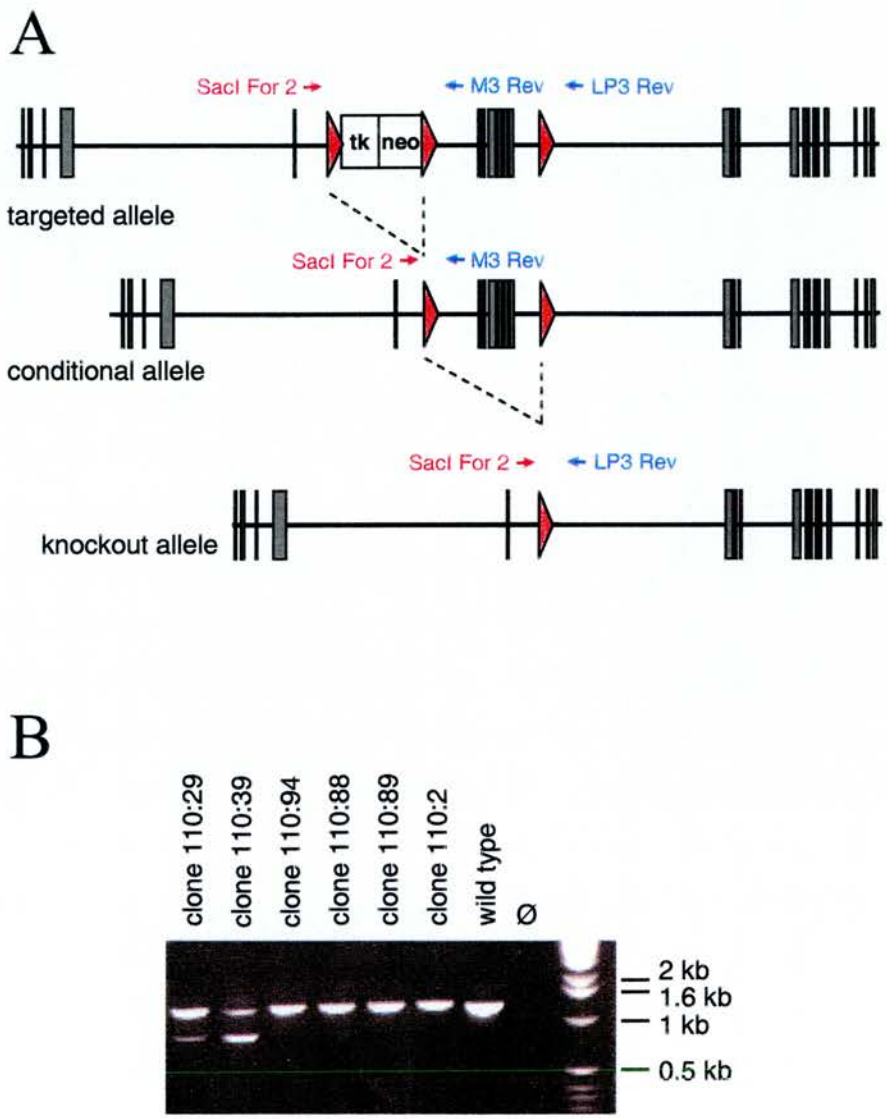


**Figure 4.4 PCR screening for selection cassette excision .** ***A:*** The targeted *PSD-95* allele is shown (top) with 2 possible recombination events shown: conditional allele (middle) and knockout allele (bottom). Primers used to screen clones are shown as arrows above alleles; red for forward primers and blue for reverse primers. ***B:*** Extension times were set such that SacI For 2 and LP3 were unable to generate product in the conditional allele. Knockout alleles (clones 110:29 and 110:39) were identified by an ~0.8 kb product. Conditional alleles (110:94, 110:88, 110:89 and 110:2) were identified by an ~1.4 kb product that did not resolve from the wild type product.

The level of Cre expression determines the balance between partial and complete recombination and in earlier studies this balance was difficult to achieve, such that only complete recombination was observed (A. J. S. Smith – personal communication). An appropriate level of Cre expression could, however, be obtained using the weak MC1 promotor. Electroporation of clones 110 and 132 with pMC1-Cre thus yielded clones with either partial or complete recombination.

PCR and Southern blotting was used to screen clones following transient Cre transfection. The PCR strategy utilised a common forward primer with a two reverse primers that generated products specific to either partial or complete recombination (Fig. 4.4B). Southern hybridisation of the 5' probe with NotI-EcoRV digested gDNA produced a 12kb band with the cassette excised while total recombination (knockout allele) produced a positively hybridising band of 8 kb (Fig. 4.5). PCR was used to confirm the presence of 5' and 3' loxP sites in clones containing the conditional allele (Fig. 4.6).

From 24 screened clones derived from Cre transfection of clone 110, 15 (63%) had undergone partial recombination. Clones 110:88 and 110:26, which had undergone partial recombination (*PSD-95*$^{+/flox}$), grew well as ES cells and were therefore used for the generation of chimeras. From 24 screened clones derived from Cre transfection of clone 132, 7 (29%) exhibited partial recombination. *PSD-95*$^{+/flox}$ clone 132:65 thrived on thawing and was used for blastocyst injection. All clones identified as carrying the condition allele were confirmed to contain both loxP sites by PCR. The different percentages of partial recombinants probably represent transfection variation. Fewer copies of pMC1-Cre transfected into an ES cell would result in a lower expression level, favouring partial recombination.

**Figure 4.5 Southern blot screening for selection cassette excision.** ***A:*** The targeted *PSD-95* allele is shown (top) with 2 possible recombination events shown: the conditional allele (middle) containing 2 loxP sites and the knockout allele (bottom) that contains 1 loxP site. Probes used to screen clones are shown as thick lines above the targeted allele, red for the 5' probe and blue for the 3' probe. ***B:*** Southern blots using NotI-EcoRV digested DNA with the 5' probe identify excision of the selection cassette from the *PSD-95* locus (conditional allele; clones 110:88, 110:89 and 110:2) by the hybridising fragment reverting back to the wild type size of 12 kb. Excision of both selection cassette and exons 3 to 8 (knockout allele; 110:4) is identified by an 8 kb band. A locus that has not undergone recombination is also shown (clone 132). Southern blots using EcoRI digested DNA with the 3' probe cannot differentiate between conditional (clones 110:88, 110:89 and 110:2) and unrecombined (clone 132) alleles, both generating 11.5 kb hybridising fragments. Knockout alleles are identified by a 15.5 kb band that fails to resolve from the wild type 19.5 kb band. Wild type DNA is shown in the far right lane.

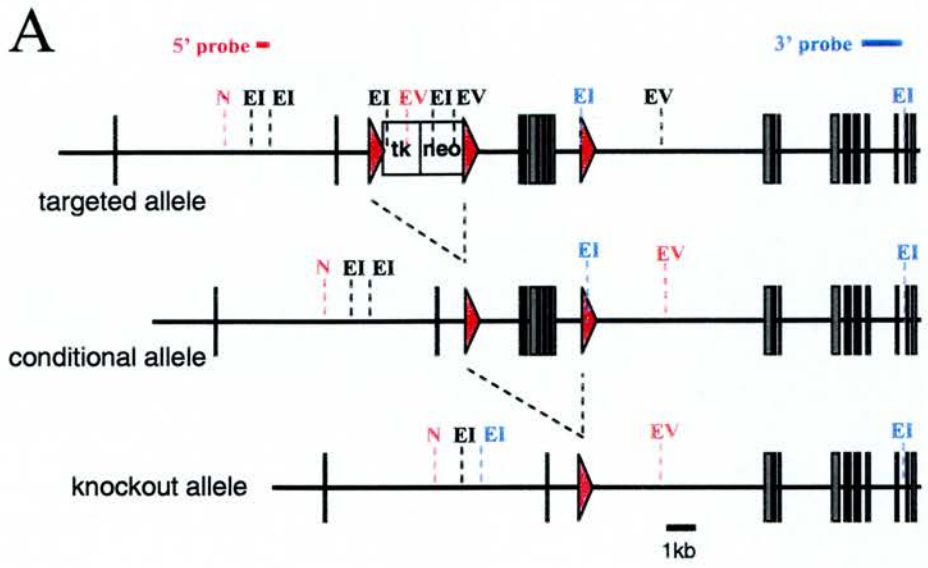
A
5' probe
3' probe
N EI EI
EI EV EI EV
EI
EV
EI
tk
neo
targeted allele
conditional allele
knockout allele
1kb

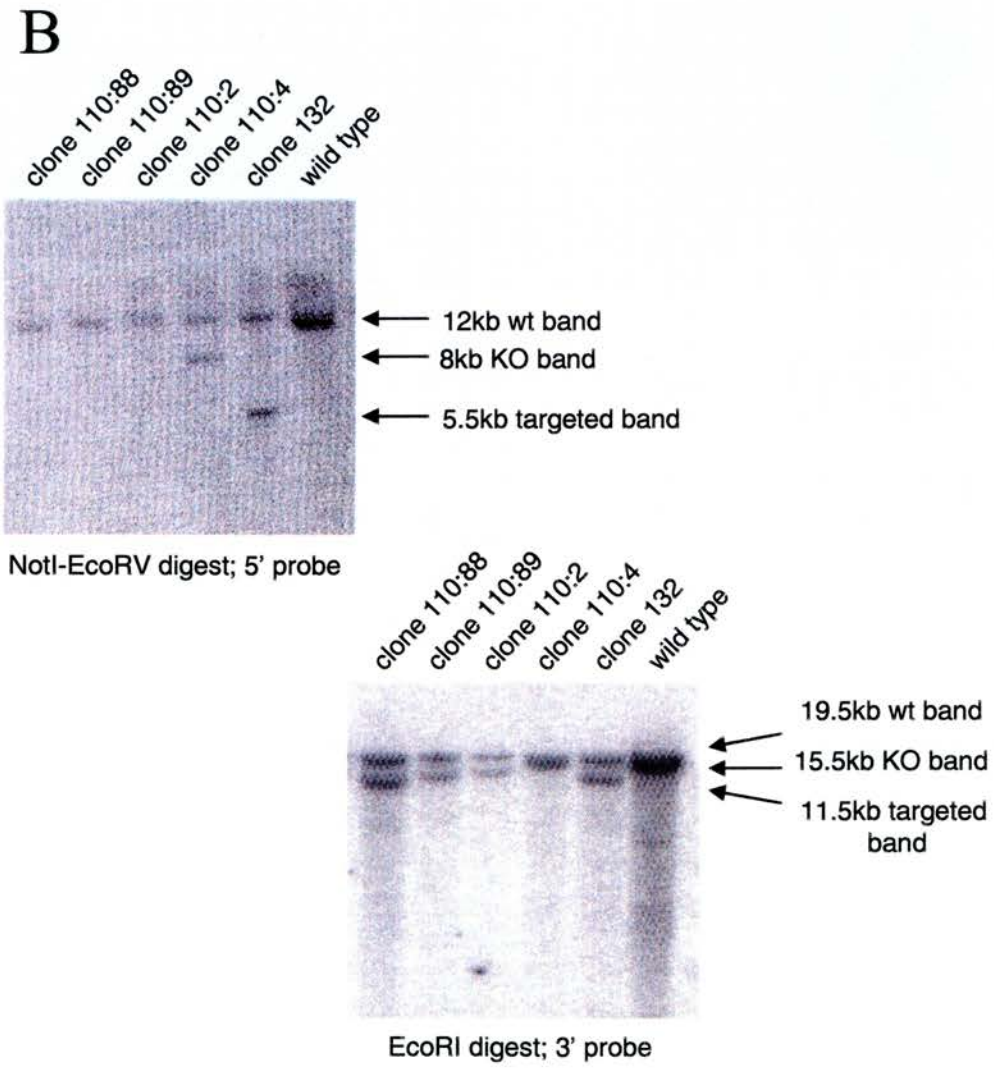
B
clone 110:88
clone 110:89
clone 110:2
clone 110:4
clone 132
wild type
12kb wt band
8kb KO band
5.5kb targeted band
NotI-EcoRV digest; 5' probe
19.5kb wt band
15.5kb KO band
11.5kb targeted band
band
EcoRI digest; 3' probe

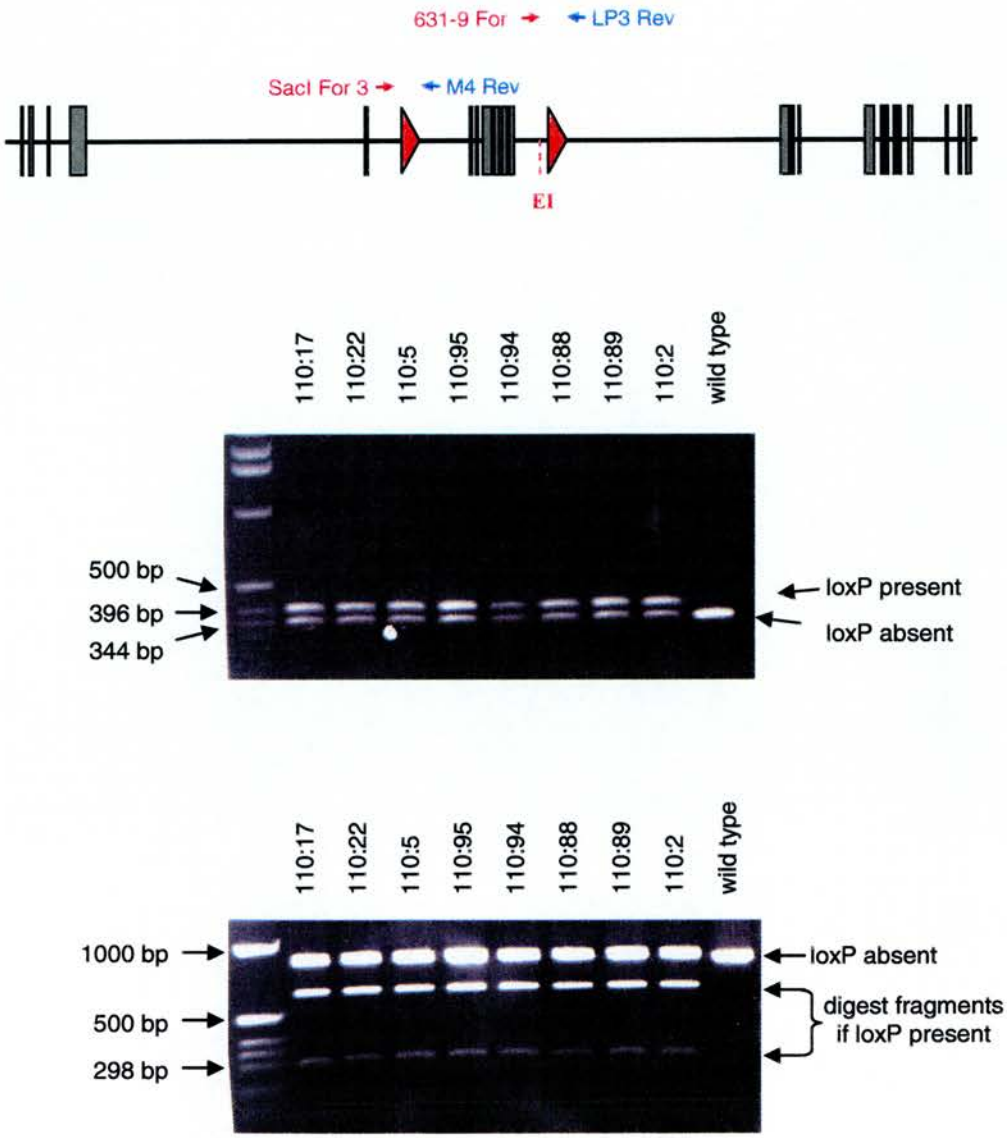


**Figure 4.6 PCR screening of 5' and 3' loxP sites.** The conditional *PSD-95* allele is shown (top) with primers used to screen clones shown as arrows above the allele; red for forward primers and blue for reverse primers. The small size of the PCR products allowed the size difference resulting from the presence of the 32 bp loxP site to be resolved. SacI For 3 and M4 Rev primers were used to screen for the 5' loxP site and generated a wild type product of ~350 bp and a product of ~390bp when the loxP site was present (middle panel). 631-9 For and LP3 Rev primers were used to screen for the 3' loxP site. These PCR products were digested with the restriction enzyme EcoRI to determine the presence of the 3' loxP site oligo that included an EcoRI site. The wild type product could not be digested by EcoRI and was seen as a single band. Products containing the loxP site and the EcoRI site generated 2 bands (bottom panel).

## 4.7 Generation of Chimeras

Clones 110:88 and 110:26 were injected into blastocysts to generate chimeras. 110:88 produced one female and four male chimeras, 110:26 produced one male and two female chimeras. At six weeks of age test crosses were set up using the male chimeras and monitored for at least eight months. Each male was caged with two MF1 females, however three chimeras proved sterile while the two fertile chimeras did not transmit the mutation down the germline (see table 4.2 below).

| | **Litter DOB** | **Number of pups** | **Coat colour** |
|---|---|---|---|
| **110:88 chimera 1** (set up 17/07/01) | 20/08/01 | 11 | All black |
| | 01/09/01 | 2 | All black |
| | 06/11/01 | 2 | Found dead at birth |
| | Breeding terminated 04/04/02 | | |
| **110:88 chimera 2** (set up 17/07/01) | 07/08/01 | 12 | All black |
| | 15/09/01 | 17 | All black |
| | 25/09/01 | 2 | All black |
| | 26/10/01 | 5 | All black |
| | 28/10/01 | 5 | All black |
| | 05/11/01 | 14 | All black |
| | 04/12/01 | 10 | All black |
| | 06/02/02 | 6 | All black |
| | 03/03/02 | 4 | All black |
| | Breeding terminated 04/04/02 | | |
| **110:88 chimera 3** (set up 17/07/01) | No litters | | |
| | Breeding terminated 04/04/02 | | |
| **110:88 chimera 4** (set up 17/07/01) | No litters | | |
| | Breeding terminated 04/04/02 | | |
| **110:26 chimera** (set up 31/07/01) | No litters | | |
| | Breeding terminated 04/04/02 | | |

**Table 4.2 Results of test crosses set up using male chimeras.**

With the failure of the male chimeras to either breed or transmit the mutation down the germline, each female chimera was subsequently set up with a single male MF1 mouse. Unfortunately, the females were over 6 months old when they were set up for test crosses and died before any litters were produced.

Since chimeras generated in the first round of blastocyst injection did not produce germline transmission, further blastocyst injections were performed using a different clone, 132:65. While the earlier injections were performed in a well established facility at the Centre for Genome Research, the second round of injections were carried out in new, unproven facilities at the Department of Neuroscience. Unfortunately, the second round of injections failed to generate any chimeras and further injections were prevented by the closure of the Centre for Genome Research animal facility to new mutant lines, the availability of staff trained to perform blastocyst injection and the deadline for the completion of this project.

## 4.8 Discussion

A conditional allele of *PSD-95* has been generated using Cre-loxP technology. This allows *PSD-95* to be deleted in a temporally and spatially defined manner such that its function in specific brain regions can be studied. This may prove particularly useful in addressing the role of PSD-95 in learning and memory, specifically its role in the hippocampus.

To generate the conditional allele, the targeting vector was designed, constructed and electroporated into ES cells. Transient Cre transfection of correctly targeted clones removed the selection cassette, producing a conditional allele in which the endogenous locus was disrupted to the absolute minimum. Partial recombinants were selected, expanded and injected into blastocysts. Clone 132:65 failed to produce chimeras and chimeras generated from clones 110:88 and 110:26 did not transmit the mutation down the germline. Potential reasons for the failure of germline transmission are numerous, however the ES cells were not obviously unhealthy and their chromosome number was normal (D. Rout – personal communication). Further blastocyst injections, particularly of clone 132:65, are therefore required.

# Chapter 5: RESULTS PSD-95 and Halothane Anaesthesia

## 5.1 Introduction

Anaesthesia is defined as unconsciousness, amnesia and immobility in response to noxious stimuli. Volatile anaesthetics are an important and widely used class of general anaesthetic, however, their mechanism of action is still not fully understood.

### 5.1.1 Volatile Anaesthetic Mode of Action

There are two main theories for the action of volatile anaesthetics, both related to their hydrophobicity. Meyer and Overton observed that the potency of a volatile anaesthetic correlated with its lipid solubility (Meyer 1899; Overton 1901), solubility and potency increasing with increasing hydrocarbon length. Anaesthesia has therefore been proposed to result from changes in membrane function precipitated by anaesthetics dissolving in the cell membrane. This change in membrane function may take the form of membrane expansion (increasing in volume) or loss of membrane organisation. However, the changes in membrane properties induced by physiologically relevant anaesthetic concentrations are of a magnitude that could also be produced by temperature changes of <1°C, which do not induce anaesthesia (reviewed by Wann and MacDonald 1988; Franks and Lieb 1994). Furthermore, the Meyer-Overton correlation is limited by a cut-off in the size of the anaesthetic, beyond which increasing hydrocarbon length does not increase potency, despite an increase in lipid solubility. The lipid theory has therefore fallen from favour and considerable research has been focused on determining the protein targets of volatile anaesthetics.

#### *5.1.1.1 Effects on Receptors and Ion Channels*

The binding of volatile anaesthetics to a protein hydrophobic pocket is now a more commonly favoured theory. Ligand and voltage gated ion channels have been the focus of many studies into the action of anaesthetics and $GABA_A$ receptors, glycine receptors and two-pore $K^+$ channels appear to be major targets for volatile anaesthetics (Wakamori *et al.* 1991; Harrison *et al.* 1993; Lin *et al.* 1993; Patel *et al.* 1999). The

existence of anaesthetic binding sites can be inferred from the size cut-off seen with the Meyer-Overton correlation while further studies provide more convincing evidence: The action of isoflurane, both *in vitro* and *in vivo*, was found to be stereoselective (Franks and Lieb 1991; Moody *et al.* 1993; Lysko *et al.* 1994); halothane and enflurane preferentially enhanced GABA and glycine receptor currents in primary neurons, with little effect on glutamate receptor currents (Wakamori *et al.* 1991) while ρ1 homomeric GABA receptors expressed in HEK293 cells were insensitive to isoflurane (Harrison *et al.* 1993).

Studies in mutant mice suggest that different volatile anaesthetic targets are important for distinct anaesthetic end points. The loss of righting reflex (LORR) test is used as a measure of hypnosis and assesses the ability of the animal to right itself after being turned on its back during exposure to an anaesthetic agent. The minimum alveolar concentration (MAC) determines the immobilising effect of an anaesthetic by measuring the concentration of anaesthetic required to prevent movement in 50% of subjects in response to a noxious stimulus, such as application of a clamp. Mice deficient in the AMPA receptor subunit, GluR2, were more sensitive to halothane, isoflurane- and sevoflurane-induced LORR but were no different from wild type animals when MAC was tested by tail clamp (Joo *et al.* 2001). The AMPA receptor is not, however, a major site of action for volatile anaesthetics. Mice lacking GluR2 exhibited reduced AMPA receptor-mediated excitatory transmission (Joo *et al.* 2001), potentially making the mutants more susceptible to enhanced inhibitory transmission induced by volatile anaesthetics. The lack of difference in MAC between mutants and wild type animals was therefore explained by absence of GluR2 subunits from spinal motor neurons (Joo *et al.* 2001), mutants maintaining the normal balance of excitatory and inhibitory influence on these neurons.

Mice lacking the β3 $GABA_A$ subunit exhibited reduced sensitivity to enflurane when tested using tail clamp yet were indistinguishable from wild type animals in the LORR test (Quinlan *et al.* 1998). The β3 subunit is widely expressed through the CNS and knockout animals exhibit a severe phenotype including hyperactivity, incoordination

and epilepsy (Homanics *et al.* 1997). In the light of such obvious and widespread impairment in inhibitory neurotransmission, the lack of LORR phenotype is unlikely to represent a regional difference in the balance in excitatory and inhibitory influences. It more likely reflects an important role for β3-containing $GABA_A$ receptors in mediating enflurane effects in the spinal cord, while other mechanisms contribute to its LORR effect. Thus volatile anaesthetics appear to have multiple, though specific targets through which they produce multiple anaesthetic end points.

## 5.1.2 Volatile Anaesthetic Site of Action in the CNS

The multiple effects of anaesthetics (unconsciousness, amnesia and immobility in response to a noxious stimulus) require them to act in both brain and spinal cord and the interaction between the two appears to be important.

### *5.1.2.1 Spinal Cord*

The role of different regions of the CNS in anaesthesia is dependent on the anaesthetic end point being determined. MAC appears to measure primarily spinal reflexes, since cerebral lesions and hypothermic isolation of spinal cord from the brain does not alter MAC (Rampil *et al.* 1993; Todd *et al.* 1993; Rampil 1994). Additional support for the importance of the spinal cord over the brain in determining MAC was generated by elegant experiments exploiting the unique goat cerebral circulation, which utilises only the external carotid artereies to perfuse brain regions higher than the medulla, venous blood draining via the external jugular vein. The brain can therefore be isolated and preferentially perfused by the use of a bypass system such that blood draining from the external jugular vein is gassed and returned to the carotid artery by means of a peristaltic pump. In this manner, brain isoflurane concentrations can be altered independent of the rest of the body. With low torso isoflurane concentrations (0.2–0.3%), the brain isoflurane concentration required to prevent response was 3%, considerably higher than the previously observed whole body MAC of 1.3% (Antognini and Schwartz 1993). Another study in the goat showed low brain isoflurane concentrations to reduce MAC (Borges and Antognini 1994), suggesting an increase in descending inhibition at low brain concentrations of isoflurane. However, the brain does not appear to influence

MAC at higher concentrations of anaesthetic since hypothermic transection of rat spinal cord had no effect on MAC (Rampil 1994).

#### *5.1.2.2 Brain*

The brain is the almost certainly the site of action for anaesthetic-induced amnesia and unconsciousness, specifically the midbrain reticular formation, thalamus, hippocampus and cortex. Damage to the reticular formation or thalamus causes unconsciousness while damage to the cortex produces sensory and motor disturbances, though not loss of consciousness. As described in the introduction, damage to the hippocampus can cause antero- and retrograde amnesia, though this brain region is not required for consciousness, as demonstrated by patients with bilateral hippocampal lesions. There is, however, evidence that the spinal cord can influence these anaesthesia end-points: Volatile anaesthetics can decrease spinal cord activity in response to noxious stimuli (Namiki *et al.* 1980; Yamauchi *et al.* 2002) and reduce transmission of noxious information to the brain (Antognini and Carstens 1999; Antognini *et al.* 2000), reducing arousal and thus the level of consciousness. This is supported by decreased hypnotic requirements observed in patients under epidural anaesthesia (Tverskoy *et al.* 1996).

## 5.2 *PSD-95* Deletion Mutants Are More Sensitive to Halothane

PSD-95 is expressed in the spinal cord and is required for NMDA-dependent processes in the spinal cord, such as generation of NMDA- and peripheral nerve crush-induced thermal hyperalgesia (Tao *et al.* 2000; Garry *et al.* 2001). Halothane has been reported to bind PSD-95 (R. A. Johns – personal communication) and antisense reduction of PSD-95 protein levels in the rat spinal cord reduced the MAC of a closely related volatile anaestheitc, isoflurane (Tao and Johns 2001). PSD-95 therefore appears to be a target for volatile anaesthetics and is involved in anaesthesia endpoints dependent on primarily spinal processes. However, the study by Tao and coworkers (2001) could not address the role of PSD-95 in other anaesthetic processes that require the brain.

To assess the anaesthesia phenotype of *PSD-95* deletion mutant mice and to determine the involvement of PSD-95 in anaesthetic endpoints other than MAC, the animals were tested for LORR in response to halothane. Since the LORR test requires motor coordination, it should be noted that *PSD-95* deletion mutant mice do not exhibit overt motor dysfunction and their righting reflex is indistinguishable from littermate controls in the absence of anaesthesia.

Temperature and $CO_2$ concentration can affect anaesthetic requirements, thus both were carefully monitored and maintained within narrow ranges: 33.5±1.0°C, maximum $CO_2$ 0.3kPa. In four experiments rectal temperature was monitored. Mouse rectal temperature was stable at 36.9±0.3°C for at least 10 min, the internal temperature of any one mouse not varying by more than 0.3°C over that time.

LORR was tested at a range of concentrations and the dose-response curve plotted (Fig. 5.1). The *PSD-95* deletion mutants were significantly ($P<0.05$) more sensitive to halothane, exhibiting a 23% reduction in $EC_{50}$ (wild type $EC_{50}$ 1.23%, PSD-$95^{-/-}$ $EC_{50}$ 0.95%). Thus PSD-95 appears to affect anaesthetic requirements for both MAC (Tao 2001) and LORR, in contrast to other studies of knockout mice, which have showed altered sensitivity either MAC or LORR tests, but not both.

## 5.3 Halothane Does Not Alter PSD-95 binding to Receptors and Ion Channels

Studies of anaesthetics usually focus on their action on voltage or ligand gated ion channels. Since PSD-95 associates with a number of receptors and ion channels, it seemed pertinent to address whether halothane might alter these interactions. Therefore, the effect of halothane on PSD-95 associations was assessed, focusing on 3 well-documented binding partners of PSD-95: the NMDA receptor, the kainite receptor and Kv1.4.

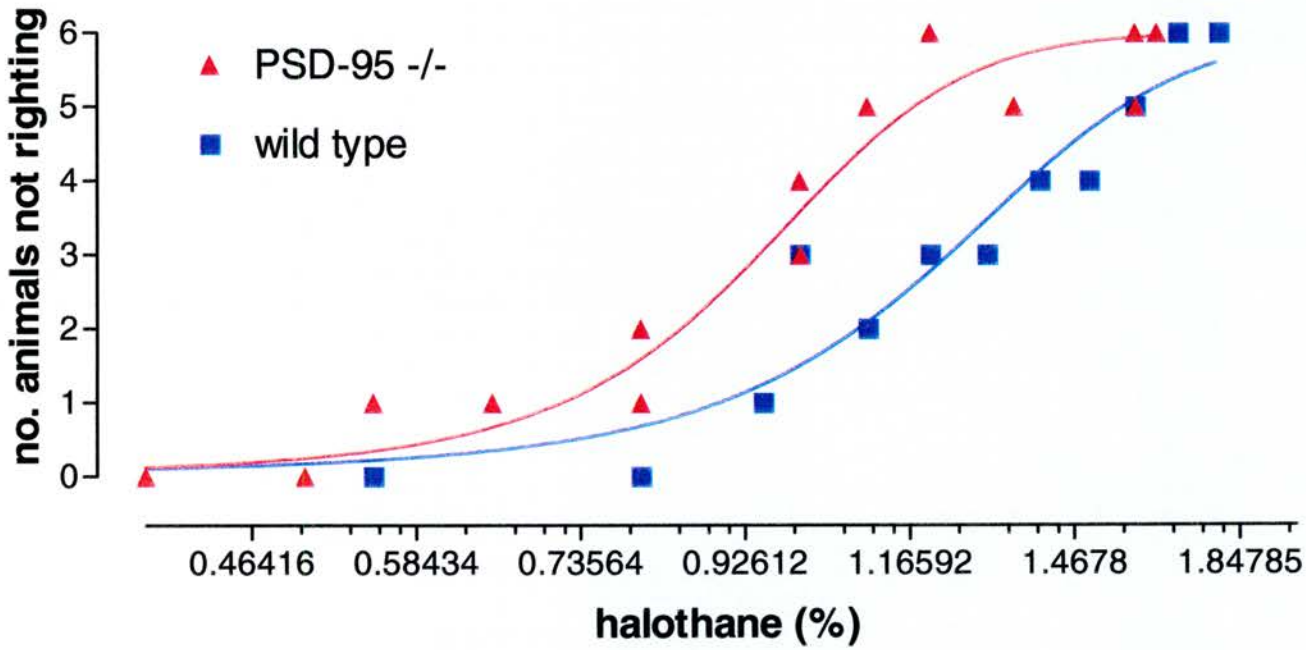


**Figure 5.1 The effect of halothane on LORR in *PSD-95* deletion mutants.** PSD-95$^{-/-}$ mice (red triangle symbols, red regression line) are more sensitive than wild type mice (blue square symbols, blue regression line) to the effects of halothane in the LORR test. Graph shows data from at least 4 experiments per genotype.

The effect of halothane on PSD-95 interactions was determined by immunoprecipitation of brain homogenate from anaesthetised and non-anaesthetised wild type mice. Anaesthetised mice were maintained in approximately 2.2% halothane for 10 min after they had stopped moving. Both anaesthetised and non-anaesthetised mice were killed, their brains rapidly removed and homogenised on ice. Immunoprecipitation was performed using antibodies to the channel or receptor of interest and the resulting Western blot probed with an anti-PSD-95 antibody.

In some blots loading was not uniform, but using the IgG band to gauge loading differences, it was clear that there was no difference in the association of PSD-95 with NR2B-containing NMDA receptors, KA2-containing kainite receptors or Kv1.4 channels (Fig. 5.2). Halothane therefore does not alter these interactions, although this does not rule out the disruption of other PSD-95 binding activities.

## 5.4 Discussion

The increased sensitivity observed in *PSD-95* deletion mutants may reflect a phenomenon specific to halothane and related volatile anaesthetics, consistent with a specific binding site being influenced in the *PSD-95* deletion mutant. PSD-95 itself may be acting as a halothane binding site, or PSD-95 may mask a halothane binding site on an ion channel, such that halothane and PSD-95 binding to a specific target is mutually exclusive. Another possibility is that loss of PSD-95 may produce a general alteration in neuronal physiology that increases sensitivity to all anaesthetics. To address these possibilities, *PSD-95* deletion mutants should be tested with different classes of anaesthetics, for example barbiturates and ketamine. A general physiological alteration would be supported if *PSD-95* deletion mutants are more sensitive to all classes of anaesthetic, however, PSD-95 may be implicated as a specific site of action for halothane if *PSD-95* deletion mutants are more sensitive to only halothane, but not other classes of anaesthetic.

It should be noted that there is a clearly demonstrated genetic basis for anaesthetic sensitivity (Koblin 1980; McCrae 1993; Quinlan 1994), therefore it is possible that the

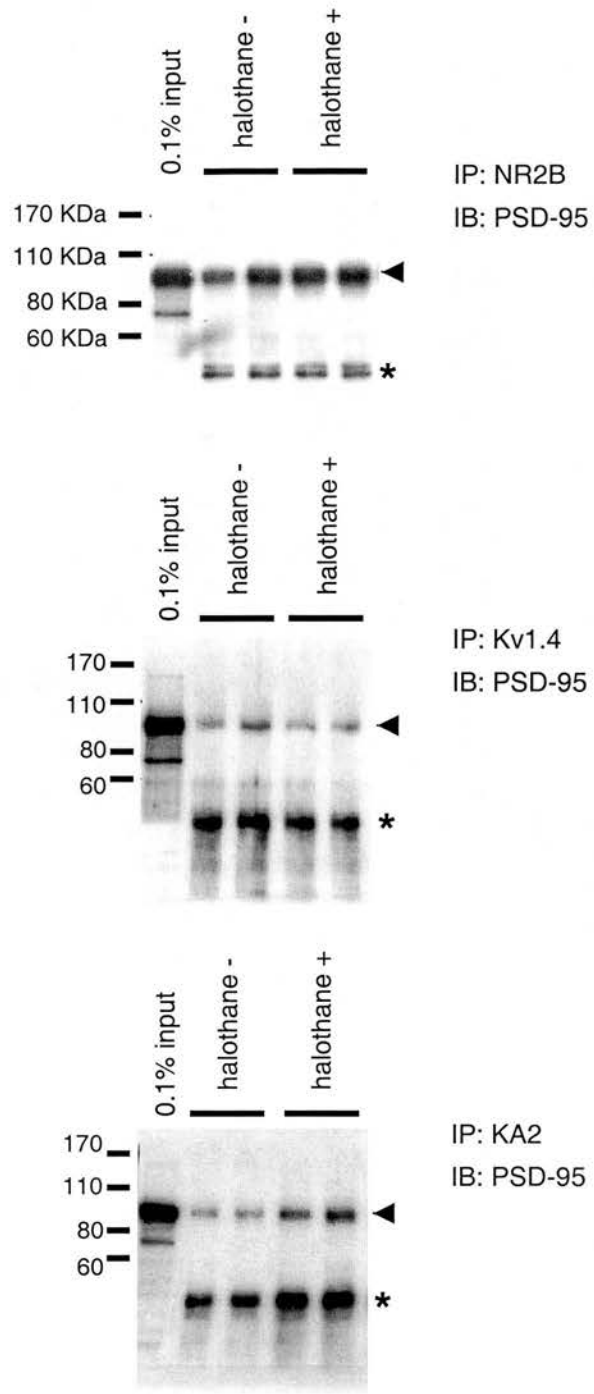


**Figure 5.2 The effect of halothane on PSD-95 binding activity.** PSD-95 (marked with arrowhead) immunoprecipitated with the NR2B NMDA receptor subunit, the KA2 kainate receptor subunit or the Kv1.4 potassium channel is unaffected by halothane anaesthesia when loading differences are gauged by the strength of signal from the IgG band (marked with asterisk). Immunoprecipitations (IP) were performed with NR2B, Kv1.4 or KA2 antibodies and immunoblots (IB) were performed with a PSD-95 antibody. Protein size markers (KDa) are displayed at the right of each blot. 4 wild type mice were used, 2 exposed exposed to halothane (halothane +) and 2 not (halothane -), each lane showing an IP from an individual mouse brain.

increased sensitivity of *PSD-95* deletion mutants resulted not from the *PSD-95* mutation, but from co-segregation of linked genes. However, when sensitive and resistant lines were intercrossed, the offspring exhibited an intermediate anaesthetic sensitivity, implying that the phenotype was under the control of more than one gene (Koblin and Eger 1981) and so unlikely to explain the phenotype of *PSD-95* deletion mutants.

PSD-95 therefore appears to play an important role in determining anaesthetic sensitivity of different anaesthesia end points. Considering the learning deficits in *PSD-95* deletion mutant mice, it would be interesting to also study the role of PSD-95 in the amnesia end point of anaesthesia.

# Chapter 6: DISCUSSION

The assembly and regulation of NRC components may play an important role in producing appropriate neuronal adaptations to stimuli such as those that generate synaptic plasticity. Many mechanisms involved in synaptic plasticity are also important for behavioural tests of learning, so synaptic plasticity appears to be a reasonable *in vitro* model of learning and memory. PSD-95 is an adaptor protein that interacts with a number of proteins important in synaptic plasticity and learning, including the NMDA receptor. PSD-95 can physically cluster components of NMDA receptor-stimulated signal transduction pathways to this receptor. This function of PSD-95 may be important since in *Drosophila* another adaptor protein, INAD, is required for phototranduction in the eye. Mutation of *inaD* results in profound phototransduction signalling defects and mislocalisation of complex constituents (Tsunoda *et al.* 1997).

Mutation of *PSD-95* in the mouse results in altered synaptic plasticity and profound defects in learning and memory. Localisation and channel function of the NMDA receptor is normal, therefore it is believed the phenotype results from altered signalling downstream of the NMDA receptor. This is supported by observations in stimulated hippocampal slices that CaMKII activation is greater in *PSD-95* deletion mutants than slices from wild type animals.

## 6.1 The *PSD-95* Conditional Allele

A conditional *PSD-95* targeting vector was designed, constructed and targeted to the *PSD-95* locus in ES cells. ES cell clones were injected into blastocysts to generate chimeric animals, however, the mutation was not transmitted through the germline.

### 6.1.1 Possible Reasons Why Germline Transmission of the Conditional *PSD-95* Allele Did Not Occur

The existence of the *PSD-95* deletion mutant implies that mutation of *PSD-95* does not prevent the establishment of mutant mouse lines. In addition, the conditional *PSD-95* allele was designed such that *PSD-95* gene function should not be affected by the insertion of loxP sites. This may not necessarily be the case though, since some

functions of PSD-95 may have been maintained in the *PSD-95* deletion mutant through the expression of the truncated protein containing PDZ domains 1 and 2. Furthermore, the loxP sites that make up the conditional *PSD-95* allele may have been inserted into an enhancer element, interfering with *PSD-95* transcription in a manner that produced a constitutive null allele. Thus, the *PSD-95* conditional allele may not have been transmitted because the gene was inactivated and PSD-95 is required for either spermatogenesis or embryonic development. However, PSD-95 protein was only detected at postnatal stages of development (Cho *et al.* 1992; Sans *et al.* 2000) arguing against a role for PSD-95 in embryonic development, while PSD-95 expression was not detected in the testes (Cho *et al.* 1992; Kistner *et al.* 1993) making it unlikely that PSD-95 was required for spermatogenesis.

Interfering with *PSD-95* gene function was therefore unlikely to be the reason for the *PSD-95* conditional allele not being transmitted through the germline, however, targeting the *PSD-95* locus with loxP sites might have interfered with the expression of a distant gene that was required for embryogenesis or spermatogenesis. Enhancer elements control gene expression but may be located either 5' or 3' to the gene's promotor at sites that can be many kb distant (reviewed by Blackwood and Kadonaga 1998). The insertion of loxP sites into the *PSD-95* locus may therefore have disrupted an enhancer element controlling the transcription of another gene necessary for spermatogenesis or embryogenesis and thereby prevented transmission of the mutation.

It is perhaps more likely that the pluripotency of the ES cells influenced the transmission of mutations through the germline. ES cells were grown in the cytokine DIA/LIF to maintain them in an undifferentiated state, sustaining their pluripotency. When injected into a blastocyst, pluripotent ES cells should have contributed to all tissues, including the germ cells, however, culturing ES cells in DIA/LIF does not guarantee their pluripotency. It is therefore possible that the ES cells carrying the conditional *PSD-95* allele were unable to contribute to the germ cells of the testes, although little differentiation was observed in ES cell clones used for blastocyst injection based on observation of their morphology.

Only 2 fertile chimeras were generated from ES cells carrying the *PSD-95* conditional allele, both derived from a single ES cell clone, 110:88. It is possible that targeted ES cells simply did not contribute to the germ cells in these chimeras and that generation of more chimeras will result ES cell contribution to the germ cells and the establishment of a conditional *PSD-95* mouse line. Generation of chimeras using additional targeted clones (110:26, 110:2, 132:65, 132:17 and 132:42) is also required to address whether an intrinsic problem existed with the previously injected clones; this may be due to either the genetic alteration itself or because the ES cell clones used previously were no longer pluripotent. Even if clone 110:88 was no longer pluripotent, it is likely that independently derived clones, such as 132:65, 132:17 or 132:42, maintained their pluripotency and will therefore be competent to generate conditional *PSD-95* mouse lines.

### 6.1.2 Analysis of *PSD-95* Expression in Conditional and Knockout Alleles

An initial experiment to perform with *PSD-95*$^{flox/flox}$ mice would be to cross them with Cre deleter transgenic mice. Cre deleter mice express Cre in all tissues from an early embryonic age by driving *Cre* with a constitutive promotor such as the cytomagalovirus promotor (Schwenk *et al.* 1995). In the presence of Cre, loxP sites are recombined, therefore a *PSD-95*$^{flox/flox}$ mouse carrying the Cre deleter transgene would represent a ubiquitous null allele (*PSD-95*$^{-/-}$). To analyse *PSD-95* expression in *PSD-95*$^{-/-}$ and *PSD-95*$^{flox/flox}$ mice, brain tissue would be taken from these animals and compared with tissue from wild type mice by Western blotting, Northern blotting and/or RT-PCR. These analyses would answer 2 basic questions:

1) Does the conditional allele affect normal *PSD-95* expression?

   The placement of loxP sites in the *PSD-95* targeting vector was carefully considered to avoid interfering with spice donor or splice acceptor sequences. Therefore, one would not expect the loxP sites to alter *PSD-95* expression in *PSD-95*$^{flox/flox}$ mice; expression levels should be comparable between *PSD-95*$^{flox/flox}$ and wild type animals.

2) Is the knockout allele a null allele?

Following recombination of the loxP sites flanking exons 3-8, a frameshift would be produced, resulting in a stop codon being encoded by exon 9. The major transcript (PSD-95α) generated following recombination would be 56 amino acids in length and probably unstable. Although unlikely, it is possible that the transcriptional machinery could splice to a different exon 3' to the deleted region (exons 3-8), however, only exons 13 and 17 are in frame with exon 2. Splicing to exon 13 would produce a protein encoding the N-terminus and GK domain while splicing to exon 17 would encode the N-terminus and the C-terminal portion of the GK domain. Northern blotting and RT-PCR would probably only identify transcripts that spliced to exon 9 and Western blotting would determine if the potential 56 amino acid protein product was stable.

### 6.1.3 Studying Synaptic Plasticity and Learning using *PSD-95* Conditional Mutants

The main aim of this thesis was the generation of a conditional *PSD-95* allele that would allow the role of PSD-95 to be studied in greater depth, particularly its involvement in learning and memory. How could conditional *PSD-95* (*PSD-95*$^{flox/flox}$) mutants be used?

#### *6.1.3.1 Comparison of Ubiquitous Null Allele Mice with PSD-95 Deletion Mutants*

*PSD-95* deletion mice were found to express a truncated form of PSD-95 containing PDZ domains 1 and 2. The truncated protein was expressed at <20% the level of the normal protein, was not found in synaptic fractions of brain homogenate preparations (Migaud *et al.* 1998) and was therefore thought not to be functional. However, it remained a formal possibility that the truncated protein acted in a dominant negative manner. Ubiquitous null allele *PSD-95*$^{-/-}$ mice would be able to directly address this issue.

Comparing the performance of *PSD-95* deletion mutants and *PSD-95*$^{-/-}$ mice in the water maze could determine the contribution of the truncated protein to the phenotype of the *PSD-95* deletion mutants. If the truncated protein were inert, *PSD-95* deletion mutants and *PSD-95*$^{-/-}$ mice would exhibit similar learning deficits in the water maze.

However, if the truncated PSD-95 protein were acting in a dominant negative manner, one would expect the *PSD-95* deletion mutants to exhibit a more severe learning deficit than *PSD-95*$^{-/-}$ mice. Hippocampal synaptic plasticity could also be compared in slice derived from *PSD-95* deletion mutants and *PSD-95*$^{-/-}$ mice. Again, similar phenotypes in *PSD-95* deletion mutants and *PSD-95*$^{-/-}$ mice would be expected if the truncated protein were inert.

In both behavioural and electrophysiological paradigms, control animals should include wild type animals, *PSD-95*$^{+/+}$ mice carrying the *Cre* transgene and *PSD-95*$^{flox/flox}$ mice that do not carry the *Cre* transgene. These controls would test whether the *Cre* transgene, or the floxed *PSD-95* allele affects either learning or synaptic plasticity. Either *PSD-95*$^{+/+}$ mice carrying the *Cre* transgene or *PSD-95*$^{flox/flox}$ mice would not be expected to differ from wild type animals, as was seen in CA1-restricted NR1 knockout mice (Tsien *et al.* 1996).

### 6.1.3.2 A Hippocampal-Dependent Role for PSD-95?

The hippocampus has been shown to be required for spatial learning and it would therefore be interesting to test the importance of PSD-95 in this brain region by knocking out *PSD-95* specifically in the hippocampus (*PSD-95*$^{hipp}$). The phenotype of such a regional-specific knockout could then be compared with the ubiquitous *PSD-95*$^{-/-}$ null mutant.

Generating *PSD-95*$^{hipp}$ mutants would require hippocampal-specific *Cre* expression. One way to achieve this would be by crossing *PSD-95*$^{flox/flox}$ mice with transgenic mice that preferentially express *Cre* in the hippocampus. In house, Cre-Pr1 mice are available that exhibit hippocampal-specific *Cre* expression, using the *αCaMKII* promotor to drive *Cre* expression. Another method that might be used would be to stereotactically inject *Cre*-expressing adenovirus into the hippocampus of *PSD-95*$^{flox/flox}$ mice.

Comparing *PSD-95*$^{hipp}$ and *PSD-95*$^{-/-}$ mutants, there would be a range of possible outcomes:

1) *PSD-95$^{hipp}$* mutants are indistinguishable from ubiquitous mutants, displaying profoundly impaired learning, indicating that PSD-95 is required only for hippocampal-dependent plasticity and learning processes.
2) *PSD-95$^{hipp}$* mutants exhibit a similar, but less extreme phenotype than ubiquitous mutants, indicating that other brain regions are also involved in the performance of mutants in learning paradigms.
3) *PSD-95$^{hipp}$* mutants learn normally indicating that the ubiquitous mutant phenotype is not due to hippocampal dysfunction but rather some other behavioural system is affected.

The first 2 possibilities would be the most probable outcomes. Control experiments performed with *PSD-95* deletion mutants in the water maze (visual platform training) did not identify motor or visual deficits (Migaud *et al.* 1998), therefore it would be unlikely that their poor performance was entirely independent of the hippocampus. However, without a hippocampal-specific knockout of *PSD-95*, the contribution of other brain regions to the phenotype cannot be assessed and so outcome 3 remains a formal possibility.

#### *6.1.3.3 The Role of PSD-95 in Synaptic Plasticity: Pre- or Postsynaptic?*

Enhanced LTP was observed in the hippocampi of *PSD-95* deletion mutants, however, these animal could not address whether the role of PSD-95 was more important pre- or postsynaptically, or if PSD-95 was equally important in both pre- and postsynaptic neurons. It might be expected that PSD-95 would have a more important role postsynaptically since it is enriched in the PSD.

Stereotactic injection could deliver *Cre*-expressing adenovirus specifically to the CA3 or CA1 regions of the hippocampus, knocking out *PSD-95* in these regions and generating *PSD-95$^{CA3}$* or *PSD-95$^{CA1}$* mutants respectively. Alternatively, *PSD-95$^{flox/flox}$* mice could be crossed with CA1- and CA3-specific *Cre*-expressing transgenic mice such as the T29-1 (Tsien *et al.* 1996) and G32-4 (Nakazawa *et al.* 2002) lines respectively. Hippocampi from subregion-specific knockout animals could then be used for synaptic plasticity experiments. Synaptic plasticity in the CA1 region would be

induced by placing stimulation electrodes in the CA3 region (presynaptic) and recording electrodes placed in the CA1 region (postsynaptic). A comparison of *PSD-95*$^{CA3}$ and *PSD-95*$^{CA1}$ synaptic plasticity phenotypes would allow the contribution of pre- and postsynaptic PSD-95 to be assessed.

#### 6.1.3.4 A Role for PSD-95 in Encoding and Retrieval of Memories?

There are considered to be 3 phases of learning: encoding, consolidation and retrieval. Encoding is the initial laying down of a memory, while consolidation is the phase in which pertinent memories are strengthened. Retrieval is the use of a memory, for instance, to find a hidden platform.

Encoding of spatial memories has been shown to be NMDA receptor dependent (Morris *et al.* 1986; Morris 1989), however, retrieval did not require NMDA receptor activity (Morris 1989). It is therefore likely that PSD-95 plays an important role in the encoding phase, however, the binding of PSD-95 to other proteins may also make it important in retrieval. The temporal control possible with *PSD-95*$^{flox/flox}$ mutants can be exploited to ask whether PSD-95 is required for encoding or retrieval or both.

Temporal control of *PSD-95* ablation could be achieved by crossing *PSD-95*$^{flox/flox}$ mice with *Cre* transgenics that express a Cre-steroid binding domain fusion protein. Application of a synthetic ligand would activate Cre, inducing the deletion of *PSD-95*. Using the water maze, this system could knockout *PSD-95* either prior to spatial training (encoding) or after training but before the transfer test (retrieval). In this way, the role of PSD-95 in encoding and retrieval could be investigated. An alternative method to knockout *PSD-95* with reasonable temporal control would be to deliver *Cre*-expressing adenovirus to the hippocampus either before encoding or retrieval.

## 6.2 PSD-95 and Anaesthesia

General anaesthetics must act on both spinal cord and brain to induce anaesthesia, which is described as loss of consciousness, amnesia and immobility in response to noxious stimuli. The multiple effects of anaesthetics make it unlikely that a single protein target mediates their action, although mice carrying mutations in single genes have exhibited

differing sensitivities to anaesthetic agents. The increased sensitivity of *GluR2* knockout mice to volatile anaesthetics in the LORR tests was explained by an imbalance between excitatory and inhibitory transmission, unmasked by the anaesthetic. In *PSD-95* deletion mice, no obvious imbalances were observed (Migaud *et al.* 1998), therefore PSD-95 may have acted as a specific target for halothane-related anaesthetics; halothane might have stimulated the dissociation of PSD-95 from a receptor or channel, altering the function of that protein in a manner that contributed to anaesthesia. Alternatively, PSD-95 may have masked a halothane binding site on an ion channel, such that the binding site only became available with the dissociation of PSD-95 from the ion channel. In the absence of PSD-95, this halothane binding site would be constitutively unmasked, possibly explaining the reduced anaesthetic requirements observed in PSD-95 mice and following antisense knockdown (Tao and Johns 2001), determined by LORR and MAC respectively. In light of the profound learning deficit in *PSD-95* deletion mutant mice, it is also tempting to speculate that halothane and PSD-95 might interact to influence the amnesia component of anaesthesia.

The brain regions important in the induction of anaesthesia have not yet been well defined. *PSD-95*$^{flox/flox}$ mice could be used to elucidate the brain regions that mediated the increased halothane sensitivity in the LORR test observed in *PSD-95* deletion mutants. *PSD-95* could be systematically knocked out in candidate brain regions such as the midbrain reticular formation and the thalamus and the mice then analysed in the LORR test. To produce such regional-specific knockouts, *Cre*-expressing adenovirus would be stereotactically injected into target brain regions of *PSD-95*$^{flox/flox}$ mice.

In summary, murine *PSD-95* was cloned, characterised and novel mouse PSD-95 variants identified. A conditional *PSD-95* allele was generated that will allow the role of PSD-95 to be studied in much greater detail. The capacity for temporal and/or regional control over *PSD-95* ablation engendered by this conditional allele will facilitate interesting studies of the involvement of PSD-95 in synaptic plasticity, learning and anaesthesia.

# Appendix 1: Diagrams of genomic subclones

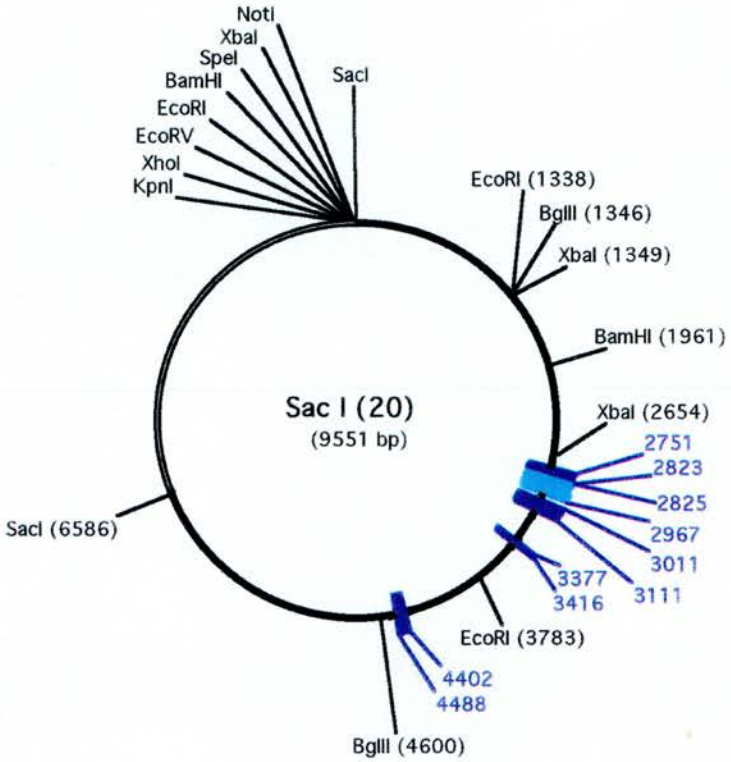


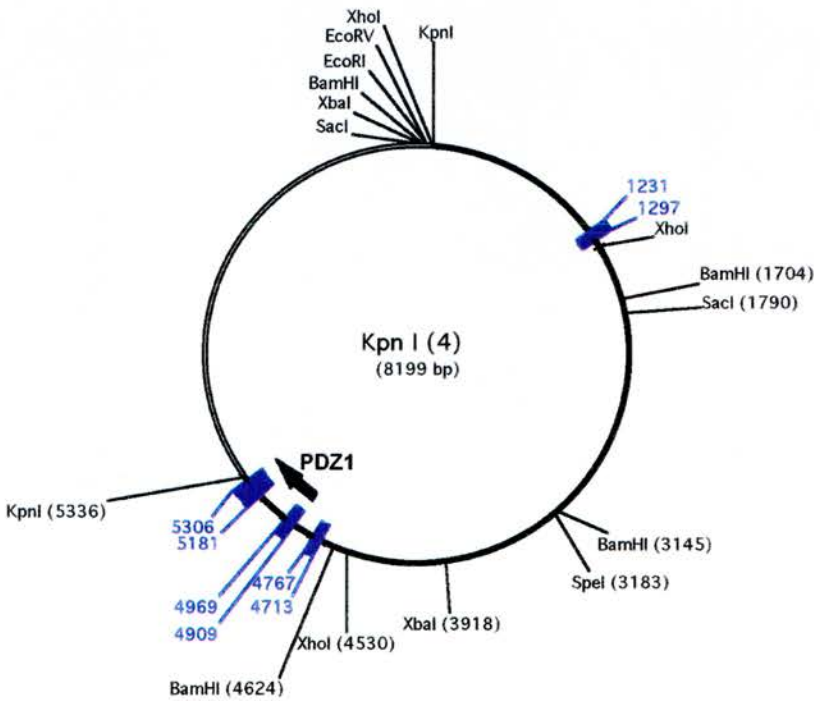

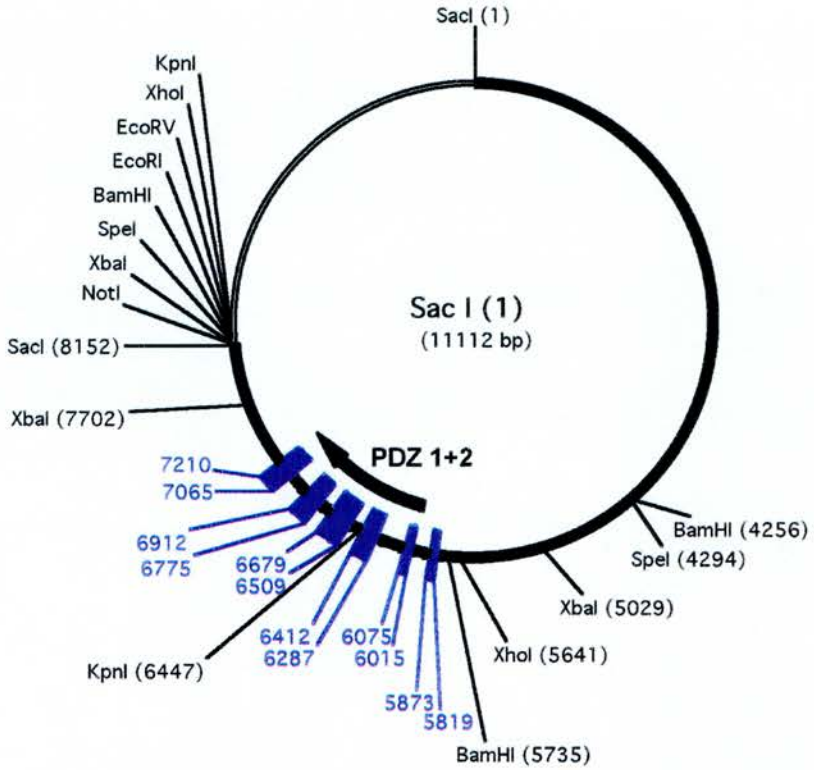
SacI (1)
KpnI
XhoI
EcoRV
EcoRI
BamHI
SpeI
XbaI
NotI
SacI (8152)
XbaI (7702)
Sac I (1)
(11112 bp)
PDZ 1+2
7210
7065
6912
6775
6679
6509
6412
6287
6075
6015
5873
5819
KpnI (6447)
BamHI (4256)
SpeI (4294)
XbaI (5029)
XhoI (5641)
BamHI (5735)

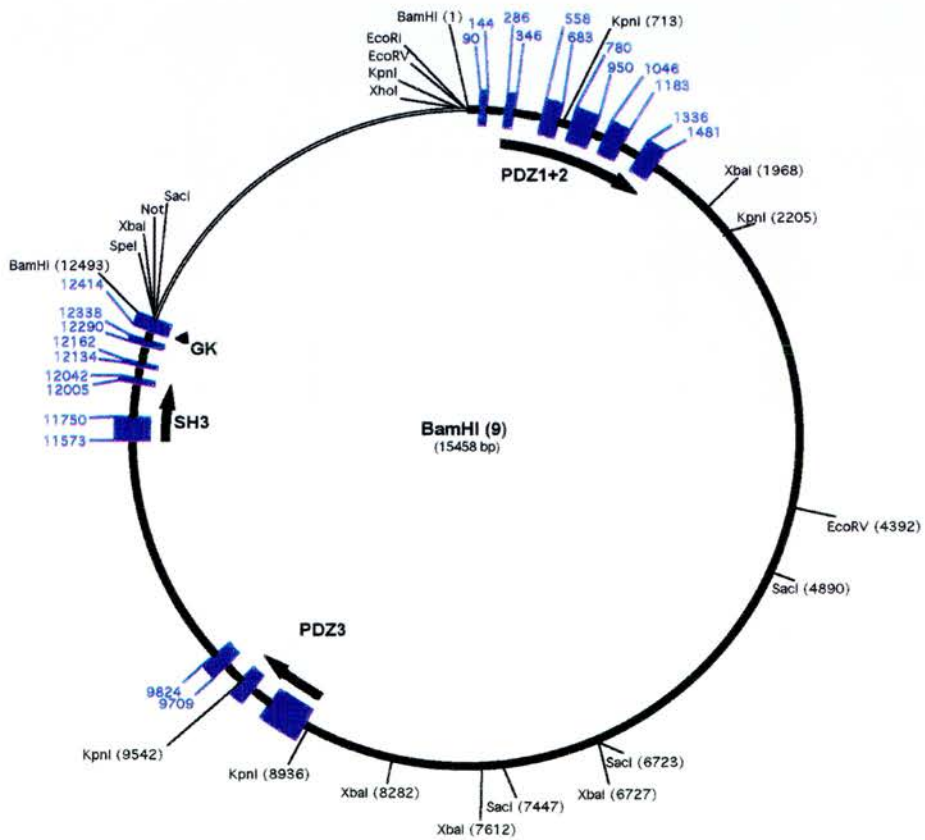
BamHI (1)
144
286
558
KpnI (713)
EcoRI
EcoRV
KpnI
XhoI
90
346
683
780
950
1046
1183
1336
1481
PDZ1+2
XbaI (1968)
KpnI (2205)
SacI
NotI
XbaI
SpeI
BamHI (12493)
12414
12338
12290
12162
12134
12042
12005
GK
11750
11573
SH3
BamHI (9)
(15458 bp)
EcoRV (4392)
SacI (4890)
PDZ3
9824
9709
KpnI (9542)
KpnI (8936)
XbaI (8282)
SacI (7447)
XbaI (7612)
SacI (6723)
XbaI (6727)

# Appendix 2: Sequence of SacI (20) subclone

α1, β1, β1' and β1'' exons are highlighted in dark blue, γ1 exon is highlighted in light blue.

```
   1 GCAGCCCGGG GGATCCACTA GTTCTAGAGC GGCCGCCACC GCGGTGGAGC TCTGGTCATC
  61 CCTTACCTCA AAGAACCGGG CCACTGGTCC CACCAGCTCT TTGAGAAATT GTGCCTGTTC
 121 TTCACTGAGC ACTGTATAAT GGGAGAGAAG AGCAGGCTAG TCAGGCAGAG AGGGCTCCCC
 181 TGCCCACACT GTCAGTGACT GACTAAGCCT TTACTTACCA GATGGGTATG GGAACACCTG
 241 ATCAATGGTA AGCTGGCCTT TGAACATCCC CACAGCAAAG GACTTCGATT CCTAGGCAAG
 301 GAAGGAAAGG ATCTTAGGTG GGTGCCTGGG GTGATTCTAC TCCTGGTTTT TAAGTGTCAG
 361 TCCAGTTTCC AGTCACTTAC TGCCCTGGCT GGTTTTTCTC TGGTGGAAGC ATCAGAGGAG
 421 AGGGTTTCTG GCTTGTCCAG AACTGCCTGG AGGGAAGGGC AGAGCAGTTA GGCTGGAGAT
 481 GGGTCTTAAA AGGTGTGCAG GAAGCGCTAG CTCTAGGAAG TGCGTTTGGT GCATGTTCCA
 541 TTACTTTCTC ACTAGGGCAC CCTGGCGTGC CCTTTCCCCT ACTTTCAGTG ACAGAACTGC
 601 CACCAGGTGA CTGGGTCGAA GAGAGAGACC CCTGTCGGTC GCAGGCTAGT GGGAACTGGC
 661 AACTCGCATT TCTACGTCCG TCTCCCTCAT CCACTGTCAC TTACCTGAGT GGCCTCCCTG
 721 GCATAAAGTC GCTGGGCAGA GATAGGCCGG GGTTGTCCCT GAAGCACAGT AGTAGATCGC
 781 GAGCTGTAAG GAGTCGGGGT TCAAGTTCTG CCCTGGTTCC CANACCCAGT GTCCCCTTGC
 841 TATATACGGA CCTTCGGGCC CCCAGCCGCA GCAGCTGTCG CCCCACACTC GGGGTCATCC
 901 GAGCCGACTG CATCTCCAAA GCCGCCGCCG AAGTCTTGAC CACTGACCTC TTCTCTTCGC
 961 GTCTCGCCTG CCCAAAGGTT GTGTGTCTGG GCCCTGACTC ATGCTCCACA ATGCACTGCG
1021 TGGTGGGGGC GTGGTCTTGG GCCTCNATGC ATGGTGGGAG CTGAAGTTCC NACGTGTGCC
1081 CGGTCCCTGT ATTCTACCTG ACCTAGGGTG ATCCATCTTC AAACGATCCG TTTTCTTTCC
1141 CAAACTCTAT AGAGCCGCTG GTCTAAACTA AAGTCTGATC CACTAAAAAG GGAAGAGATT
1201 AGATAAGAGA AGGAAGAATT AAATGACTAG AAGGTTGGAG GTAGACTGGA GGGAGGACTT
1261 CCTAGCTAAA GTTAAAAGAG AGAAAGGAAA ATATCAGATG CAGAGACCTG GATTATAAGG
1321 AAAAAAATTC TCCTTCAAAT AAAGAGGGGC CGTGAGGTGG CANACTCAAG CTGGGGTGTN
1381 CTCTAAGCGA ATTCTGAGAT CTAGAAGATT TCACCAACTT AAAACACTTC TNAAAGCGCG
1441 TAGTAGGCAC CTCTAGTCTC TCATGGACTT TGGGAGATAA TAAATCACGA TCACTATGAA
1501 TTTGANGCCA CATATACCCT GCTNGAGTGA NGACTCCAAA TACATAAGTC TTAGGAAATG
1561 AATACTTTTT TTTAAAAAAG AACTTTATGT GTGTCTCTGT GTGTCTGTAT ATTAACCGTG
1621 TGCACATGGG TGCANTGCCT ATTGATACAN NANACCAGAA GCTGTGGAGC TGGAGGGAAG
1681 TTGTGAGTCT CCCGACGTGG TTGCTGAGAA CAGAACTAAG GTCCTCTGGA AGAGCAAAAT
1741 GCATCGTGTG TGTGTNGTAT GGTTTTTGTT GTTGTTGGAG GAGGTTTGTT TTTCTGAGAC
1801 AGGGTTTCTC TGTGTAGCCC TGACTGTCCT GGAACTTACT CTGTAAACAA GACTGGTCTT
1861 GAACTCAGAA ATCTGCCTGC CTCTCCTTCC CAAGTACTGG GATTAAAGGT GTGCGCCACC
1921 ACTGCCAGGC TAGTTTTTTT GTTTGTTTGT TTTTTAATTT ATGTATGTGA GTACACTGTA
1981 GCTGTCCTCA GACACATCAN AAGAGGGCAT CGGATCCCAT TATAGATGGC TGTGAGCCAC
2041 AATGTGGTTG CTGGGTATTG AACTCAGGGC CTCTGGAAGA GCAGTCAGTG CTTTTAACCC
2101 CTGAGACATC TCTCCAGCCC TCCCTTTTTT TTTTTTTTTT TTAGGCTTTA AAGGTTTATT
2161 TTAAAATTTT TATATATATG AGTGTTTTGG GTGTATATAT ATATATATAT ATATATATAT
2221 ATATANCCCA CCAAGGTCAG AAGAAGGCAT TAGATCACCT GCAACTGGAA TTACATACAG
2281 TTAGCTGTAC ACTGCCATGT ATGTGGACAC TGGAGACTGA ACACAAGTCC TCTGCCTAAG
2341 AGCAACGCAT GCTCTGATTG CTGAGCTGTC TTGAACCTCA TCTAAAAGTC TGCTTATGCG
2401 AGTGTGCACT CACATAAGCC CTTATCAGAA GACAACTTCC AATAGTTCTC TCCACATTTA
2461 TGTGGGTCCC TGATGACAGG CTTGGCAGTG AGTTCCTTTA CTCAGTGAGC CATGTCACTG
2521 CCCCCGACCC CTTCTCAGTA TGGTCAGGCC TGGGGAGAAA AAGAGCTTAA CTCTGGGTTG
2581 CTGGGACTGC CTTAAATAAA ATCCTCTTTC CCACTCACAG AAAAGCAGCT AAATTATGCC
2641 TGGCATTTGG GAAGGNNCAC TATGCGGAGC AAAGTGTTAC CTGGNGACCT GGGGAAGAAT
                                                          exon β1
2701 GGAATCTAGA CCGATTGTCC ACTTTACTAG CTACAACTGC GTAGGCTGAA GGCAGCTCAA
2761 CTTCAATCTT GGCGGATTAG GGAGATTAAA TCGAGAGAAG AGAGATGTCC CAGAGACCAA
```

exon γ1

2821 GAGGTGAAAA AAAAAAACCA ACCCGGGTCT TTGAGGGGGT GATCTGGATC TGGGATGGGG
2881 GCCCAGGGGC TCCTTCTCTT CCTGAATCTA TCCATGGTGT CTGGAAAAAG AAGACAAAGG
2941 CTGGGAAACC TTAGATGACT AAGTGGGTAA GTGGCTTGGT CTCGATCCTT TGTCACTTGC

exon β1'

3001 TTTTTTACCA GCTCCCAGGT CAGCCCTCTG GCTACTGGCC CCCCCACTAC TGCGGTGGGC
3061 ACCTCCCCTC CTCACAGTGC TGCACAGTGA TCTCTTCCAG GCCTTGCTGG GTGAGTAAGG
3121 CTGGTGTTCT GAGGGGCCAC AGTGGACAGG GCTGGCCTGT GGTATGGGGT CAAGCATTAC
3181 AGGTTCTAGG CTGGTTGGAA ATACTCAGAG CATCTAGTCC AGGCTCTCGC TTGTATAGAG
3241 CCATCACACT GTACCTCCTA GCAGCATCCA TCCTAGCCGG AGGAGCCTCT CTTGACACAC
3301 AGAAGCCAGG GGTAGCAGGG GTGGCCAGAG GGCCCCGGGA TTTGGGAGGG TGACTTAATT

exon β1"

3361 CTGTTCCTGT GACAGACATC CTGGACTATT ATGAGGCTTG TATCTCAGAG AGTCAGGTAA
3421 GGTGATGACG GTGGGTGCCT GGCTTCCTGA CTGCCTGAGC TGGCAGGACT GGAGGGACAA
3481 GAGTACATTC TTCTAATTCT AAACTGAGAC TTAGGGGCCC AGGCAACATG ATCCCTAGTN
3541 CTGACTGAGG AGTTGGGGCA CCAGCAGTGC TGTCTGTGGG CAGCCAGCCC TATGCCCTTT
3601 CTCCTTTCTT CTCCCCTTTC TTGCATTGCC CCAATTTCAA TACCAGGAAG TCCAGGTCAT
3661 ACTTAATTAC TTTTCAGACT TCTTCCTGTG ACTCCTAGGG GAGAACTAGG TCCCCAAGAT
3721 TCTCTACTGC CAGCCCCTCC CTCAACCCCT TACCCCACGC TATGGCCTCC CTCCTGCACT
3781 CAACCAAGGA GGGATGCTCC CCTCCCAGCT GTGGGCTTTT TTCCTCTAAG GAGGAATTCC
3841 ATCCTCCTCA TCTTTGCTGT CATCACCGAG GTTAGCCAGG TCTCCATGTT TGCCGTAGGG
3901 CCTCTCTGCT TGTGCTTCTA GCTCCTTTCC CATTATCCGG GTTCCTGCCA GCAGTGAAGG
3961 AGTTAACACT GCCAAGGCAC CCCCCCCATT CTGGCTCCTA GCTCCCTCCC TCCCTCCCCC
4021 TGCTTCCTCT CTCCTCCTCT CTCCCCTTCC CTCCTCGGCT CCGCGGCTAC ATCGGCCGCT

exon α1

4081 GCCATCTCCA ACCCCCCCCA CCCCACTCCC CCGCCACGGC CCCTAGCCCC TGGCCGTTTG
4141 GCAAGACCCC CGCATACCCC GGGGCTTCCC GAAATCCAGT TCCCCTCCCC CATCCCAGCT
4201 CATGCCCCAG CCCCAGAACT CCGGGGCTGC CAGCCCCCTG TGCCCCTACC CCTCCTGAGA
4261 ATCGGGGTGT GCTCCTCAAG CCCCCTCCCC TCCACTGGGG AGCCCCTTTT AGGGTCCCCC
4321 CTCCCTTCCA CGCTCCCCTA CCCTTCTCTT CTCCAACCTT CTCCTTCCCC TCTCACCCCT
4381 CCCCCCATCC TGGCCCCCCC TGCAAAAGTG GGGTGCGGAG GGGGGAGGGG TGAGAACCCA
4441 CCGAGGGGAG GAACAAAACT CCAATGAAGT CAGAGCCCCC TACTCGCCGC CGCGGCCAGG
4501 CCCCCCAACA TGGACTGTCT CTGTATAGTG ACAACCAAGG TAAGCATGAT GGGGAAGCCG
4561 TGGGGAGGGG GAGTAGGTAA TGAATTTGTG GAGAAGGGTT AGGTAGGCCT TATCTAGGGC
4621 TGCAGGCNCT GGAGTGAGAG CCTCAGAAGT AAGATCTATT AGAGGGGGTC ACAGTTTAGT
4681 TTTGGGGTTC ACATCTGAGA AAAGGATGGA TTTGGCCACA GGTGCCTCCT GGAGTGATCA
4741 TTTTGTACCT ATAAGGAAAT GGAGAATCTG GTGTTTGGGG TGGCTTGGTG AGCTTTAGTG
4801 TTCACCANCA NTGTTTTGAG GGCAATTTAT TTAAGGAGAA GCCTGCCTGC CTCACATGGG
4861 AGTTCTGCTC ATATATGTGG GAAGGTGGGC TATGTGAGTG TGCTGGGGGG GAGGGTTGTC
4921 TTCCTTTCTG GGCAAAAAAG CTCATTTTGA GATACTGACC AATTTTTGGG GGGTCTCTTG
4981 GCATGAGGGT AAAGGTTACT GGTTGTGAGT GTCTGGCTTG TATGGCGGTG TCAACTAGCA
5041 GGTAAGGGTG GGCCTTCAGG TGGTAGAACA TCTTGTGCTA GACATGTTTG GGATGCTCCT
5101 GCTTTGAGGG AATTGTACAT TGAGGGTTTA ATTATGTGGA ATAGAGTGAC CTGGGAGTTG
5161 TCAGAGGCCT GAGGCCTGAT ACAGCCTTAC CTGAGAGAAT GGACCAGGTG GGATTAGGAT
5221 GTGGGGTACT CCCCTGGGAG CTAGAAGCTT GCAACAGCTG AGGTTGCCAT CTCCTAAGAA
5281 GGATGAGGTT TGGGGTAGCA GGAGAGAAAG AAGGTAGTTG AGGACCATGT GGGTGGTNCA
5341 AAATTTGGGG GTAGCCCAGG CAGGTGCCCA NTATTCCCAT CTCCCACATT TTATCTANCC
5401 CTGGTCAAGA NAACANANNA ACAGATGCGG GGGGGGGGGG GGCAGGGGAT GTTACCCTTA
5461 CTCTTGGGAG GACTCCTGGA TCTCAGGAGG CTTGTGAGGT CAAGAGGCCA CTGGGGTAAA
5521 AAGGTGTAGG AAGAGGGCAG GGCTGGGGGG GCTGGAACCC ATACACGGGT ACAAGGGTGT
5581 CCCTGTGATC AGAGCCTGGA AAGAGTGGGA TGGAAGCCCA AGGAGCTGAG GCCCGTTTGC
5641 TCCCANACTC TGGGACTGGC NAGCTGGATG CCTGGTGTGT GGAGGGAGGC TTGGGCAGGG
5701 TGGCAGGCAG CTGGGGGTTG GGGGGTGGGA CAGGAAGTGG GGGCCGGGGG AGGCGGGGTC

```
5761 CGTGTGAGTC ACAGGCTGGG GAGGGGGTTA TATTTAGTGG GAACTGCAGC TTCTTATGGG
5821 AGGAAGCTGA GGACACACAT GTTCCTTGCC ACAAACTCAC ACATGTGTAT ACACATGCAT
5881 TGTGCACGTG TGGACATGAT TANAGACTGG GGACTGAAGA CTTTAGTTCT GTATCCCTCA
5941 CCCCATCTAC AGGGCTGCTT GTTTTTCTAC TGGTCTGTGG GTTTTGGGCG TTCTTCCAGG
6001 TTGCTGGCTC TCTCATCCCC TGTAGTTTTC AGTACATTTT TGTGCCTCAG TTCTTCTGGC
6061 CCTCTTTCAG TCAGTGTCTG CCTGTGCTCT TTGTGTCTCT TGTCCTTAGG CCTAATCNTT
6121 GGCCTTGGCA ACNTAACTTG TCATCACCTT TGTGCAGATA GGAAACCCAT TGGAATATGT
6181 GGGTTCTCCT AACGCATGAG CACATGAAAT CCAGTAAGGG TGAGGGGCTC CGCAGCACTG
6241 GTTAACTATT CTGGGTGGAT GCATTTATTC ATTTTTCTGC CCCAAATTCC TGTGTGTTCG
6301 ATGGAGCACA TGATTGAGCA GCCCTGAAGG TAGGAGGCTT GTAGAGAGGA TCATATGCAT
6361 TCGGGTCTTA CTGGTTTGGA GACCCAGGTT TGCCACATTC ATTGGCCAGA AAACTTGTCA
6421 GCCTCAGGAT GGAGGGACTC CAACTCCCAT AAGGCCTTGA GGTACTAGAT CCTTCAATGG
6481 TAGCGTGTGG TTGTCCACTG GACTGTTGGG AGTTGTGGTT CCTCTCNATC CAGGCCAGTG
6541 GAGGGTGGCC CAGGACCAAC CAGCAGGGGG CACATGGCTT CTGCCCTCCG CAAATGNTGG
6601 GGAGTGGGAT TAGGAGTGNT CAGCCTTTGT AGTCACCGAG CTCCAATTCG CCCTN
```

# Appendix 3: Illustrated PSD-95α cDNA

The published PSD-95α cDNA is shown (Genbank Acc. No. D50621) with residue number labelled on the right. PDZ domains are highlighted in green, the SH3 domain is highlighted in yellow and the GK domain is highlighted in pink. Start and stop codons are underlined and in bold. Forward primers are highlighted in blue and labelled in black, reverse primers are boxed in red and labelled in red. Intron-exon boundaries are marked by a vertical black line.

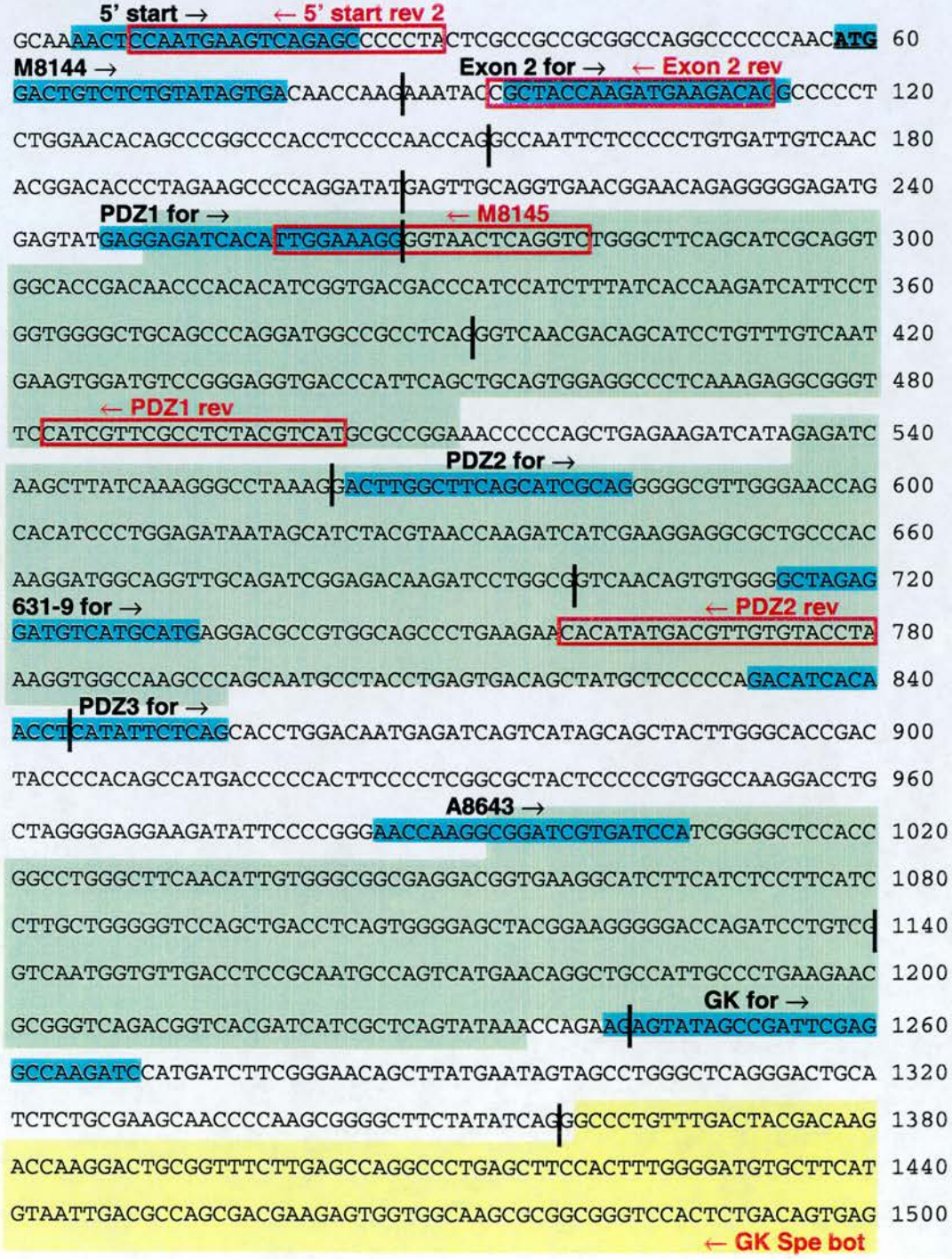

## Appendix 3: Illustrated PSD-95α cDNA

```
ACCGATGACATTGGCTTCATTCCCAGCAAACGGCGGGTCGAGCGACGAGAGTGGTCAAGG 1560
TTAAAGGCCAAGGACTGGGGCTCCAGCTCTGGATCACAGGGTCGAGAAGACTCGGTTCTG 1620
AGCTATGAGACGGTGACGCAGATGGAAGTGCACTACGCTCGCCCCATCATCATCCTTGGG 1680
CCTACCAAAGACCGTGCCAACGATGATCTTCTCTCCGAGTTCCCCGACAAGTTTGGATCC 1740
TGTGTCCCTCATACGACACGTCCTAAGCGGGAATATGAGATAGACGGCCGCGATTACCAC 1800
TTTGTCTCCTCCCGGGAGAAAATGGAGAAGGACATTCAGGCGCACAAGTTCATTGAGGCT 1860
GGCCAGTACAACAGCCACCTCTACGGGACCAGCGTCCAGTCTGTGCGAGAGGTAGCAGAG 1920
CAGGGGAAGCACTGCATCCTTGATGTCTCAGCCAATGCCGTGCGGCGGCTGCAGGCGGCC 1980
CACCTGCACCCTATCGCCATCTTCATCCGTCCCCGCTCCCTGGAGAATGTGCTAGAGATC 2040
AATAAGCGGATCACAGAGGAGCAAGCCCGGAAAGCCTTCGACAGGGCCACGAAGCTGGAG 2100
CAGGAGTTCACGGAGTGCTTCTCAGCCATCGTAGAGGGCGACAGCTTTGAAGAGATCTAT 2160
CACAAAGTGAAACGTGTCATCGAAGACCTCTCAGGCCCCTACATCTGGGTCCCAGCCCGA 2220
GAGAGACTCTGATTCCTGCCCTGGCTTGGCCTGGACTCACCCTGCCTCCACCACCTGGGC 2280
CCTTGGTCTGGACTGAATAGCCCAATAACCCTACCCCTAGCCCCCCAACTAATTACCT   2338
```

# Appendix 4: Primer sequences

**pBluescript KSII Primers**

| | |
|---|---|
| t3 KSII | 5' CCAAGCTCGAAATTAACCCTCAC 3' |
| t7 KSII | 5' GCCAGTGAATTGTAATACGACTCAC 3' |

***PSD-95* Forward Primers**

| | |
|---|---|
| 4 For 1 | 5' GGTGTGGGAGGTTCTTGTTCTGG 3' |
| 5' Kpn For | 5' TGCTGTCACCCCCTAAATGCCG 3' |
| 5' Start | 5' AACTCCAATGAAGTCAGAGC 3' |
| 20 For 1 | 5' GTGTCAGTCCAGTTTCCAGTC 3' |
| 20 For 2 | 5' GTTCAAGTTCTGCCCTGGTTCC 3' |
| 20 For 3 | 5' AGAAGGTTGGAGGTAGACTGGAGG 3' |
| 20 For 4 | 5' GCTGGAGGGAAGTTGTGAGTC 3' |
| 20 For 5 | 5' GACACATCAGAAGAGGGCATCG 3' |
| 20 For 6 | 5' TAAAAGTCTGCTTATGCGAGTGTG 3' |
| 20 For 7 | 5' CGAGAGAAGAGAGATGTCCCAGAG 3' |
| 20 For 8 | 5' TGACACACAGAAGCCAGGGGTAG 3' |
| 20 For 9 | 5' ATTCTCTACTGCCAGCCCCTCC 3' |
| 20 For 10 | 5' TTATCCGGGTTCCTGCCAGC 3' |
| 631-9 For | 5' GCTAGAGGATGTCATGCATG 3' |
| A8643 | 5' AACCAAGGCGGATCGTGATCCA 3' |
| AGAP For | 5' GATTCAGCTAGAGACCATG 3' |
| Exon 2 For | 5' GCTACCAAGATGAAGACACG 3' |
| GK For | 5' AGAGTAATAGCCATTCGACCGGAAGATC 3' |
| Int 1 For | 5' TGGCTTGGTGAGCTTTAGTG 3' |
| Int 1 For 3 | 5' AAGGTGTAGGAAGAGGGCAGG 3' |
| Int 1 For 4 | 5' GGTCTGTGGGTTTTGGGCG 3' |
| Int 1 For 5 | 5' CCAGGTTTGCCACATTCATTG 3' |
| Int 2 For 1 | 5' TGGGGGAAAAGATGGGGTG 3' |
| LP3 Rev | 5' GTGTTCTAAACGTAAGCCTGTCTG 3' |
| LR For 1 | 5' GAGCAGCTTTCTCCCACTCCGTCC 3' |

| | |
|---|---|
| LR Rev 1 | 5' CCAAGTAGGGTTACATATCAAGACGC 3' |
| LTNL Rev | 5' GTTTGCTCGACATTGGGTGG 3' |
| M8144 | 5' ATGGACTGTCTCTGTATAGTGA 3' |
| PDZ1 For | 5' GAGGAGATCACATTGGAAAGG 3' |
| PDZ2 For | 5' ACTTGGCTTCAGCATCGCAG 3' |
| Sac 1 For 1 | 5' CAGTTTCCCGTTTGTCTCTTG 3' |
| Sac 1 For 2 | 5' GGAAAGTGGGAAGGGCAAGG 3' |
| Sac 1 For 3 | 5' AGGTGGCAGGTGAGGATAGGAG 3' |
| Sac 1 For 3a | 5' AGGGGTCCAGGATGAGGTAAAG 3' |
| Sub O For | 5' CAGGGCTACATAGGGAAAAACC 3' |
| Sub O For 2 | 5' GTGAGAAGGAAGGTTGTGGTGG 3' |

***PSD-95* Reverse Primers**

| | |
|---|---|
| 3N | 5' AGGACTCTCTTTGGTGGGCA 3' |
| 3' Sac 20 | 5' CCCTCTCTGCCTGACTAGCCTG 3' |
| 4 Rev 1 | 5' TGGAGACTCGGGAACAGGCAG 3' |
| 5' Kpn | 5' ACTATCCCAACTCCAGACTCC 3' |
| 5' Start Rev 2 | 5' TAGGGGGCTCTGACTTCATTGG 3' |
| 20 Rev 3 | 5' AGGGGCGTGAGGTGGCAGAC 3' |
| 20 Rev 4 | 5' TTGGTGGTGGTTTGTTTTTCTGAG 3' |
| A8646 | 5' AGGACTCTCTTTGGTGGGCA 3' |
| B7524 | 5' AATCGCGGCCGTCTATCTCAT 3' |
| Exon 2 Rev | 5' GTGTCTTCATCTTGGTAGCG 3' |
| GK Spe Bot | 5' CTTGGCCTTTAAACTAGTCCACTCTCGT 3' |
| Hu Exon 2 For | 5' GGTCAGCCCTCTGGCTACTGG 3' |
| Hu Exon 3 For | 5' CATCCTGGACTATTATGAGGCTTG 3' |
| Int 2 Rev | 5' ACAAGTTCCTCTCCGCCACG 3' |
| LP3 Rev | 5' GTGTTCTAAACGTAAGCCTGTCTG 3' |
| M1 Rev | 5' GTCCGTGTTGACAATCACAG 3' |
| M2 Rev | 5' CGCATTACACCCCAGAGTTC 3' |
| M3 Rev | 5' CAGGAGGATTCTATTCGTGG 3' |

| | |
|---|---|
| M4 Rev | 5' GCCCATAATAGATTCCATACCC 3' |
| M8145 | 5' GACCTGAGTTACCCCTTTCCAA 3' |
| Oligo 4 | 5' AGCGGTTAAGAGCACTGACTG 3' |
| PDZ1 Rev | 5' ATGACGTAGAGGCGAACGATG 3' |
| PDZ2 Rev | 5' TAGGTACACAACGTCATATGTG 3' |
| RPD | 5' ACTGAGCCCCCGAAAAGAGG 3' |
| Sac 1 Rev 1 | 5' GTTTCAGGACAGCCAGGACTATG 3' |
| Sac 1 Rev 2 | 5' GCGCTCTCGGAAGACCCTG 3' |
| Sac 20 Rev | 5' GAACAGTTAGGCTGGAGATG 3' |
| Sac 20 Rev 2 | 5' GCCGCCGAAGTCTTGACCAC 3' |
| SH3 Spe bot | 5' GGGAGAAAATACTAGTGAGCAGTCGG 3' |

**Oligonucleotides**

| | |
|---|---|
| SalI-NotI polylinker top | 5' TCGACGAATTCGGATCCCGGAAGATCTGC 3' |
| SalI-NotI polylinker bottom | 5' GGCCGCAGATCTTCCGGGATCCGAATTCG 3' |

EcoRI-loxP top

5' P-CTAGAGAATTCATAACTTCGTATAATGTATGCTATACGAAGTTATT 3'

EcoRI-loxP bottom

5' P-CTAGAATAACTTCGTATAGCATACATTATACGAAGTTATGAATTCT 3'

NB: P = phosphorylation

# Index of Figures

# Index of Tables

# References

Abe, K. and H. Saito (1993). Tyrosine kinase inhibitors, herbimycin A and lavendustin A, block formation of long-term potentiation in the dentate gyrus in vivo. *Brain Res* **621**(1): 167-70.

Abel, T., P. V. Nguyen, M. Barad, T. A. Deuel, E. R. Kandel and R. Bourtchouladze (1997). Genetic demonstration of a role for PKA in the late phase of LTP and in hippocampus-based long-term memory. *Cell* **88**(5): 615-26.

Abeliovich, A., C. Chen, Y. Goda, A. J. Silva, C. F. Stevens and S. Tonegawa (1993). Modified hippocampal long-term potentiation in PKC gamma-mutant mice. *Cell* **75**(7): 1253-62.

Abeliovich, A., R. Paylor, C. Chen, J. J. Kim, J. M. Wehner and S. Tonegawa (1993). PKC gamma mutant mice exhibit mild deficits in spatial and contextual learning. *Cell* **75**(7): 1263-71.

Adams, J. P. and J. D. Sweatt (2002). Molecular psychology: roles for the ERK MAP kinase cascade in memory. *Annu Rev Pharmacol Toxicol* **42**: 135-63.

Akagi, K., V. Sandig, M. Vooijs, M. Van der Valk, M. Giovannini, M. Strauss and A. Berns (1997). Cre-mediated somatic site-specific recombination in mice. *Nucleic Acids Res* **25**(9): 1766-73.

Antequera, F. and A. Bird (1999). CpG islands as genomic footprints of promoters that are associated with replication origins. *Current Biology* **9**(17): R661-7.

Antognini, J. F. and E. Carstens (1999). Isoflurane blunts electroencephalographic and thalamic-reticular formation responses to noxious stimulation in goats. *Anesthesiology* **91**(6): 1770-9.

Antognini, J. F., E. Carstens, M. Sudo and S. Sudo (2000). Isoflurane depresses electroencephalographic and medial thalamic responses to noxious stimulation via an indirect spinal action. *Anesth Analg* **91**(5): 1282-8.

Antognini, J. F. and K. Schwartz (1993). Exaggerated anesthetic requirements in the preferentially anesthetized brain. *Anesthesiology* **79**(6): 1244-9.

Aoki, C., I. Miko, H. Oviedo, T. Mikeladze_Dvali, L. Alexandre, N. Sweeney and D. S. Bredt (2001). Electron microscopic immunocytochemical detection of PSD-95, PSD-93, SAP-102, and SAP-97 at postsynaptic, presynaptic, and nonsynaptic sites of adult and neonatal rat visual cortex. *Synapse* **40**(4): 239-57.

Arnold, D. B. and D. E. Clapham (1999). Molecular determinants for subcellular localization of PSD-95 with an interacting K+ channel. *Neuron* **23**(1): 149-57.

Augustine, G. J. (2001). How does calcium trigger neurotransmitter release? *Curr Opin Neurobiol* **11**(3): 320-6.

Avila-Flores, A., E. Rendon-Huerta, J. Moreno, S. Islas, A. Betanzos, M. Robles-Flores and L. Gonzalez-Mariscal (2001). Tight-junction protein zonula occludens 2 is a target of phosphorylation by protein kinase C. *Biochem J* **360**(Pt 2): 295-304.

Bach, M. E., R. D. Hawkins, M. Osman, E. R. Kandel and M. Mayford (1995). Impairment of spatial but not contextual memory in CaMKII mutant mice with a selective loss of hippocampal LTP in the range of the theta frequency. *Cell* **81**(6): 905-15.

Bannerman, D. M., M. A. Good, S. P. Butcher, M. Ramsay and R. G. Morris (1995). Distinct components of spatial learning revealed by prior training and NMDA receptor blockade. *Nature* **378**(6553): 182-6.

Bayer, K. U., P. De_Koninck, A. S. Leonard, J. W. Hell and H. Schulman (2001). Interaction with the NMDA receptor locks CaMKII in an active conformation. *Nature* **411**(6839): 801-5.

Bishop, J. (1999). *Transgenic mammals*. Harlow, Pearson Education Ltd.

Blackwood, E. M. and J. T. Kadonaga (1998). Going the distance: a current view of enhancer action. *Science* **281**(5373): 61-3.

Bland, B. H. (1986). The physiology and pharmacology of hippocampal formation theta rhythms. *Progress in Neurobiology* **26**(1): 1-54.

Blaszczyk, J., Y. Li, H. Yan and X. Ji (2001). Crystal structure of unligated guanylate kinase from yeast reveals GMP-induced conformational changes. *Journal of Molecular Biology* **307**(1): 247-57.

Bliss, T. V. and T. Lomo (1973). Long-lasting potentiation of synaptic transmission in the dentate area of the anaesthetized rabbit following stimulation of the perforant path. **232**(2): 331-56.

Blum, S., A. N. Moore, F. Adams and P. K. Dash (1999). A mitogen-activated protein kinase cascade in the CA1/CA2 subfield of the dorsal hippocampus is essential for long-term spatial memory. *The Journal of Neuroscience* **19**(9): 3535-44.

Borges, M. and J. F. Antognini (1994). Does the brain influence somatic responses to noxious stimuli during isoflurane anesthesia? *Anesthesiology* **81**(6): 1511-5.

Bradley, A., M. Evans, M. H. Kaufman and E. Robertson (1984). Formation of germ-line chimaeras from embryo-derived teratocarcinoma cell lines. *Nature* **309**(5965): 255-6.

Brandon, E. P., M. Zhuo, Y. Y. Huang, M. Qi, K. A. Gerhold, K. A. Burton, E. R. Kandel, G. S. McKnight and R. L. Idzerda (1995). Hippocampal long-term depression and depotentiation are defective in mice carrying a targeted disruption of the gene encoding the RI beta subunit of cAMP-dependent protein kinase. *Proceedings of the National Academy of Sciences of the United States of America* **92**(19): 8851-5.

Brenman, J. E., K. S. Christopherson, S. E. Craven, A. W. McGee and D. S. Bredt (1996a). Cloning and characterization of postsynaptic density 93, a nitric oxide synthase interacting protein. *J Neurosci* **16**(23): 7407-15.

Brenman, J. E., D. S. Chao, S. H. Gee, A. W. McGee, S. E. Craven, D. R. Santillano, Z. Wu, F. Huang, H. Xia, M. F. Peters, S. C. Froehner and D. S. Bredt (1996b). Interaction of nitric oxide synthase with the postsynaptic density protein PSD-95 and alpha1-syntrophin mediated by PDZ domains. *Cell* **84**(5): 757-67.

Brenman, J. E., J. R. Topinka, E. C. Cooper, A. W. McGee, J. Rosen, T. Milroy, H. J. Ralston and D. S. Bredt (1998). Localization of postsynaptic density-93 to dendritic microtubules and interaction with microtubule-associated protein 1A. *The Journal of Neuroscience* **18**(21): 8805-13.

Budnik, V., Y. H. Koh, B. Guan, B. Hartmann, C. Hough, D. Woods and M. Gorczyca (1996). Regulation of synapse structure and function by the Drosophila tumor suppressor gene dlg. *Neuron* **17**(4): 627-40.

Butler, L. S., A. J. Silva, A. Abeliovich, Y. Watanabe, S. Tonegawa and J. O. McNamara (1995). Limbic epilepsy in transgenic mice carrying a Ca2+/calmodulin-dependent kinase II alpha-subunit mutation. *Proceedings of the National Academy of Sciences of the United States of America* **92**(15): 6852-5.

Caruana, G. and A. Bernstein (2001). Craniofacial dysmorphogenesis including cleft palate in mice with an insertional mutation in the discs large gene. *Molecular and Cellular Biology* **21**(5): 1475-83.

Castillo, P. E., R. C. Malenka and R. A. Nicoll (1997). Kainate receptors mediate a slow postsynaptic current in hippocampal CA3 neurons. *Nature* **388**(6638): 182-6.

Chen, H. J., M. Rojas-Soto, A. Oguni and M. B. Kennedy (1998). A synaptic Ras-GTPase activating protein (p135 SynGAP) inhibited by CaM kinase II. *Neuron* **20**(5): 895-904.

Chen, L., D. M. Chetkovich, R. S. Petralia, N. T. Sweeney, Y. Kawasaki, R. J. Wenthold, D. S. Bredt and R. A. Nicoll (2000). Stargazin regulates synaptic targeting of AMPA receptors by two distinct mechanisms. *Nature* **408**(6815): 936-43.

Chetkovich, D. M., R. C. Bunn, S.-H. Kuo, Y. Kawasaki, M. Kohwi and D. S. Bredt (2002). Postsynaptic targeting of alternative Postsynaptic Density-95 isoforms by distinct mechanisms. *The Journal of Neuroscience* **22**(15): 6415-6423.

Chetkovich, D. M., L. Chen, T. J. Stocker, R. A. Nicoll and D. S. Bredt (2002). Phosphorylation of the Postsynaptic Density-95 (PSD-95)/Discs Large/Zona Occludens-1 Binding Site of Stargazin Regulates Binding to PSD-95 and Synaptic Targeting of AMPA Receptors. *The Journal of Neuroscience* **22**(14): 5791-6.

Cho, K. O., C. A. Hunt and M. B. Kennedy (1992). The rat brain postsynaptic density fraction contains a homolog of the Drosophila discs-large tumor suppressor protein. *Neuron* **9**(5): 929-42.

Choi, J., J. Ko, E. Park, J. R. Lee, J. Yoon, S. Lim and E. Kim (2002). Phosphorylation of stargazin by protein kinase A regulates its interaction with PSD-95. *The Journal of Biological Chemistry* **277**(14): 12359-63.

Cicchetti, P., B. J. Mayer, G. Thiel and D. Baltimore (1992). Identification of a protein that binds to the SH3 region of Abl and is similar to Bcr and GAP-rho. *Science* **257**(5071): 803-6.

Cipolotti, L., T. Shallice, D. Chan, N. Fox, R. Scahill, G. Harrison, J. Stevens and P. Rudge (2001). Long-term retrograde amnesia...the crucial role of the hippocampus. *Neuropsychologia* **39**(2): 151-72.

Coan, E. J., W. Saywood and G. L. Collingridge (1987). MK-801 blocks NMDA receptor-mediated synaptic transmission and long term potentiation in rat hippocampal slices. *Neuroscience Letters* **80**(1): 111-4.

Cohen, G. B., R. Ren and D. Baltimore (1995). Modular binding domains in signal transduction proteins. *Cell* **80**(2): 237-48.

Cohen, N. A., J. E. Brenman, S. H. Snyder and D. S. Bredt (1996). Binding of the inward rectifier K+ channel Kir 2.3 to PSD-95 is regulated by protein kinase A phosphorylation. *Neuron* **17**(4): 759-67.

Cohen, R. S., F. Blomberg, K. Berzins and P. Siekevitz (1977). The structure of postsynaptic densities isolated from dog cerebral cortex. I. Overall morphology and protein composition. *J Cell Biol* **74**(1): 181-203.

Colledge, M., R. A. Dean, G. K. Scott, L. K. Langeberg, R. L. Huganir and J. D. Scott (2000). Targeting of PKA to glutamate receptors through a MAGUK-AKAP complex. *Neuron* **27**(1): 107-19.

Collingridge, G. L., S. J. Kehl and H. McLennan (1983). Excitatory amino acids in synaptic transmission in the Schaffer collateral-commissural pathway of the rat hippocampus. *J Physiol* **334**: 33-46.

Cotman, C. W., G. Banker, L. Churchill and D. Taylor (1974). Isolation of postsynaptic densities from rat brain. *J Cell Biol* **63**(2 Pt 1): 441-55.

Craven, S. E. and D. S. Bredt (2000). Synaptic targeting of the postsynaptic density protein PSD-95 mediated by a tyrosine-based trafficking signal. *Journal of Biological Chemistry* **275**(26): 20045-51.

Craven, S. E., A. E. El_Husseini and D. S. Bredt (1999). Synaptic targeting of the postsynaptic density protein PSD-95 mediated by lipid and protein motifs. *Neuron* **22**(3): 497-509.

Dawson, V. L., V. M. Kizushi, P. L. Huang, S. H. Snyder and T. M. Dawson (1996). Resistance to neurotoxicity in cortical cultures from neuronal nitric oxide synthase-deficient mice. *J Neurosci* **16**(8): 2479-87.

Deguchi, M., Y. Hata, M. Takeuchi, N. Ide, K. Hirao, I. Yao, M. Irie, A. Toyoda and Y. Takai (1998). BEGAIN (brain-enriched guanylate kinase-associated protein), a novel neuronal PSD-95/SAP90-binding protein. *The Journal of Biological Chemistry* **273**(41): 26269-72.

Doyle, D. A., A. Lee, J. Lewis, E. Kim, M. Sheng and R. MacKinnon (1996). Crystal structures of a complexed and peptide-free membrane protein-binding domain: molecular basis of peptide recognition by PDZ. *Cell* **85**(7): 1067-76.

Dudek, S. M. and M. F. Bear (1992). Homosynaptic long-term depression in area CA1 of hippocampus and effects of N-methyl-D-aspartate receptor blockade. *Proceedings of the National Academy of Sciences of the United States of America* **89**(10): 4363-7.

El-Husseini, A. E., S. E. Craven, D. M. Chetkovich, B. L. Firestein, E. Schnell, C. Aoki and D. S. Bredt (2000). Dual palmitoylation of PSD-95 mediates its vesiculotubular sorting, postsynaptic targeting, and ion channel clustering. *Journal of Cell Biology* **148**(1): 159-72.

El-Husseini, A. e. l.-D., E. Schnell, S. Dakoji, N. Sweeney, Q. Zhou, O. Prange, C. Gauthier_Campbell, A. Aguilera_Moreno, R. A. Nicoll and D. S. Bredt (2002). Synaptic strength regulated by palmitate cycling on PSD-95. *Cell* **108**(6): 849-63.

English, J. D. and J. D. Sweatt (1996). Activation of p42 mitogen-activated protein kinase in hippocampal long term potentiation. *The Journal of Biological Chemistry* **271**(40): 24329-32.

English, J. D. and J. D. Sweatt (1997). A requirement for the mitogen-activated protein kinase cascade in hippocampal long term potentiation. *The Journal of Biological Chemistry* **272**(31): 19103-6.

Evans, M. J. and M. H. Kaufman (1981). Establishment in culture of pluripotential cells from mouse embryos. *Nature* **292**(5819): 154-6.

Firestein, B. L., J. E. Brenman, C. Aoki, A. M. Sanchez_Perez, A. E. El_Husseini and D. S. Bredt (1999). Cypin: a cytosolic regulator of PSD-95 postsynaptic targeting. *Neuron* **24**(3): 659-72.

Forrest, D., M. Yuzaki, H. D. Soares, L. Ng, D. C. Luk, M. Sheng, C. L. Stewart, J. I. Morgan, J. A. Connor and T. Curran (1994). Targeted disruption of NMDA receptor 1 gene abolishes NMDA response and results in neonatal death. *Neuron* **13**(2): 325-38.

Franks, N. P. and W. R. Lieb (1991). Stereospecific effects of inhalational general anesthetic optical isomers on nerve ion channels. *Science* **254**(5030): 427-30.

Franks, N. P. and W. R. Lieb (1994). Molecular and cellular mechanisms of general anaesthesia. *Nature* **367**(6464): 607-14.

Frey, U., Y. Y. Huang and E. R. Kandel (1993). Effects of cAMP simulate a late stage of LTP in hippocampal CA1 neurons. *Science* **260**(5114): 1661-4.

Fukaya, M., H. Ueda, K. Yamauchi, Y. Inoue and M. Watanabe (1999). Distinct spatiotemporal expression of mRNAs for the PSD-95/SAP90 protein family in the mouse brain. *Neuroscience Research* **33**(2): 111-8.

Fukaya, M. and M. Watanabe (2000). Improved immunohistochemical detection of postsynaptically located PSD-95/SAP90 protein family by protease section pretreatment: a study in the adult mouse brain. *Journal of Comparative Neurology* **426**(4): 572-86.

Garcia, E. P., S. Mehta, L. A. Blair, D. G. Wells, J. Shang, T. Fukushima, J. R. Fallon, C. C. Garner and J. Marshall (1998). SAP90 binds and clusters kainate receptors causing incomplete desensitization. *Neuron* **21**(4): 727-39.

Gardoni, F., A. Caputi, M. Cimino, L. Pastorino, F. Cattabeni and M. Di_Luca (1998). Calcium/calmodulin-dependent protein kinase II is associated with NR2A/B subunits of NMDA receptor in postsynaptic densities. *Journal of Neurochemistry* **71**(4): 1733-41.

Gardoni, F., L. H. Schrama, A. Kamal, W. H. Gispen, F. Cattabeni and M. Di_Luca (2001). Hippocampal synaptic plasticity involves competition between Ca2+/calmodulin-dependent protein kinase II and postsynaptic density 95 for binding to the NR2A subunit of the NMDA receptor. *The Journal of Neuroscience* **21**(5): 1501-9.

Gardoni, F., L. H. Schrama, J. J. van_Dalen, W. H. Gispen, F. Cattabeni and M. Di_Luca (1999). AlphaCaMKII binding to the C-terminal tail of NMDA receptor subunit NR2A and its modulation by autophosphorylation. *Febs Letters* **456**(3): 394-8.

Garner, C. C., J. Nash and R. L. Huganir (2000). PDZ domains in synapse assembly and signalling. *Trends Cell Biol* **10**(7): 274-80.

Garry, E., A. Moss, F. O'Neill, J. Blakemore, J. Bowen, R. Mitchell, H. Husi, S. G. N. Grant and S. M. Fleetwood-Walker (2001). Evidence for a role of the NMDA receptor-interacting protein PSD-95 in neuropathic pain. *Society for Neuroscience Abstracts.*

Giese, K. P., N. B. Fedorov, R. K. Filipkowski and A. J. Silva (1998). Autophosphorylation at Thr286 of the alpha calcium-calmodulin kinase II in LTP and learning. *Science* **279**(5352): 870-3.

Gossen, M. and H. Bujard (1992). Tight control of gene expression in mammalian cells by tetracycline- responsive promoters. *Proc Natl Acad Sci U S A* **89**(12): 5547-51.

Gossen, M., S. Freundlieb, G. Bender, G. Muller, W. Hillen and H. Bujard (1995). Transcriptional activation by tetracyclines in mammalian cells. *Science* **268**(5218): 1766-9.

Gossler, A., T. Doetschman, R. Korn, E. Serfling and R. Kemler (1986). Transgenesis by means of blastocyst-derived embryonic stem cell lines. *Proc Natl Acad Sci U S A* **83**(23): 9065-9.

Grant, S. G., T. J. O'Dell, K. A. Karl, P. L. Stein, P. Soriano and E. R. Kandel (1992). Impaired long-term potentiation, spatial learning, and hippocampal development in fyn mutant mice. *Science* **258**(5090): 1903-10.

Gray, E. G. (1959). Axo-somatic and axo-dendritic synapses of the cerebral cortex: an electron microscope study. *J. Anat.* **93**: 420-433.

Griffith, L. C., L. M. Verselis, K. M. Aitken, C. P. Kyriacou, W. Danho and R. J. Greenspan (1993). Inhibition of calcium/calmodulin-dependent protein kinase in Drosophila disrupts behavioral plasticity. *Neuron* **10**(3): 501-9.

Guzowski, J. F., G. L. Lyford, G. D. Stevenson, F. P. Houston, J. L. McGaugh, P. F. Worley and C. A. Barnes (2000). Inhibition of activity-dependent arc protein expression in the rat hippocampus impairs the maintenance of long-term potentiation and the consolidation of long-term memory. *J Neurosci* **20**(11): 3993-4001.

Harding, T. C., B. J. Geddes, D. Murphy, D. Knight and J. B. Uney (1998). Switching transgene expression in the brain using an adenoviral tetracycline-regulatable system. *Nat Biotechnol* **16**(6): 553-5.

Hardingham, G. E., F. J. Arnold and H. Bading (2001). A calcium microdomain near NMDA receptors: on switch for ERK-dependent synapse-to-nucleus communication. *Nat Neurosci* **4**(6): 565-6.

Harris BZ and Lim WA (2001). Mechanism and role of PDZ domains in signaling complex assembly. *J Cell Sci* **114**, 3219-31.

Harrison, N. L., J. L. Kugler, M. V. Jones, E. P. Greenblatt and D. B. Pritchett (1993). Positive modulation of human gamma-aminobutyric acid type A and glycine receptors by the inhalation anesthetic isoflurane. *Mol Pharmacol* **44**(3): 628-32.

Haskins, J., L. Gu, E. S. Wittchen, J. Hibbard and B. R. Stevenson (1998). ZO-3, a novel member of the MAGUK protein family found at the tight junction, interacts with ZO-1 and occludin. *Journal of Cell Biology* **141**(1): 199-208.

Hasty, P., J. Rivera_Perez and A. Bradley (1991). The length of homology required for gene targeting in embryonic stem cells. *Molecular and Cellular Biology* **11**(11): 5586-91.

Hebb, D. O. (1949). *The organization of behaviour*. New York, Wiley.

Hibino, H., A. Inanobe, M. Tanemoto, A. Fujita, K. Doi, T. Kubo, Y. Hata, Y. Takai and Y. Kurachi (2000). Anchoring proteins confer G protein sensitivity to an inward-rectifier K(+) channel through the GK domain. *Embo Journal* **19**(1): 78-83.

Hillier, B. J., K. S. Christopherson, K. E. Prehoda, D. S. Bredt and W. A. Lim (1999). Unexpected modes of PDZ domain scaffolding revealed by structure of nNOS-syntrophin complex. *Science* **284**(5415): 812-5.

Holscher, C. (1997). Nitric oxide, the enigmatic neuronal messenger: its role in synaptic plasticity. *Trends Neurosci* **20**(7): 298-303.

Homanics, G. E., T. M. DeLorey, L. L. Firestone, J. J. Quinlan, A. Handforth, N. L. Harrison, M. D. Krasowski, C. E. Rick, E. R. Korpi, R. Makela, M. H. Brilliant, N. Hagiwara, C. Ferguson, K. Snyder and R. W. Olsen (1997). Mice devoid of gamma-aminobutyrate type A receptor beta3 subunit have epilepsy, cleft palate, and hypersensitive behavior. *Proc Natl Acad Sci U S A* **94**(8): 4143-8.

Hough, C. D., D. F. Woods, S. Park and P. J. Bryant (1997). Organizing a functional junctional complex requires specific domains of the Drosophila MAGUK Discs large. *Genes and Development* **11**(23): 3242-53.

Hsueh, Y. P. and M. Sheng (1999). Requirement of N-terminal cysteines of PSD-95 for PSD-95 multimerization and ternary complex formation, but not for binding to potassium channel Kv1.4. *Journal of Biological Chemistry* **274**(1): 532-6.

Hsueh, Y. P., T. F. Wang, F. C. Yang and M. Sheng (2000). Nuclear translocation and transcription regulation by the membrane-associated guanylate kinase CASK/LIN-2. *Nature* **404**(6775): 298-302.

Hu, L. A., Y. Tang, W. E. Miller, M. Cong, A. G. Lau, R. J. Lefkowitz and R. A. Hall (2000). beta 1-adrenergic receptor association with PSD-95. Inhibition of receptor internalization and facilitation of beta 1-adrenergic receptor interaction with N-methyl-D-aspartate receptors. *The Journal of Biological Chemistry* **275**(49): 38659-66.

Huang, Y. Y., E. R. Kandel, L. Varshavsky, E. P. Brandon, M. Qi, R. L. Idzerda, G. S. McKnight and R. Bourtchouladze (1995). A genetic test of the effects of mutations in PKA on mossy fiber LTP and its relation to spatial and contextual learning. *Cell* **83**(7): 1211-22.

Huang, Z., P. L. Huang, N. Panahian, T. Dalkara, M. C. Fishman and M. A. Moskowitz (1994). Effects of cerebral ischemia in mice deficient in neuronal nitric oxide synthase. *Science* **265**(5180): 1883-5.

Husi, H., M. A. Ward, J. S. Choudhary, W. P. Blackstock and S. G. Grant (2000). Proteomic analysis of NMDA receptor-adhesion protein signaling complexes. *Nature Neuroscience* **3**(7): 661-9.

Inanobe, A., A. Fujita, M. Ito, H. Tomoike, K. Inageda and Y. Kurachi (2002). Inward rectifier K+ channel Kir2.3 is localized at the postsynaptic membrane of excitatory synapses. *American Journal of Physiology. Cell Physiology* **282**(6): C1396-403.

Indra, A. K., X. Warot, J. Brocard, J. M. Bornert, J. H. Xiao, P. Chambon and D. Metzger (1999). Temporally-controlled site-specific mutagenesis in the basal layer of the epidermis: comparison of the recombinase activity of the tamoxifen- inducible Cre-ER(T) and Cre-ER(T2) recombinases. *Nucleic Acids Res* **27**(22): 4324-7.

Ishidate, T., A. Matsumine, K. Toyoshima and T. Akiyama (2000). The APC-hDLG complex negatively regulates cell cycle progression from the G0/G1 to S phase. *Oncogene* **19**(3): 365-72.

Ito, I., H. Hidaka and H. Sugiyama (1991). Effects of KN-62, a specific inhibitor of calcium/calmodulin-dependent protein kinase II, on long-term potentiation in the rat hippocampus. *Neurosci Lett* **121**(1-2): 119-21.

Jesaitis, L. A. and D. A. Goodenough (1994). Molecular characterization and tissue distribution of ZO-2, a tight junction protein homologous to ZO-1 and the Drosophila discs-large tumor suppressor protein. *The Journal of Cell Biology* **124**(6): 949-61.

Joo, D. T., D. Gong, J. M. Sonner, Z. Jia, J. F. MacDonald, E. I. Eger, 2nd and B. A. Orser (2001). Blockade of AMPA receptors and volatile anesthetics: reduced anesthetic requirements in GluR2 null mutant mice for loss of the righting reflex and antinociception but not minimum alveolar concentration. *Anesthesiology* **94**(3): 478-88.

Jugloff, D. G., R. Khanna, L. C. Schlichter and O. T. Jones (2000). Internalization of the Kv1.4 potassium channel is suppressed by clustering interactions with PSD-95. *Journal of Biological Chemistry* **275**(2): 1357-64.

Jun, K., G. Choi, S. G. Yang, K. Y. Choi, H. Kim, G. C. Chan, D. R. Storm, C. Albert, G. W. Mayr, C. J. Lee and H. S. Shin (1998). Enhanced hippocampal CA1 LTP but

normal spatial learning in inositol 1,4,5-trisphosphate 3-kinase(A)-deficient mice. *Learning & Memory* **5**(4-5): 317-30.

Kay, B. K., M. P. Williamson and M. Sudol (2000). The importance of being proline: the interaction of proline-rich motifs in signaling proteins with their cognate domains. *Faseb J* **14**(2): 231-41.

Kellendonk, C., F. Tronche, E. Casanova, K. Anlag, C. Opherk and G. Schutz (1999). Inducible site-specific recombination in the brain. *J Mol Biol* **285**(1): 175-82.

Kellendonk, C., F. Tronche, A. P. Monaghan, P. O. Angrand, F. Stewart and G. Schutz (1996). Regulation of Cre recombinase activity by the synthetic steroid RU 486. *Nucleic Acids Res* **24**(8): 1404-11.

Kennedy, M. B. (1997). The postsynaptic density at glutamatergic synapses. *Trends Neurosci* **20**(6): 264-8.

Kennedy, M. B. (2000). Signal-processing machines at the postsynaptic density. *Science* **290**(5492): 750-4.

Khaldi, A., C. C. Chiueh, M. R. Bullock and J. J. Woodward (2002). The significance of nitric oxide production in the brain after injury. *Ann N Y Acad Sci* **962**: 53-9.

Kim, E., K. O. Cho, A. Rothschild and M. Sheng (1996). Heteromultimerization and NMDA receptor-clustering activity of Chapsyn-110, a member of the PSD-95 family of proteins. *Neuron* **17**(1): 103-13.

Kim, E., S. Naisbitt, Y. P. Hsueh, A. Rao, A. Rothschild, A. M. Craig and M. Sheng (1997). GKAP, a novel synaptic protein that interacts with the guanylate kinase-like domain of the PSD-95/SAP90 family of channel clustering molecules. *The Journal of Cell Biology* **136**(3): 669-78.

Kim, E., M. Niethammer, A. Rothschild, Y. N. Jan and M. Sheng (1995). Clustering of Shaker-type K+ channels by interaction with a family of membrane-associated guanylate kinases. *Nature* **378**(6552): 85-8.

Kim, J. J. and M. S. Fanselow (1992). Modality-specific retrograde amnesia of fear. *Science* **256**(5057): 675-7.

Kistner, U., C. C. Garner and M. Linial (1995). Nucleotide binding by the synapse associated protein SAP90. *Febs Letters* **359**(2-3): 159-63.

Kistner, U., B. M. Wenzel, R. W. Veh, C. Cases_Langhoff, A. M. Garner, U. Appeltauer, B. Voss, E. D. Gundelfinger and C. C. Garner (1993). SAP90, a rat presynaptic protein related to the product of the Drosophila tumor suppressor gene dlg-A. *Journal of Biological Chemistry* **268**(7): 4580-3.

Kiyono, T., A. Hiraiwa, M. Fujita, Y. Hayashi, T. Akiyama and M. Ishibashi (1997). Binding of high-risk human papillomavirus E6 oncoproteins to the human homologue of the Drosophila discs large tumor suppressor protein. *Proceedings of the National Academy of Sciences of the United States of America* **94**(21): 11612-6.

Koblin, D. D. and E. I. Eger, 2nd (1981). Cross-mating of mice selectively bred for resistance or susceptibility to nitrous oxide anesthesia: potencies of nitrous oxide in offspring. *Anesth Analg* **60**(9): 646-8.

Koh, Y. H., E. Popova, U. Thomas, L. C. Griffith and V. Budnik (1999). Regulation of DLG localization at synapses by CaMKII-dependent phosphorylation. *Cell* **98**(3): 353-63.

Kornau, H. C., L. T. Schenker, M. B. Kennedy and P. H. Seeburg (1995). Domain interaction between NMDA receptor subunits and the postsynaptic density protein PSD-95. *Science* **269**(5231): 1737-40.

Kuhlendahl, S., O. Spangenberg, M. Konrad, E. Kim and C. C. Garner (1998). Functional analysis of the guanylate kinase-like domain in the synapse-associated protein SAP97. *European Journal of Biochemistry* **252**(2): 305-13.

Kutsuwada, T., K. Sakimura, T. Manabe, C. Takayama, N. Katakura, E. Kushiya, R. Natsume, M. Watanabe, Y. Inoue, T. Yagi, S. Aizawa, M. Arakawa, T. Takahashi, Y. Nakamura, H. Mori and M. Mishina (1996). Impairment of suckling response, trigeminal neuronal pattern formation, and hippocampal LTD in NMDA receptor epsilon 2 subunit mutant mice. *Neuron* **16**(2): 333-44.

Lahey, T., M. Gorczyca, X. X. Jia and V. Budnik (1994). The Drosophila tumor suppressor gene dlg is required for normal synaptic bouton structure. *Neuron* **13**(4): 823-35.

Larson, J., D. Wong and G. Lynch (1986). Patterned stimulation at the theta frequency is optimal for the induction of hippocampal long-term potentiation. *Brain Research* **368**(2): 347-50.

Lee, S. S., R. S. Weiss and R. T. Javier (1997). Binding of human virus oncoproteins to hDlg/SAP97, a mammalian homolog of the Drosophila discs large tumor suppressor protein. *Proceedings of the National Academy of Sciences of the United States of America* **94**(13): 6670-5.

Leonard, A. S., M. A. Davare, M. C. Horne, C. C. Garner and J. W. Hell (1998). SAP97 is associated with the alpha-amino-3-hydroxy-5-methylisoxazole-4-propionic acid receptor GluR1 subunit. *The Journal of Biological Chemistry* **273**(31): 19518-24.

Leonard, A. S., I. A. Lim, D. E. Hemsworth, M. C. Horne and J. W. Hell (1999). Calcium/calmodulin-dependent protein kinase II is associated with the N-methyl-D-

aspartate receptor. *Proceedings of the National Academy of Sciences of the United States of America* **96**(6): 3239-44.

Leonoudakis, D., W. Mailliard, K. Wingerd, D. Clegg and C. Vandenberg (2001). Inward rectifier potassium channel Kir2.2 is associated with synapse-associated protein SAP97. *Journal of Cell Science* **114**(Pt 5): 987-98.

Lin, L. H., P. Whiting and R. A. Harris (1993). Molecular determinants of general anesthetic action: role of GABAA receptor structure. *J Neurochem* **60**(4): 1548-53.

Link, W., U. Konietzko, G. Kauselmann, M. Krug, B. Schwanke, U. Frey and D. Kuhl (1995). Somatodendritic expression of an immediate early gene is regulated by synaptic activity. *Proc Natl Acad Sci U S A* **92**(12): 5734-8.

Lovinger, D. M., K. L. Wong, K. Murakami and A. Routtenberg (1987). Protein kinase C inhibitors eliminate hippocampal long-term potentiation. *Brain Res* **436**(1): 177-83.

Lu, Y. M., J. C. Roder, J. Davidow and M. W. Salter (1998). Src activation in the induction of long-term potentiation in CA1 hippocampal neurons. *Science* **279**(5355): 1363-7.

Lue, R. A., E. Brandin, E. P. Chan and D. Branton (1996). Two independent domains of hDlg are sufficient for subcellular targeting: the PDZ1-2 conformational unit and an alternatively spliced domain. *Journal of Cell Biology* **135**(4): 1125-37.

Lue, R. A., S. M. Marfatia, D. Branton and A. H. Chishti (1994). Cloning and characterization of hdlg: the human homologue of the Drosophila discs large tumor suppressor binds to protein 4.1. *Proceedings of the National Academy of Sciences of the United States of America* **91**(21): 9818-22.

Lyford, G. L., K. Yamagata, W. E. Kaufmann, C. A. Barnes, L. K. Sanders, N. G. Copeland, D. J. Gilbert, N. A. Jenkins, A. A. Lanahan and P. F. Worley (1995). Arc, a growth factor and activity-regulated gene, encodes a novel cytoskeleton-associated protein that is enriched in neuronal dendrites. *Neuron* **14**(2): 433-45.

Lynch, G., J. Larson, S. Kelso, G. Barrionuevo and F. Schottler (1983). Intracellular injections of EGTA block induction of hippocampal long- term potentiation. *Nature* **305**(5936): 719-21.

Lysko, G. S., J. L. Robinson, R. Casto and R. A. Ferrone (1994). The stereospecific effects of isoflurane isomers in vivo. *Eur J Pharmacol* **263**(1-2): 25-9.

Makino, K., H. Kuwahara, N. Masuko, Y. Nishiyama, T. Morisaki, J. Sasaki, M. Nakao, A. Kuwano, M. Nakata, Y. Ushio and H. Saya (1997). Cloning and characterization of NE-dlg: a novel human homolog of the Drosophila discs large (dlg) tumor suppressor protein interacts with the APC protein. *Oncogene* **14**(20): 2425-33.

Malenka, R. C., J. A. Kauer, D. J. Perkel, M. D. Mauk, P. T. Kelly, R. A. Nicoll and M. N. Waxham (1989). An essential role for postsynaptic calmodulin and protein kinase activity in long-term potentiation. *Nature* **340**(6234): 554-7.

Malinow, R., D. V. Madison and R. W. Tsien (1988). Persistent protein kinase activity underlying long-term potentiation. *Nature* **335**(6193): 820-4.

Malinow, R., H. Schulman and R. W. Tsien (1989). Inhibition of postsynaptic PKC or CaMKII blocks induction but not expression of LTP. *Science* **245**(4920): 862-6.

Malleret, G., U. Haditsch, D. Genoux, M. W. Jones, T. V. Bliss, A. M. Vanhoose, C. Weitlauf, E. R. Kandel, D. G. Winder and I. M. Mansuy (2001). Inducible and reversible enhancement of learning, memory, and long-term potentiation by genetic inhibition of calcineurin. *Cell* **104**(5): 675-86.

Mansuy, I. M., D. G. Winder, T. M. Moallem, M. Osman, M. Mayford, R. D. Hawkins and E. R. Kandel (1998). Inducible and reversible gene expression with the rtTA system for the study of memory. *Neuron* **21**(2): 257-65.

Manzoni, O., L. Prezeau, P. Marin, S. Deshager, J. Bockaert and L. Fagni (1992). Nitric oxide-induced blockade of NMDA receptors. *Neuron* **8**(4): 653-62.

Marfatia, S. M., O. Byron, G. Campbell, S. C. Liu and A. H. Chishti (2000). Human homologue of the Drosophila discs large tumor suppressor protein forms an oligomer in solution. Identification of the self-association site. *J Biol Chem* **275**(18): 13759-70.

Martin, G. R. (1981). Isolation of a pluripotent cell line from early mouse embryos cultured in medium conditioned by teratocarcinoma stem cells. *Proc Natl Acad Sci U S A* **78**(12): 7634-8.

Masuko, N., K. Makino, H. Kuwahara, K. Fukunaga, T. Sudo, N. Araki, H. Yamamoto, Y. Yamada, E. Miyamoto and H. Saya (1999). Interaction of NE-dlg/SAP102, a neuronal and endocrine tissue-specific membrane-associated guanylate kinase protein, with calmodulin and PSD-95/SAP90. A possible regulatory role in molecular clustering at synaptic sites. *Journal of Biological Chemistry* **274**(9): 5782-90.

Matsumine, A., A. Ogai, T. Senda, N. Okumura, K. Satoh, G. H. Baeg, T. Kawahara, S. Kobayashi, M. Okada, K. Toyoshima and T. Akiyama (1996). Binding of APC to the human homolog of the Drosophila discs large tumor suppressor protein. *Science* **272**(5264): 1020-3.

Matthies, H. and K. G. Reymann (1993). Protein kinase A inhibitors prevent the maintenance of hippocampal long-term potentiation. *Neuroreport* **4**(6): 712-4.

Mayer, B. J. (2001). SH3 domains: complexity in moderation. *J Cell Sci* **114**(Pt 7): 1253-63.

Mayford, M., M. E. Bach, Y. Y. Huang, L. Wang, R. D. Hawkins and E. R. Kandel (1996). Control of memory formation through regulated expression of a CaMKII transgene. *Science* **274**(5293): 1678-83.

Mayford, M., J. Wang, E. R. Kandel and T. J. O_Dell (1995). CaMKII regulates the frequency-response function of hippocampal synapses for the production of both LTD and LTP. *Cell* **81**(6): 891-904.

Mazzucchelli, C., C. Vantaggiato, A. Ciamei, S. Fasano, P. Pakhotin, W. Krezel, H. Welzl, D. P. Wolfer, G. Pages, O. Valverde, A. Marowsky, A. Porrazzo, P. C. Orban, R. Maldonado, M. U. Ehrengruber, V. Cestari, H. P. Lipp, P. F. Chapman, J. Pouyssegur and R. Brambilla (2002). Knockout of ERK1 MAP kinase enhances synaptic plasticity in the striatum and facilitates striatal-mediated learning and memory. *Neuron* **34**(5): 807-20.

McCulloch, J., K. J. Horsburgh and S. G. N. Grant (2001). Deficiency of PSD-95 markedly reduces neuronal damage after global ishemia. *Society for Neuroscience Abstracts*.

McGee, A. W. and D. S. Bredt (1999). Identification of an intramolecular interaction between the SH3 and guanylate kinase domains of PSD-95. *The Journal of Biological Chemistry* **274**(25): 17431-6.

McGee, A. W., S. R. Dakoji, O. Olsen, D. S. Bredt, W. A. Lim and K. E. Prehoda (2001). Structure of the SH3-guanylate kinase module from PSD-95 suggests a mechanism for regulated assembly of MAGUK scaffolding proteins. *Molecular Cell* **8**(6): 1291-301.

McLaughlin, M., R. Hale, D. Ellston, S. Gaudet, R. A. Lue and A. Viel (2002). The distribution and function of alternatively spliced insertions in hDlg. *J Biol Chem* **277**(8): 6406-12.

Meyer, H. H. (1899). Theorie der Alkoholnarkose. *Archives of Experimental and Pathological Pharmakology* **42**: 109-18.

Meyers, E. N., M. Lewandoski and G. R. Martin (1998). An Fgf8 mutant allelic series generated by Cre- and Flp-mediated recombination. *Nat Genet* **18**(2): 136-41.

Migaud, M., P. Charlesworth, M. Dempster, L. C. Webster, A. M. Watabe, M. Makhinson, Y. He, M. F. Ramsay, R. G. Morris, J. H. Morrison, T. J. O'Dell and S. G. Grant (1998). Enhanced long-term potentiation and impaired learning in mice with mutant postsynaptic density-95 protein. *Nature* **396**(6710): 433-9.

Montell, C. (1998). TRP trapped in fly signaling web. *Current Opinion in Neurobiology* **8**(3): 389-97.

Monyer, H., N. Burnashev, D. J. Laurie, B. Sakmann and P. H. Seeburg (1994). Developmental and regional expression in the rat brain and functional properties of four NMDA receptors. *Neuron* **12**(3): 529-40.

Moody, E. J., B. D. Harris and P. Skolnick (1993). Stereospecific actions of the inhalation anesthetic isoflurane at the GABAA receptor complex. *Brain Res* **615**(1): 101-6.

Morais-Cabral, J. H., C. Petosa, M. J. Sutcliffe, S. Raza, O. Byron, F. Poy, S. M. Marfatia, A. H. Chishti and R. C. Liddington (1996). Crystal structure of a PDZ domain. *Nature* **382**(6592): 649-52.

Mori, H., T. Manabe, M. Watanabe, Y. Satoh, N. Suzuki, S. Toki, K. Nakamura, T. Yagi, E. Kushiya, T. Takahashi, Y. Inoue, K. Sakimura and M. Mishina (1998). Role of the carboxy-terminal region of the GluR epsilon2 subunit in synaptic localization of the NMDA receptor channel. *Neuron* **21**(3): 571-80.

Morris, D. R. and A. P. Geballe (2000). Upstream open reading frames as regulators of mRNA translation. *Mol Cell Biol* **20**(23): 8635-42.

Morris, R. G. (1989). Synaptic plasticity and learning: selective impairment of learning rats and blockade of long-term potentiation in vivo by the N-methyl-D-aspartate receptor antagonist AP5. *The Journal of Neuroscience* **9**(9): 3040-57.

Morris, R. G., E. Anderson, G. S. Lynch and M. Baudry (1986). Selective impairment of learning and blockade of long-term potentiation by an N-methyl-D-aspartate receptor antagonist, AP5. *Nature* **319**(6056): 774-6.

Morris, R. G., P. Garrud, J. N. Rawlins and J. O_Keefe (1982). Place navigation impaired in rats with hippocampal lesions. *Nature* **297**(5868): 681-3.

Morris, R. G., F. Schenk, F. Tweedie and L. E. Jarrard (1990). Ibotenate Lesions of Hippocampus and/or Subiculum: Dissociating Components of Allocentric Spatial Learning. *Eur J Neurosci* **2**(12): 1016-1028.

Moser, E., M. B. Moser and P. Andersen (1993). Spatial learning impairment parallels the magnitude of dorsal hippocampal lesions, but is hardly present following ventral lesions. *The Journal of Neuroscience* **13**(9): 3916-25.

Mulkey, R. M. and R. C. Malenka (1992). Mechanisms underlying induction of homosynaptic long-term depression in area CA1 of the hippocampus. *Neuron* **9**(5): 967-75.

Muller, B. M., U. Kistner, S. Kindler, W. J. Chung, S. Kuhlendahl, S. D. Fenster, L. F. Lau, R. W. Veh, R. L. Huganir, E. D. Gundelfinger and C. C. Garner (1996). SAP102, a novel postsynaptic protein that interacts with NMDA receptor complexes in vivo. *Neuron* **17**(2): 255-65.

Muller, B. M., U. Kistner, R. W. Veh, C. Cases_Langhoff, B. Becker, E. D. Gundelfinger and C. C. Garner (1995). Molecular characterization and spatial distribution of SAP97, a novel presynaptic protein homologous to SAP90 and the Drosophila discs-large tumor suppressor protein. *Journal of Neuroscience* **15**(3 Pt 2): 2354-66.

Nagy, A., C. Moens, E. Ivanyi, J. Pawling, M. Gertsenstein, A. K. Hadjantonakis, M. Pirity and J. Rossant (1998). Dissecting the role of N-myc in development using a single targeting vector to generate a series of alleles. *Curr Biol* **8**(11): 661-4.

Nakazawa, K., M. C. Quirk, R. A. Chitwood, M. Watanabe, M. F. Yeckel, L. D. Sun, A. Kato, C. A. Carr, D. Johnston, M. A. Wilson and S. Tonegawa (2002). Requirement for hippocampal CA3 NMDA receptors in associative memory recall. *Science* **297**(5579): 211-8.

Namiki, A., J. G. Collins, L. M. Kitahata, H. Kikuchi, E. Homma and J. G. Thalhammer (1980). Effects of halothane on spinal neuronal responses to graded noxious heat stimulation in the cat. *Anesthesiology* **53**(6): 475-80.

Nehring, R. B., E. Wischmeyer, F. Doring, R. W. Veh, M. Sheng and A. Karschin (2000). Neuronal inwardly rectifying K(+) channels differentially couple to PDZ proteins of the PSD-95/SAP90 family. *The Journal of Neuroscience* **20**(1): 156-62.

Niethammer, M., E. Kim and M. Sheng (1996). Interaction between the C terminus of NMDA receptor subunits and multiple members of the PSD-95 family of membrane-associated guanylate kinases. *Journal of Neuroscience* **16**(7): 2157-63.

Niethammer, M., J. G. Valtschanoff, T. M. Kapoor, D. W. Allison, T. M. Weinberg, A. M. Craig and M. Sheng (1998). CRIPT, a novel postsynaptic protein that binds to the third PDZ domain of PSD-95/SAP90. *Neuron* **20**(4): 693-707.

Nieto Sampedro, M., C. M. Bussineau and C. W. Cotman (1981). Postsynaptic density antigens: preparation and characterization of an antiserum against postsynaptic densities. *Journal of Cell Biology* **90**(3): 675-86.

Nieto Sampedro, M., C. M. Bussineau and C. W. Cotman (1982). Isolation, morphology, and protein and glycoprotein composition of synaptic junctional fractions from the brain of lower vertebrates: antigen PSD-95 as a junctional marker. *Journal of Neuroscience* **2**(6): 722-34.

Nieto Sampedro, M., C. M. Bussineau and C. W. Cotman (1982). Turnover of brain postsynaptic densities after selective deafferentation: detection by means of an antibody to antigen PSD-95. *Brain Research* **251**(2): 211-20.

Nix, S. L., A. H. Chishti, J. M. Anderson and Z. Walther (2000). hCASK and hDlg associate in epithelia, and their src homology 3 and guanylate kinase domains

participate in both intramolecular and intermolecular interactions. *The Journal of Biological Chemistry* **275**(52): 41192-200.

O'Dell, T. J., E. R. Kandel and S. G. Grant (1991). Long-term potentiation in the hippocampus is blocked by tyrosine kinase inhibitors. *Nature* **353**(6344): 558-60.

Osoegawa, K., M. Tateno, P. Y. Woon, E. Frengen, A. G. Mammoser, J. J. Catanese, Y. Hayashizaki and P. J. de_Jong (2000). Bacterial artificial chromosome libraries for mouse sequencing and functional analysis. *Genome Research* **10**(1): 116-28.

Overton, E. (1901). Studien uber die Narkose Zugleich ein Beitrag zur Allgemeinen Pharmacology. Jena, Germany: Verlag von Gustav Fischer.

Pak, D. T., S. Yang, S. Rudolph_Correia, E. Kim and M. Sheng (2001). Regulation of dendritic spine morphology by SPAR, a PSD-95-associated RapGAP. *Neuron* **31**(2): 289-303.

Palay, S. L. (1958). The morphology of synapses in the central nervous system. *Exp. Cell. Res. Suppl.* **5**: 275-293.

Patel, A. J., E. Honore, F. Lesage, M. Fink, G. Romey and M. Lazdunski (1999). Inhalational anesthetics activate two-pore-domain background K+ channels. *Nat Neurosci* **2**(5): 422-6.

Pesole, G., S. Liuni, G. Grillo, F. Licciulli, F. Mignone, C. Gissi and C. Saccone (2002). UTRdb and UTRsite: specialized databases of sequences and functional elements of 5' and 3' untranslated regions of eukaryotic mRNAs. Update 2002. *Nucleic Acids Research (Online)* **30**(1): 335-40.

Piserchio, A., M. Pellegrini, S. Mehta, S. M. Blackman, E. P. Garcia, J. Marshall and D. F. Mierke (2002). The PDZ1 domain of SAP90. Characterization of structure and binding. *The Journal of Biological Chemistry* **277**(9): 6967-73.

Platenik, J., N. Kuramoto and Y. Yoneda (2000). Molecular mechanisms associated with long-term consolidation of the NMDA signals. *Life Sci* **67**(4): 335-64.

Qi, M., M. Zhuo, B. S. Skalhegg, E. P. Brandon, E. R. Kandel, G. S. McKnight and R. L. Idzerda (1996). Impaired hippocampal plasticity in mice lacking the Cbeta1 catalytic subunit of cAMP-dependent protein kinase. *Proceedings of the National Academy of Sciences of the United States of America* **93**(4): 1571-6.

Quinlan, J. J., G. E. Homanics and L. L. Firestone (1998). Anesthesia sensitivity in mice that lack the beta3 subunit of the gamma- aminobutyric acid type A receptor. *Anesthesiology* **88**(3): 775-80.

Rampil, I. J. (1994). Anesthetic potency is not altered after hypothermic spinal cord transection in rats. *Anesthesiology* **80**(3): 606-10.

Rampil, I. J., P. Mason and H. Singh (1993). Anesthetic potency (MAC) is independent of forebrain structures in the rat. *Anesthesiology* **78**(4): 707-12.

Rasband MN, Park EW, Zhen D, Arbuckle MI, Poliak S, Peles E, Grant SG and Trimmer JS (2002). Clustering of neuronal potassium channels is independent of their interaction with PSD-95. *J Cell Biol* **159**, 663-72.

Ren, R., B. J. Mayer, P. Cicchetti and D. Baltimore (1993). Identification of a ten-amino acid proline-rich SH3 binding site. *Science* **259**(5098): 1157-61.

Reymann, K. G., R. Brodemann, H. Kase and H. Matthies (1988). Inhibitors of calmodulin and protein kinase C block different phases of hippocampal long-term potentiation. *Brain Res* **461**(2): 388-92.

Riedel, G., J. Micheau, A. G. Lam, E. Roloff, S. J. Martin, H. Bridge, L. Hoz, B. Poeschel, J. McCulloch and R. G. Morris (1999). Reversible neural inactivation reveals hippocampal participation in several memory processes. *Nat Neurosci* **2**(10): 898-905.

Robertson, E., A. Bradley, M. Kuehn and M. Evans (1986). Germ-line transmission of genes introduced into cultured pluripotential cells by retroviral vector. *Nature* **323**(6087): 445-8.

Roche, K. W., S. Standley, J. McCallum, C. Dune Ly, M. D. Ehlers and R. J. Wenthold (2001). Molecular determinants of NMDA receptor internalization. *Nat Neurosci* **4**(8): 794-802.

Rosenbaum, R. S., G. Winocur and M. Moscovitch (2001). New views on old memories: re-evaluating the role of the hippocampal complex. *Behav Brain Res* **127**(1-2): 183-97.

Russwurm, M., N. Wittau and D. Koesling (2001). Guanylyl cyclase/PSD-95 interaction: targeting of the nitric oxide-sensitive alpha2beta1 guanylyl cyclase to synaptic membranes. *The Journal of Biological Chemistry* **276**(48): 44647-52.

Rutter, A. R. and F. A. Stephenson (2000). Coexpression of postsynaptic density-95 protein with NMDA receptors results in enhanced receptor expression together with a decreased sensitivity to L-glutamate. *Journal of Neurochemistry* **75**(6): 2501-10.

Sans, N., R. S. Petralia, Y. X. Wang, J. Blahos, J. W. Hell and R. J. Wenthold (2000). A developmental change in NMDA receptor-associated proteins at hippocampal synapses. *Journal of Neuroscience* **20**(3): 1260-71.

Sans, N., C. Racca, R. S. Petralia, Y. X. Wang, J. McCallum and R. J. Wenthold (2001). Synapse-associated protein 97 selectively associates with a subset of AMPA receptors early in their biosynthetic pathway. *Journal of Neuroscience* **21**(19): 7506-16.

Sattler, R., Z. Xiong, W. Y. Lu, M. Hafner, J. F. MacDonald and M. Tymianski (1999). Specific coupling of NMDA receptor activation to nitric oxide neurotoxicity by PSD-95 protein. *Science* **284**(5421): 1845-8.

Savinainen, A., E. P. Garcia, D. Dorow, J. Marshall and Y. F. Liu (2001). Kainate receptor activation induces mixed lineage kinase-mediated cellular signaling cascades via post-synaptic density protein 95. *Journal of Biological Chemistry* **276**(14): 11382-6.

Schuster, C. M., G. W. Davis, R. D. Fetter and C. S. Goodman (1996). Genetic dissection of structural and functional components of synaptic plasticity. II. Fasciclin II controls presynaptic structural plasticity. *Neuron* **17**(4): 655-67.

Schwenk, F., U. Baron and K. Rajewsky (1995). A cre-transgenic mouse strain for the ubiquitous deletion of loxP- flanked gene segments including deletion in germ cells. *Nucleic Acids Res* **23**(24): 5080-1.

Schwenk, F., R. Kuhn, P. O. Angrand, K. Rajewsky and A. F. Stewart (1998). Temporally and spatially regulated somatic mutagenesis in mice. *Nucleic Acids Res* **26**(6): 1427-32.

Scoville, W. B. and B. Milner (1957). Loss of recent memory after bilateral hippocampal lesions. *J. Neurol Neurosurg Psychiatry* **20**: 11-21.

Silva, A. J., R. Paylor, J. M. Wehner and S. Tonegawa (1992). Impaired spatial learning in alpha-calcium-calmodulin kinase II mutant mice. *Science* **257**(5067): 206-11.

Silva, A. J., C. F. Stevens, S. Tonegawa and Y. Wang (1992). Deficient hippocampal long-term potentiation in alpha-calcium-calmodulin kinase II mutant mice. *Science* **257**(5067): 201-6.

Smith, A. G. (1991). Culture and differentiation of embryonic stem cells. *Journal of Tissue Culture Methods* **13**: 89-94.

Smith, W. B., G. Aakalu and E. M. Schuman (2001). Local protein synthesis in neurons. *Curr Biol* **11**(22): R901-3.

Spiers, H. J., E. A. Maguire and N. Burgess (2001). Hippocampal amnesia. *Neurocase* **7**(5): 357-82.

Sprengel, R., B. Suchanek, C. Amico, R. Brusa, N. Burnashev, A. Rozov, O. Hvalby, V. Jensen, O. Paulsen, P. Andersen, J. J. Kim, R. F. Thompson, W. Sun, L. C. Webster, S. G. Grant, J. Eilers, A. Konnerth, J. Li, J. O. McNamara and P. H. Seeburg (1998). Importance of the intracellular domain of NR2 subunits for NMDA receptor function in vivo. *Cell* **92**(2): 279-89.

Stathakis, D. G., K. B. Hoover, Z. You and P. J. Bryant (1997). Human postsynaptic density-95 (PSD95): location of the gene (DLG4) and possible function in nonneural as well as in neural tissues. *Genomics* **44**(1): 71-82.

Stathakis, D. G., N. Udar, O. Sandgren, S. Andreasson, P. J. Bryant, K. Small and K. Forsman_Semb (1999). Genomic organization of human DLG4, the gene encoding postsynaptic density 95. *Journal of Neurochemistry* **73**(6): 2250-65.

Staubli, U. and G. Lynch (1990). Stable depression of potentiated synaptic responses in the hippocampus with 1-5 Hz stimulation. *Brain Research* **513**(1): 113-8.

Steigerwald, F., T. W. Schulz, L. T. Schenker, M. B. Kennedy, P. H. Seeburg and G. Kohr (2000). C-Terminal truncation of NR2A subunits impairs synaptic but not extrasynaptic localization of NMDA receptors. *Journal of Neuroscience* **20**(12): 4573-81.

Stevenson, B. R., J. D. Siliciano, M. S. Mooseker and D. A. Goodenough (1986). Identification of ZO-1: a high molecular weight polypeptide associated with the tight junction (zonula occludens) in a variety of epithelia. *The Journal of Cell Biology* **103**(3): 755-66.

Stewart, M., C. Murphy and J. W. Fristrom (1972). The recovery and preliminary characterization of X chromosome mutants affecting imaginal discs of Drosophila melanogaster. *Developmental Biology* **27**(1): 71-83.

St-Onge, L., P. A. Furth and P. Gruss (1996). Temporal control of the Cre recombinase in transgenic mice by a tetracycline responsive promoter. *Nucleic Acids Res* **24**(19): 3875-7.

Strack, S., S. Choi, D. M. Lovinger and R. J. Colbran (1997). Translocation of autophosphorylated calcium/calmodulin-dependent protein kinase II to the postsynaptic density. *The Journal of Biological Chemistry* **272**(21): 13467-70.

Strack, S. and R. J. Colbran (1998). Autophosphorylation-dependent targeting of calcium/ calmodulin-dependent protein kinase II by the NR2B subunit of the N-methyl-D-aspartate receptor. *Journal of Biological Chemistry* **273**(33): 20689-92.

Sun, Y., A. Savanenin, P. H. Reddy and Y. F. Liu (2001). Polyglutamine-expanded huntingtin promotes sensitization of N-methyl-D-aspartate receptors via post-synaptic density 95. *Journal of Biological Chemistry* **276**(27): 24713-8.

Suzuki, T., J. Ito, H. Takagi, F. Saitoh, H. Nawa and H. Shimizu (2001). Biochemical evidence for localization of AMPA-type glutamate receptor subunits in the dendritic raft. *Brain Res Mol Brain Res* **89**(1-2): 20-8.

Tanemoto, M., A. Fujita, K. Higashi and Y. Kurachi (2002). PSD-95 mediates formation of a functional homomeric Kir5.1 channel in the brain. *Neuron* **34**(3): 387-97.

Tao, Y. X., Y. Z. Huang, L. Mei and R. A. Johns (2000). Expression of PSD-95/SAP90 is critical for N-methyl-D-aspartate receptor-mediated thermal hyperalgesia in the spinal cord. *Neuroscience* **98**(2): 201-6.

Tao, Y. X. and R. A. Johns (2001). Effect of the deficiency of spinal PSD-95/SAP90 on the minimum alveolar anesthetic concentration of isoflurane in rats. *Anesthesiology* **94**(6): 1010-5.

Tavares, G. A., E. H. Panepucci and A. T. Brunger (2001). Structural characterization of the intramolecular interaction between the SH3 and guanylate kinase domains of PSD-95. *Molecular Cell* **8**(6): 1313-25.

Tejedor, F. J., A. Bokhari, O. Rogero, M. Gorczyca, J. Zhang, E. Kim, M. Sheng and V. Budnik (1997). Essential role for dlg in synaptic clustering of Shaker K+ channels in vivo. *Journal of Neuroscience* **17**(1): 152-9.

Thomas, K. R. and M. R. Capecchi (1987). Site-directed mutagenesis by gene targeting in mouse embryo-derived stem cells. *Cell* **51**(3): 503-12.

Thomas, M. J., A. M. Watabe, T. D. Moody, M. Makhinson and T. J. O'Dell (1998). Postsynaptic complex spike bursting enables the induction of LTP by theta frequency synaptic stimulation. *J Neurosci* **18**(18): 7118-26.

Thomas, U., S. Ebitsch, M. Gorczyca, Y. H. Koh, C. D. Hough, D. Woods, E. D. Gundelfinger and V. Budnik (2000). Synaptic targeting and localization of discs-large is a stepwise process controlled by different domains of the protein. *Current Biology* **10**(18): 1108-17.

Thomas, U., E. Kim, S. Kuhlendahl, Y. H. Koh, E. D. Gundelfinger, M. Sheng, C. C. Garner and V. Budnik (1997). Synaptic clustering of the cell adhesion molecule fasciclin II by discs-large and its role in the regulation of presynaptic structure. *Neuron* **19**(4): 787-99.

Thomas, U., B. Phannavong, B. Muller, C. C. Garner and E. D. Gundelfinger (1997). Functional expression of rat synapse-associated proteins SAP97 and SAP102 in Drosophila dlg-1 mutants: effects on tumor suppression and synaptic bouton structure. *Mechanisms of Development* **62**(2): 161-74.

Tischmeyer, W. and R. Grimm (1999). Activation of immediate early genes and memory formation. *Cell Mol Life Sci* **55**(4): 564-74.

Tochio, H., F. Hung, M. Li, D. S. Bredt and M. Zhang (2000). Solution structure and backbone dynamics of the second PDZ domain of postsynaptic density-95. *Journal of Molecular Biology* **295**(2): 225-37.

Todd, M. M., J. B. Weeks and D. S. Warner (1993). A focal cryogenic brain lesion does not reduce the minimum alveolar concentration for halothane in rats. *Anesthesiology* **79**(1): 139-43.

Topinka, J. R. and D. S. Bredt (1998). N-terminal palmitoylation of PSD-95 regulates association with cell membranes and interaction with K+ channel Kv1.4. *Neuron* **20**(1): 125-34.

Torres, R. M. and R. Kuhn (1997). *Laboratory protocols for conditional gene targeting*, Oxford University Press.

Tsien, J. Z., D. F. Chen, D. Gerber, C. Tom, E. H. Mercer, D. J. Anderson, M. Mayford, E. R. Kandel and S. Tonegawa (1996). Subregion- and cell type-restricted gene knockout in mouse brain. *Cell* **87**(7): 1317-26.

Tsien, J. Z., P. T. Huerta and S. Tonegawa (1996). The essential role of hippocampal CA1 NMDA receptor-dependent synaptic plasticity in spatial memory. *Cell* **87**(7): 1327-38.

Tsunoda, S., J. Sierralta, Y. Sun, R. Bodner, E. Suzuki, A. Becker, M. Socolich and C. S. Zuker (1997). A multivalent PDZ-domain protein assembles signalling complexes in a G- protein-coupled cascade. *Nature* **388**(6639): 243-9.

Tverskoy, M., V. Shifrin, J. Finger, G. Fleyshman and I. Kissin (1996). Effect of epidural bupivacaine block on midazolam hypnotic requirements. *Reg Anesth* **21**(3): 209-13.

van Huizen, R., K. Miller, D. M. Chen, Y. Li, Z. C. Lai, R. W. Raab, W. S. Stark, R. D. Shortridge and M. Li (1998). Two distantly positioned PDZ domains mediate multivalent INAD- phospholipase C interactions essential for G protein-coupled signaling. *Embo J* **17**(8): 2285-97.

Vega, M. A., Ed. (1995). *Gene Targeting*. London, CRC Press.

Vignes, M. and G. L. Collingridge (1997). The synaptic activation of kainate receptors. *Nature* **388**(6638): 179-82.

Wakamori, M., Y. Ikemoto and N. Akaike (1991). Effects of two volatile anesthetics and a volatile convulsant on the excitatory and inhibitory amino acid responses in dissociated CNS neurons of the rat. *J Neurophysiol* **66**(6): 2014-21.

Waltereit, R., B. Dammermann, P. Wulff, J. Scafidi, U. Staubli, G. Kauselmann, M. Bundman and D. Kuhl (2001). Arg3.1/Arc mRNA induction by Ca2+ and cAMP requires protein kinase A and mitogen-activated protein kinase/extracellular regulated kinase activation. *J Neurosci* **21**(15): 5484-93.

Wang, J., J. J. Renger, L. C. Griffith, R. J. Greenspan and C. F. Wu (1994). Concomitant alterations of physiological and developmental plasticity in Drosophila CaM kinase II-inhibited synapses. *Neuron* **13**(6): 1373-84.

Wann, K. T. and A. G. Macdonald (1988). Actions and interactions of high pressure and general anaesthetics. *Prog Neurobiol* **30**(4): 271-307.

Wassarman, K. M., M. Lewandoski, K. Campbell, A. L. Joyner, J. L. Rubenstein, S. Martinez and G. R. Martin (1997). Specification of the anterior hindbrain and establishment of a normal mid/hindbrain organizer is dependent on Gbx2 gene function. *Development* **124**(15): 2923-34.

Weisskopf, M. G., P. E. Castillo, R. A. Zalutsky and R. A. Nicoll (1994). Mediation of hippocampal mossy fiber long-term potentiation by cyclic AMP. *Science* **265**(5180): 1878-82.

Wilding, T. J. and J. E. Huettner (1997). Activation and desensitization of hippocampal kainate receptors. *J Neurosci* **17**(8): 2713-21.

Willott, E., M. S. Balda, A. S. Fanning, B. Jameson, C. Van_Itallie and J. M. Anderson (1993). The tight junction protein ZO-1 is homologous to the Drosophila discs-large tumor suppressor protein of septate junctions. *Proceedings of the National Academy of Sciences of the United States of America* **90**(16): 7834-8.

Winocur, G. (1990). Anterograde and retrograde amnesia in rats with dorsal hippocampal or dorsomedial thalamic lesions. *Behav Brain Res* **38**(2): 145-54.

Winocur, G., R. M. McDonald and M. Moscovitch (2001). Anterograde and retrograde amnesia in rats with large hippocampal lesions. *Hippocampus* **11**(1): 18-26.

Woods, D. F. and P. J. Bryant (1989). Molecular cloning of the lethal(1)discs large-1 oncogene of Drosophila. *Developmental Biology* **134**(1): 222-35.

Woods, D. F. and P. J. Bryant (1991). The discs-large tumor suppressor gene of Drosophila encodes a guanylate kinase homolog localized at septate junctions. *Cell* **66**(3): 451-64.

Woods, D. F., C. Hough, D. Peel, G. Callaini and P. J. Bryant (1996). Dlg protein is required for junction structure, cell polarity, and proliferation control in Drosophila epithelia. *Journal of Cell Biology* **134**(6): 1469-82.

Wunderlich, F. T., H. Wildner, K. Rajewsky and F. Edenhofer (2001). New variants of inducible Cre recombinase: a novel mutant of Cre-PR fusion protein exhibits enhanced sensitivity and an expanded range of inducibility. *Nucleic Acids Res* **29**(10): E47.

Wyszynski, M., J. Lin, A. Rao, E. Nigh, A. H. Beggs, A. M. Craig and M. Sheng (1997). Competitive binding of alpha-actinin and calmodulin to the NMDA receptor. *Nature* **385**(6615): 439-42.

Xu, X. Z., A. Choudhury, X. Li and C. Montell (1998). Coordination of an array of signaling proteins through homo- and heteromeric interactions between PDZ domains and target proteins. *The Journal of Cell Biology* **142**(2): 545-55.

Yamada, Y., Y. Chochi, K. Takamiya, K. Sobue and M. Inui (1999). Modulation of the channel activity of the epsilon2/zeta1-subtype N-methyl D-aspartate receptor by PSD-95. *Journal of Biological Chemistry* **274**(10): 6647-52.

Yamauchi, M., H. Sekiyama, S. G. Shimada and J. G. Collins (2002). Halothane suppression of spinal sensory neuronal responses to noxious peripheral stimuli is mediated, in part, by both GABA(A) and glycine receptor systems. *Anesthesiology* **97**(2): 412-7.

Yoshimura, Y., C. Aoi and T. Yamauchi (2000). Investigation of protein substrates of Ca(2+)/calmodulin-dependent protein kinase II translocated to the postsynaptic density. *Brain Res Mol Brain Res* **81**(1-2): 118-28.

Zambrowicz, B. P., A. Imamoto, S. Fiering, L. A. Herzenberg, W. G. Kerr and P. Soriano (1997). Disruption of overlapping transcripts in the ROSA beta geo 26 gene trap strain leads to widespread expression of beta-galactosidase in mouse embryos and hematopoietic cells. *Proc Natl Acad Sci U S A* **94**(8): 3789-94.

Zhang, Y., C. Riesterer, A. M. Ayrall, F. Sablitzky, T. D. Littlewood and M. Reth (1996). Inducible site-directed recombination in mouse embryonic stem cells. *Nucleic Acids Res* **24**(4): 543-8.

Zito, K., R. D. Fetter, C. S. Goodman and E. Y. Isacoff (1997). Synaptic clustering of Fascilin II and Shaker: essential targeting sequences and role of Dlg. *Neuron* **19**(5): 1007-16.

Zola-Morgan, S., L. R. Squire and D. G. Amaral (1986). Human amnesia and the medial temporal region: enduring memory impairment following a bilateral lesion limited to field CA1 of the hippocampus. *The Journal of Neuroscience* **6**(10): 2950-67.

Zola-Morgan, S. M. and L. R. Squire (1990). The primate hippocampal formation: evidence for a time-limited role in memory storage. *Science* **250**(4978): 288-90.